DYNAMICS OF THE NIAGARA RIVER PLUME IN LAKE ONTARIO

C.R. Murthy (Project Leader), D.C.L. Lam,
T.J. Simons, J. Jedrasik,
K.C. Miners, J.A. Bull, W.M. Schertzer
National Water Research Institute
Burlington, Ontario, Canada L7R 4A6
Contribution #84-7

Executive Summary

The coastal zones of large lakes are not only the areas of most concern for water quality impairment but are also the zones of which understanding is most difficult, due to the complex interactions with the coastal boundaries and the influence of inflowing rivers or discharges. The findings of an intensive investigation of the interactions of the Niagara River inflow and the waters of Lake Ontario in the coastal zone of the lake are reported here.

A series of intensive measurements of the temperature and velocity structure of the Niagara River plume were carried out in 1982 that covered the thermal cycle of Lake Ontario. The measurements were made using a combination of moored current meters and Lagrangian drogues, along with ship based soundings on a fixed-grid network. A wide variety of wind and lake conditions were included in the observational data.

The observational data are employed in relation to simulation models of the current and diffusion properties of the Niagara River. The model computes the three dimensional circulations based on the daily flows of the Niagara and St. Lawrence Rivers and using the wind stress as the driving function. Simulation shows very good agreement with the observed flows.

The model of the plume dynamics is then developed as a simulation of the dispersion of contaminants carried by the river plume. It is shown that the advection and diffusion of contaminants are the primary elements of dilution, although other factors such as sedimentation and resuspension may be important.

Résumé pour la direction

Les zones littorales de grands lacs sont non seulement les secteurs qui préoccupent le plus quant à la dégradation de la qualité de l'eau, mais également ceux qui sont le plus difficile à comprendre en raison des interactions complexes avec les limites littorales et de l'influence des cours d'eau qui s'y jettent ou des écoulements qu'ils reçoivent. On présente ici les résultats d'une étude intensive des interactions entre l'apport en eau de la rivière Niagara et les eaux du lac Ontario dans la zone littorale du lac.

On a effectué en 1982 une série de mesures intensives de la température et de la structure des vitesses du panache de la rivière Niagara, mesures qui couvraient le cycle thermique du lac Ontario. Les mesures ont été effectuées au moyen d'une combinaison de courantomètres ancrés et de drogues lagrangiennes ainsi que de sondages à partir de navires d'après un quadrillage fixe. Les données d'observation englobaient également une gamme variée de conditions de vent et d'états du lac.

Les observations sont utilisées en relation avec des modèles de simulation des courants et des propriétés de diffusion de la rivière Niagara. Le modèle calcule des circulations tridimensionnelles d'après les écoulements quotidiens par la rivière Niagara et le fleuve Saint-Laurent en utilisant l'effort du vent comme fonction d'entraînement. La simulation concorde très bien avec les écoulement observés.

Le modèle de la dynamique du panache est ensuite perfectionné en une simulation de la dispersion des contaminants transportés par le panache de la rivière. On montre que l'advection et la diffusion constituent les principaux éléments de la dilution, mais que d'autres facteurs comme le dépôt et la remise en suspension peuvent s'avérer importants.

1. INTRODUCTION

In the Great Lakes, as well as in the oceans, the coastal zones are the areas of most immediate interest and concern. It is therefore not surprising that oceanographic research in recent years has placed considerable emphasis on physical processes and water quality properties of these zones. In many ways, these processes appear more complicated, more irregular and more difficult to describe in terms of mathematical models than the large-scale phenomena in the open lake or ocean. For instance, modeling studies in conjunction with the 1972 IFYGL experiment on Lake Ontario have been reasonably successful in simulating observed events in the lake, but the results of such simulations deteriorated towards the shore. The problem is not a lack of conceptual models and theoretical ideas concerning various possible mechanisms operating in coastal waters, the difficulty is to identify the relative contributions from individual processes in shaping the total observed structure and behavior of the coastal zone. This question can only be addressed by a combined experimental and modeling program which is specifically designed to try and match, by objective and statistical fitting procedures, detailed coastal zone measurements with the various available models. Once the principal mechanisms have been uniquely established, then the corresponding submodels can be reassembled to arrive at a comprehensive model of the coastal zone. The Lake Ontario Physical Limnology program is directed towards that broad goal.

Broadly stated the principal objective of the Lake Ontario coastal physical limnology study is to determine to what extent the local physical and biochemical characteristics of the nearshore zone are affected by the lake-wide processes and large-scale forcing. The following specific objectives were delineated for the purposes of planning and designing of the experimental program:

(1) To relate nearshore current reversals to wind forcing and alongshore propagation of topographic and baroclinic wave phenomenon.

(2) To analyze cross-shore variations of currents in terms of wind forcing, cross-shore depth variations, and effects of friction and diffusion in shallow water.

(3) To determine the relative effects of wind-induced upwelling, alongshore Kelvin waves, and small-scale mixing on the nearshore thermal regime in spring, summer and fall.

(4) To study the impact of mass exchanges between the coastal zone and open lake on seasonal variations of nutrients and other water quality parameters in the nearshore zone.

(5) To compute seasonal mass budgets of nutrients in the nearshore zone by recourse to observations of biochemical conversion rates, and

(6) To delineate the seasonal characteristics of the Niagara River plume in spring, summer and fall in support of toxic contaminants and other related biochemical surveys in the Niagara River plume.

This report is a first in a series based on the 1982/83 Lake Ontario coastal physical study (herein referred to as Lake Ontario Study) and addresses itself specifically to objective (6) stated above.

2. EXPERIMENTAL PROGRAM

2.1 Rationale

The multi-facet nature of the Lake Ontario study called for an imaginative design of the experimental program. Viewed purely from the scientific interests of the physcists in Aquatic Physics and Systems Division (APSD), Lake Ontario Study offered two very broad areas of research interests, they are: (1) Coastal exchange dynamics of the northshore and (2) Niagara River plume dynamics. Dovetailing these two areas of physical limnological research interests are two major biochemical and toxic contaminants studies proposed by Aquatic

Ecology Division (AED) and Environmental Contaminants Division (ECD). The AED had planned an extensive biochemical measurement study entitled "Lake Ontario Nutrient Assessment Study: LONAS" across a northsouth transect from Port Hope to Port Breeze. The ECD on the other hand had planned a study known as "Operation Niagara" to look at the transport and pathways of toxic contaminants in the Niagara River plume and their implications on the water quality of the western basin. The planning and design of the experimental program reflected these two broad areas of research interests in Lake Ontario. The rationale then is to design a comprehensive experimental program satisfying the requirements of the physical studies while giving due regard to the need for physical data in support of the "LONAS" and "OPERATION NIAGARA" experiments and the subsequent water quality modelling studies.

2.2 General Measurement Array

The dual nature of the Lake Ontario study as outlined earlier is reflected in the measurement array as indicated in Figures 2.1 and 2.2. The measurement array consists of two distinct experiments carefully designed to meet the two major objectives of the study. To realize the specific objectives of the coastal exchanges dynamics of the north shore, four cross-shore arrays at Toronto, Bowmanville, Port Hope and Ogden Pt. were established. The cross-shore array at Port Hope was extended to Port Breeze on the south shore in support of the "LONAS" experiments. Similarly the cross-shore array at Toronto was extended to Niagara in support of "OPERATION NIAGARA" experiments. Figure 2.1 shows the distribution of the instruments in each of the cross-shore arrays for the summer stratified experiments while Figure 2.2 shows the measurement array for the fall and winter experiments. Details regarding the general philosphy and design of the measurement array will be given later in subsequent reports. However, a discussion of the specific physical experiments conducted at Niagara mainly in support of "OPERATION NIAGARA" is appropriate in this report.

2.3 Niagara River Physical Experiments

A study of the temperature regime and water movements in the vicinity of the Niagara River mouth was conducted during seven, five-day intensive periods between April 13 and November 12, 1983 (see Table 2.1). Initially, the study was proposed to collect physical data to aid in the interpretation of biological and chemical data collected in and around the river plume. Such a study was recognized as an opportunity to obtain a data base for developing and testing numerical hydrodynamical models of the Niagara effluent and its interaction with Lake Ontario, with little additional effort.

The temperature of water discharging from Lake Erie through the Niagara River changes very little by the time it reaches Lake Ontario. The higher surface to volume ratio of Lake Erie enhances its response to seasonal temperature extremes with the result that, over much of the year, the temperature of Niagara effluent may be used as a tracer for tracking the river plume in Lake Ontario. Realizing that the temperature differences vanish at least twice during the year, in early summer and fall, it was still believed that temperature surveys would provide a useful means of defining the river plume over most of the study period.

Logistic and resource limitations restricted the study area to a 10 by 10 km area with its base centred on the river mouth (Figure 2.3) and the duration of individual experiments to 8 to 12 hours.

Two vessels were employed; one larger vessel used primarily for taking temperature/depth profiles and operations base; and a smaller one for drogue tracking. The CSS Advent served in the former role from April through August, being replaced by the CSL Shark for the October and November surveys. A 6 m (21 ft) MonArk launch with twin 70 HP outboard engines was used for drogue tracking throughout the study.

Fast accurate positioning was a prime requisite for both temperature and current surveys. This was achieved with Motorola Mini-Ranger III range-range positioning gear on each vessel.

The Mini-Ranger console unit displays the distance, in metres, to each of two stations of known position. These stations are equipped with transponders designed to retransmit microwave pulses (uniquely coded for their channel) from the vessels' console via a transmit/receive antenna. Distances are computed by console electronics, based on the time between transmission of the pulse and receipt of the return pulse. Selection of any pair of up to four fixed stations is possible with the channel selectors on the console unit. Other factors aside the reliability of a given fix is greatest when the lines from the position to each of the selected transponder sites are mutually perpendicular. Stations are selected to optimize this aspect over the survey area.

Initially, two transponder sites (1 & 2, Figure 2.4) were established; one on the west light at the entrance to the Welland Canal at Port Weller; and the other atop the Queenston Heights Restaurant, situated near Brock's Monument at the edge of the Niagara escarpment.

Mini-Ranger being a line-of-sight system, it was found that station 1, Port Weller, was shadowed by the shoreline inshore of about 400 metres off the river mouth. Station 2, Queenston, was blacked out in most of the nearshore area plus several patches offshore. Besides these persistent shadow areas, presumably caused by topographic and man-made obstructions (towers, etc.) between the transponder site and the lake, station 2 reception seemed to be sensitive to atmospheric conditions, probably density differences caused by different temperature regimes at the vessels' antenna and the transponder, 12 km inland and at 100 m greater elevation.

To overcome this problem, two more transponders were installed; station 3, atop the navigation pylon near Fort Mississauga on the west side of the river mouth; and station 4 on the light house near Fort Niagara on the east side of the river mouth. The short distance between 3 and 4 limited their usefulness as a pair to the immediate river mouth area; however, stations 1 and 4 were found to perform reliably over the most frequently used parts of the study area.

Prior to the start of field studies computer/plotter software was developed to produce charts and tables of Mini-Ranger coordinates for the study area. Charts were produced from a data file of X,Y coordinates digitized from a hydrographic chart at a scale of 1:80,000. Since transponders were on, or very near, features marked on the chart, the digitized values for these sites were used for all computations for the positioning data.

The plotting program produced charts with shoreline and important landmarks scaled to a user supplied value (Figure 2.3). One option provided for plotting a grid on the chart given one point on the grid plus the grid spacing and overall grid dimensions in metres.

By specifying an orientation angle the grid could be oriented to fit the local mean shoreline. A second option provided for plotting of range rings at any desired radial increment around any two points on the chart. In this manner navigation guide charts at 1:20000 scale, and 200 m ring spacing, were prepared for the Mini-Ranger system. These were done for combinations of transponder stations 1 and 2, 1 and 4, plus 3 and 4; with and without temperature sample grid. An ungridded chart for each Mini-Ranger pattern was cut into 12 segments to fit 8½x11 inch (216x279 mm) sheets. Copies were made and arranged in ring binders for reference and plotting in the field. Figure 2.3 was produced for illustration only; it shows range rings, at 1000 m spacing, for transponders 1 and 4.

The temperature stations were established at 500 m intervals on a 10x10 km square grid with its base centred on the river mouth and rotated 15° counterclockwise from true north. Shore-parallel grid lines were given double letter identifiers (AA, AF, AK, etc.) starting at the baseline. Shore-perpendicular lines were identified by three digit numbers (100, 105, 110 etc.) starting on the west side. This nomenclature provided unique identifiers for each intersect (e.g. AF115) and also allowed for expansion of the entire grid and reduction of grid spacing down to 100 metres, without altering the identification scheme. Tables of Mini-Ranger coordinates of grid stations were computed for transponder pairs 1 and 2; 1 and 4; and 3 and 4.

2.4 EBT Surveys

The primary aim of the temperature surveys was to delineate the river plume, at least in the area near the river mouth. By taking vertical profiles at sufficient known locations along the plume edge in a band extending from river water through the interface to lake water, it was hoped that not only the position of the plume, but additional knowledge about its interaction with the lake could be attained.

The Advent and later the Shark, were equipped with Guildline electronic bathythermograph (EBT) systems, consisting of temperature depth sensor head with integral electrical/support cable; remote control, variable speed electric winch, and controller/recorder electronics rack, as used for several years for temperature profiling by NWRI. Temperature vs depth profiles were recorded on standard waterproof sheets by the system's X-Y recorder.

At the beginning and end of a survey profiles were taken at station AA150 in the river mouth as baseline river temperature references. Proceeding offshore profiles were taken at selected stations, usually on the 150 line, until some indication of an interface showed up, then at every station until the profiles and visible water colour differences indicated that the open lake had been reached. At this point, the direction of sampling would be changed to move over one or more lines then a line back through the interface would be run. This zig-zag pattern was repeated along the edge of that part of the plume lying within the grid, at least once per survey, for totals of up to 75 profiles per survey.

Even when a substantial difference between the two water masses existed, absolute definition of the plume outline was difficult. Coastal waters, often mixed with effluent from the Welland Canal, and having similar temperature and optical properties to those of the river, mix with and become indistinguishable from the river water. Complex turbulence and current patterns sometimes smear the existing interface with partially mixed river/lake water.

2.5 Lagrangian Drogue Experiments

The drogues used for the Niagara study were the 'roller blind' type in use by this group for several years. Minimum depth of these drogues, measured from the water surface to the centre of the 2.4 by 3.0 m (8 by 10 ft) sail, is 3.5 metres. Greater drogue depths are achieved by adding an appropriate length of wire between the drogue bridle and the float mast. The main drogue studies were conducted using 3.5 metre drogues to avoid, as much as possible, problems with drogues grounding on the complex shoals of the Niagara bar.

In order to sample the velocity field for the entire effluent, drogues (usually 10) were released at intervals across the river. In the early studies, drogues were released starting about a kilometer and a half upstream of the mouth and attempting to maintain a transverse line as more drogues were released. This method allowed time for a couple of fixes on the drogues before they reached the river mouth; however, it was found that they would consistently cluster into a narrow band near the eastern shore by the time they reached the mouth leaving nothing to trace the movements of the western half of the effluent. Beginning with the August experiments drogues were released across the river mouth. It was still necessary to avoid releasing drogues within about one hundred and fifty metres of the western shore because of shallow water, but the most westerly drogues indicated very low, sometimes reversed, flow even at that distance offshore.

The river channel curves to the west over the last two kilometres. This plus a promontory on the eastern shore right at the river mouth further forces deflection toward the west. The funnelling effect observed with drogues released upstream was likely more of a failure on the part of more westerly drogues to "feel" the westward deflection as much as those nearer the eastern shore.

Time and Mini-Ranger coordinates were recorded for each drogue as it was released, and at intervals thereafter depending on the time required to make the circuit around all of them. For the actual position fix the tracking vessel would come slowly alongside the drogue, as close as possible depending on sea state; the button to hold range displays would be pressed; and time, drogue number, and ranges would be recorded on prepared data sheets. Time was resolved only to the minute during which the fix was taken. As the drogues spread out, time between fixes lengthened and the order in which they were fixed was sometimes changed to simplify the route. By the end of a survey drogues were usually spread over several square kilometres. When the temperature survey was completed, both vessels were used to track and recover drogues.

During 8 surveys between June 23 and August 5, 1982, 5 drogues at a nominal depth of 10 m were released about 200 m apart in a line near current meter station 34 to provide comparison data between Eulerian and Lagrangian measurements at that depth. These drogues were tracked simultaneously with, and in the same manner as, the shallow drogues with fixes taken at somewhat longer intervals.

The phenomenon described above, where shallow drogues released upstream in the river crowd into the eastern side of the river by the time they reach the mouth, raised the question of where the flow in the western side comes from. The drogues released at the river mouth did indeed show that there is a substantial outflow to within a couple of hundred metres of the western shore. In order to learn more about the behavior of the effluent at greater depth near the river mouth a simple one-off experiment was conducted on November 9, 1982. Five drogues, 3 at seven metres and 2 at ten metres, were released on a transect at about the same location upstream as the earlier shallow drogue experiments starting with a 7 metre drogue near the western shore. Drogues at the two depths were alternately released across the deep channel. These were fixed as rapidly as possible until they ran aground or passed well beyond the river mouth. Failure to observe the converging characteristics seen with the shallow drogues supported the idea that water at greater depth tends to follow the channel more faithfully, while surface water, in the deeper part of the river where boundary influences are felt less strongly, tends to deflect less in the curved channel. In this lateral shearing process deeper water is likely drawn upward in the western part of the channel.

Table 2.1. Summary of 1982 Niagara River Physical Studies

Date	Drogue Experiments: Number of Drogues	Depth (m)	Duration (Hr)	Temperature Surveys: Number of Profiles
April 14	6	3½	5	50
April 15	11	3½	8	55
April 16	11	3½	6	63
May 26	15	3½	7	18
May 27	15	3½	9	69
	5	7	3	
May 28	7	3½	4½	27
June 21	9	3½	6	29
June 22	10	3½	10	50
June 23	10	3½	12	65
	5	10	9	
June 24	10	3½	10	75
	5	10	10	
June 25	10	3½	11	59
	5	10	7½	
July 6	10	3½	10	52
	5	10	10	
July 7	10	3½	8	27
	5	10	7	
July 8	10	3½	11½	45
	5	10	11	
August 10	10	3½	3	12
August 11	10	3½	11	26
	5	10	11	
August 12	10	3½	11	60
	5	10	10	
October 5	10	3½	10	65
October 6	10	3½	10	50
October 7	10	3½	10	42
November 8	5	3½	8	47
November 9	10	3½	9½	34
	* 5	7&10	1½	
November 10	10	3½	8	45

* River mouth deepwater study

3. DATA REDUCTION AND ANALYSIS

3.1 EBT Data

EBT profiles (T(z)) were processed using the nine-point digitization scheme. Data were key-punched to computer cards coding the consecutive station number, year, month, day, hour, latitude and longitude, surface water temperature, temperature/depth pairs, and sounding depth. A permanent disc file of the digitized data base formed the basis for analysis of the Niagara River plume.

Since topogrpahic features in the vicinity of the Niagara River mouth play a dominant role on the behaviour of the plume, it was necessary to produce an accurate and detailed bathymetric map indicating the main topographic features such as the main Niagara bar, the deep channel etc. Figure 3.1 was constructed based on the average sounding depths of the EBT profiles and information derived from chart 2043 on Lower Niagara River and approaches compiled by the Canadian Hydrographic Service.

Analysis of the thermal regime required interpretation of the temperature distributions in both the horizontal and vertical planes over any chosen grid axis. Computer line-printer outputs of temperature at each grid point in the horizontal and vertical planes on any specified grid axis were produced. In the horizontal plane, temperatures can be listed over the 10x10 km grid at specified depths. In the vertical plane, temperature can be listed at any designated depth along any cross-section, taken either normal to or diagonal to the grid boundaries. Finally, the various horizontal and vertical line printer outputs were interpolated and contoured to delineate the thermal regimes of the Niagara River plume.

3.2 Lagrangian Drogue Data

Lagrangian drogue data were used to calculate the drogue trajectories and the corresponding horizontal velocity field indicative of the movement of the river plume as it interacts and merges with the lake. To calculate these quantities from the basic data, namely time series mini-range sightings of the drogue positions, a system of coordinates was established as illustrated in Figure 3.2. Here (X_0,Y_0) coordinates are directed along the east and north directions respectively. The local coordinates (X_L,Y_L) were then calculated using the following trignometric relations:

$$X_0 = X_L \cos \alpha - Y_L \sin \alpha + A_x$$

$$Y_0 = Y_L \sin \alpha + Y_L \cos \alpha + A_y$$

where α is the angle of rotation between the (E-N) and the local coordinate systems A_x and A_y are the shifts to the local coordinate system (see Figure 3.2).

These transformations allowed for the early computation of the drogue displacements and the corresponding horizontal velocity vectors. Essentially two types of plots were produced to assist in the delineation of the river plume characteristics: (i) Lagragian drogue trajectories and (ii) corresponding horizontal velocity field.

4. SEASONAL CHARACTERISTICS OF THE NR PLUME;

4.1 Thermal Regime

Topographic features in the vicinity of the Niagara River mouth play a dominant role on the behaviour of the river plume. Figure 3.1 shows an accurate and detailed bathymetric map indicating the main topographic features. The bathymetry resembles that of a continental shelf with an inner shallow shelf region (Niagara Sand Bar) which extends to about 20 m depth contour (approximately 6 km offshore) followed by something like a shelf edge from 20 m to 100 m depth contour. Some of the direct effects of these topographic features on the transport and mixing of the river plume will be evident later.

Because of the high surface to volume ratio of Lake Erie, Niagara River plume shows 2 to 3°C temperature elevation in comparison to the ambient Lake Ontario water temperature in spring and fall regimes. With the onset of spring warming, the Niagara River plume temperature is generally 2 to 3°C higher than Lake Ontario nearshore and surface water temperature by the end of May (see Figure 4.1). Thus the high density river water spreads out and generally well-mixed vertically in the shallow regions of the sand bar. At the edge of the sand bar the interaction of the warm well-mixed river plume water with lake water can be recognized by the onset of a thermal front with the intrusion of the cold lake water from deeper depths. The front itself is quite weak at this stage of its formation. In the summer period (June, July and August experiments: Figures 4.2 to 4.4) the thermal contrast of the river plume is somewhat masked by the seasonal warming of the nearshore and surface waters in Lake Ontario. Figure 4.2 shows the complex thermal patterns observed during the June experiment with intrusions of warm rings of nearshore and surface waters at the edges of the plume. Although the surface thermal structure is rather complicated, the vertical cross-section reveals the two distinct phases of the river plume, namely an initial well mixed regime on the sand bar followed by a well established thermal front at the edge of the sand bar. The front itself is quite sharp during the summer and fall experiments. The overall thermal characteristics of the river plume during the fall experiments (October and November experiments: Figures 4.5 and 4.6) is identical to the summer experiments except that the surface water temperature in Lake Ontario is cooler than the river plume temperature due to the onset of fall-winter cooling.

The dynamics of the thermal front and its interaction with the sharp bathymetry at the edge of the sand bar no doubt creates some very interesting mixing characteristics of the river plume, which will be of particular interest in tracing the toxic constituents carried by the plume into Lake Ontario.

4.2 Horizontal Flow Regime

Plots of horizontal velocities calculated from the Lagrangian drifter data for each of the experiment are summarized in Figures 4.7 to 4.25 along with a summary of the mean wind history. Within the first 5 km from the mouth of the river the flow in the plume is hydraulically controlled and the dynamics of the plume itself is jet-like. During the momentum dominated initial phase an order of magnitude reduction of horizontal velocities from 200 cm sec^{-1} to about 20 cm sec^{-1} occur and the river plume is well-mixed vertically over the entire shallow sand bar. Beyond this initial stage the river plume is bent over in response to lakewide circulation and the prevailing winds. In most cases the river plume is gradually bent over to the east and eventually caught up in the strong eastward coastal current. Superimposed on this first order flow characteristics of the plume one can see quasi-secondary flow features associated with the complex river lake interactions. For example, on several occasions large scale eddies of size 1 to 2 km were generated on the leeward edges of the plume. A striking example of this phenomenon can be seen in the June 23 experiment (Figure 4.12). We will not delve here into the detailed analysis and interpretation of how these second order flow features are generated, except to note the importance of these in the transport and dispersal of toxic and other constituents carried by the Niagara River Plume into Lake Ontario.

Although one can see day-to-day variability both in the thermal regime and horizontal flow field of the Niagara River Plume in Lake Ontario, a conceptual model of the river-lake interaction can be formulated. The conceptual model formulated here consists of the following three stages:

1. Momentum Dominated Initial Phase

This phase is hydraulically controlled and the dynamics of the river plume is almost jet-like. During this momentum dominated initial phase, the river plume merely spreads over the shallow sand bar and is completely mixed vertically due to self-generated plume turbulence and wind generated turbulence. This initial phase appears to be restricted to the shallow sand bar area as can be seen from an order of magnitude reduction of horizontal velocities from 200 cm sec^{-1} at the river mouth to about 20 cm sec^{-1} at the edge of the sand bar. The vertically well-mixed plume over the sand bar area as seen from the temperature cross-sections is another indication of the extent of the initial phase.

2. Transition Phase (Thermal Front)

Interaction of the well mixed buoyant river plume at the edge of the sand bar creates some large scale isotherm displacements indicating intense vertical mixing activity. With the intrusion of colder water from deeper depths of the lake, a sharp thermal front is generated and maintained in the vicinity of the sand bar edge. The evolution of the thermal front from the early spring warming to late fall can be identified in the vertical temperature cross-section data in all the experiments.

3. Final Phase: "Buoyant Surface Spreading"

With the momentum sufficiently dissipated, the buoyant river plume responds to the prevailing winds and the lake wide circulation. The buoyant plume hugs the free surface of the lake and the winds aid in its spreading over the surface (Buoyant Surface Spreading). As remarked earlier, the plume generally turns to the east and is eventually entrained into the strong southshore eastward coastal transport (Murthy 1969).

This data base has formed the basis for the development of the hydrodynamic models of river lake interaction and the transport models to predict the distributions of toxic and other chemical constituents carried by the river plume into Lake Ontario. These models will be discussed in detail in the subsequent sections of this report.

5. NUMERICAL SIMULATION OF CURRENTS IN THE NIAGARA RIVER PLUME

5.1 Model Structure

Since the numerical calculations are concerned only with a very small portion of Lake Ontario, a nested system of models is used. Nested grid systems or telescopic grids, consisting of small, fine-mesh domains embedded in larger, coarse-mesh domains, are well known from the meteorological literature. The simplest approach is to first calculate the solution for the whole domain with the coarse mesh and then to use this solution to specify the boundary flows for the limited area with the fine mesh. A more complete formulation would allow for feed-back from the small-scale solution into the outer area, but this effect may be ignored since our interest is essentially limited to the fine-mesh solution.

In this study, a low-resolution model covering the whole of Lake Ontario provides the boundary conditions for a medium-resolution model of the area near the Niagara River. The latter, in turn, supplies boundary flows for a high-resolution model of the mouth of the Niagara River. The lake-wide model has a 5 km grid spacing and the grid is rotated 10° counterclockwise from north. The medium-resolution model covers an area of 25x15 km with a 1 km grid rotated 13.5° counterclockwise from north. The fine-grid model has a grid mesh of 0.2 km and covers an area of 3x2 km at the mouth of the

Niagara River plus the upper 2 km of the river itself. This nested system of models is outlined in Figures 5.1 to 5.3.

The vertical model structure consists of a number of horizontal computational levels at arbitrarily fixed depths below the surface. The model computes average currents for each layer between adjacent points of computation levels. The number of layers varies in the horizontal due to intersection of these levels with the lake bottom and the thickness of the lowest layer varies as a function of the depth of the lake.

5.2 Model Equations

The model computes three-dimensional water circulations on the basis of the horizontal equations of motion and the continuity equation. The sea surface is treated as a free surface, the hydrostatic and the incompressibility approximation are used, and nonlinear acceleration terms and horizontal diffusion of momentum are neglected. In principle, the model permits calculation of temperature changes but in the present case, the temperature is assumed to be known from observation.

The model has been documented by Simons "Documentation of a multilevel model for computing stratified lake circulations and temperature changes", National Water Research Institute, January 1983, 23 pp. The equations are briefly summarized below. In these equations u and v are the components of the current in x and y direction, respectively, t is time, y is the free surface perturbation, f is the Coriolis parameter, g is the earth's gravity, T is the temperature and σ is a measure of the deviation of density from its mean value. The subscript k denote the model layers, increasing from the surface layer (k=1) to the bottom layer (k=K). The number of layers, K, and the thickness of the bottom layer, D_K, vary in the horizontal. All other layer depths have uniform thickness D_K in the horizontal direction but the thickness can vary from one layer to the next.

The equations of motion give the equations for the layer velocities in the following form:

$$\frac{\partial u_k}{\partial t} = fv_k - g\frac{\partial \eta}{\partial x} - Px_k + (\tau x_{k-1} - \tau x_k)/D_k \qquad (1a)$$

$$\frac{\partial v_k}{\partial t} = -fu_k - g\frac{\partial \eta}{\partial y} - Py_k + (\tau y_{k-1} - \tau y_k)/D_k \qquad (1b)$$

where $\vec{P}$ and $\vec{\tau}$ are pressure terms and stress terms defined as follows

$$\vec{P}_1 = \tfrac{1}{2} D_1 \nabla(g\sigma_1) \qquad \vec{P}_{k+1} - \vec{P}_k = \tfrac{1}{2}(D_k + D_{k+1})\nabla(g\sigma_{k+\frac{1}{2}}) \qquad (2)$$

$$\sigma_1 = \alpha(T_1-4°)^2 \qquad \sigma_{k+\frac{1}{2}} = \alpha[\tfrac{1}{2}(T_k+T_{k+1}) - 4°]^2 \quad \alpha = -6.8\ 10^{-6}$$

$$\vec{\tau}_k = 2A_v \frac{\vec{v}_k-\vec{v}_{k+1}}{D_k+D_{k+1}}\ (k=1,K-1) \qquad \vec{\tau}_0 = \frac{\vec{\tau}_s}{\rho} \quad \tau_K = \frac{\vec{\tau}_b}{\rho} \tag{3}$$

where A_v is an eddy viscosity coefficient for vertical fluxes of momentum, τ_s is the wind stress at the surface, and τ_b is the bottom stress. The latter is formulated on the basis of the familiar Ekman theory for shallow water

$$\frac{\vec{\tau}_b}{\rho} = \frac{b}{H^2}\vec{V} \qquad b \approx 3A_v \tag{4}$$

where H is the water depth and V is the vertically-integrated current.

The continuity equations for the layers are

$$w_{k-1} = w_k - \nabla\cdot(D\vec{v})_k \qquad w_0 = \frac{\partial\eta}{\partial t} \qquad w_K = 0 \tag{5}$$

This system of equations determines the vertical velocities at the computational levels, starting from the bottom layer, with the equation for the upper layer determining the change of surface elevation needed in the equations of motion (1a-b).

5.3 Solution of the Equations

In the horizontal, the variables are staggered to form a lattice structure. The free surface and the temperature are defined at the centre of a grid square, the east-component of the current is defined at the east and west sides of the grid square, and the north-component at the north and south sides. At the open boundaries of a high-resolution model, the only variable to be obtained from the surrounding low-resolution model is the velocity component normal to the boundary. This transboundary flow is interpolated from the coarse grid to the fine grid in such a way that the total transport across each side of the fine-grid model is the same for the fine grid as for the coarse grid. In the interior grid points, all derivatives are approximated by central differences. The Coriolis term is obtained by averaging over four adjacent points.

Time extrapolation proceeds by first preceding u, then v, then η, at all times using the last available values of all variables. For reasons of economy, the variables are separated into external and internal components. The external vertical mode consists of the surface elevation and the vertically-integrated current. The internal variables are the vertical shears of the velocity between adjacent pairs of layers. The equations for the external mode are obtained by summing (1a) and (1b) over all layers and the equations for the shears are obtained by subtracting (1a) and (1b) for adjacent layers.

The timestep for the external variables is limited by the speed of external gravity waves. The time step limits are 75 sec for the lake-wide model, 21 sec for the medium-resolution model and 9 sec for the high-resolution model. The time step for the velocity shears is restricted by friction. A value of 15 min was used for all internal calculations.

5.4 Model Inputs and Outputs

Inputs to the system of models are daily values of the Niagara River flow, a constant value of the Welland Canal flow, and daily St. Lawrence outflows balancing the above flows. The river flows increase linearly to the observed values during the first 10 days. The system of models is driven by hourly winds measured at a CCIW buoy in Western Lake Ontario. The wind stress is proportional to the square of the wind with a constant drag coefficient of 1.2×10^{-6}. Hourly values of the wind stress are interpolated in time to the time steps used by the different models.

The output of the lake-wide model consists of boundary flows for the medium-resolution model at hourly intervals. These flows are interpolated in space and time to the grid mesh and the time step of the medium-resolution model. The output of the medium-resolution model consists of the flows across the border of the Niagara River model at hourly intervals. These flows are then interpolated in space and time to the grid spacing and the time interval of the river model.

The main output of the system of models consists of maps of currents at three-hourly intervals for both the medium and the high resolution models. These currents are provided in the form of vertically-averaged currents as well as upper-layer currents. The currents represent values at the centre of each grid square as obtained by averaging the flows through the sides of the square.

5.5 Model Runs

The models described in the foregoing have been run continuously for the period May 1 to November 10, 1982. This covers the period during which the 1982 Niagara River drogue experiments were carried out. These experiments started on May 26, June 21, July 6, August 10, October 6, and November 8, respectively, and lasted from 3 to 5 days each.

The lake-wide model was run in a single-layer configuration. The medium-resolution model consisted of 4 layers separated at 10, 20 and 40 m below the surface. The high resolution model consisted of 4 layers separated at 5, 10 and 15 m below the surface. The vertical eddy viscosity coefficient was equal to 25 cm^2/s.

In these initial runs, effects of temperature have been ignored because observations show that in the area of the drogue experiments, the lake is generally well-mixed in the vertical. Effects of stratification are only expected to become noticeable beyond the 10 m depth contour shown in Figure 2, that is beyond the Niagara Bar.

In the first runs, the bottom friction coefficient b of equation (4) was assigned a value of 100 cm^2/s. The results indicated that the horizontal water displacements were underestimated by the models. The bottom friction was therefore reduced to a value of 50 cm^2/s. The resulting water displacements appear to agree more closely with the observed drogue displacements.

The computed upper-layer currents for each day of the drogue experiments are shown in Figures 5.4 to 5.21. In each Figure, the upperhalf of the page shows the currents obtained from the medium-resolution model, the lower left corner of the page shows the results from the high-resolution model and the lower right portion of the page shows the wind history before and during the drogue experiments. All current and wind vectors are plotted such that the alongshore components coincide with the horizontal axis and the offshore components with the vertical axis. The dashed line in the upper figure denotes the 20 m depth contour.

The computed currents illustrate the strong impact of wind on water circulations outside the area of the river mouth. Particularly striking is the rapid response of currents to changing winds as noted, for instance, on August 11-12 and November 8-10. This effect is so strong that, at times, it penetrates into the area covered by the high-resolution model, as seen in the lower left corners of the illustrations. As expected, however, the flow in the river and at the river mouth are completely determined by the hydraulic discharge.

A note of cautions should be added. The computer circulations of Figures 5.4 to 5.21 should not be interpreted as faithful reproductions of actual currents but rather as illustrations of the variability in time and space that may be expected to occur in this area under realistic environmental conditions. From the limited current meter data available (see Figure 5.2), it has been verified that major current reversals indeed seem correlated with wind events but superimposed on this basic flow pattern is an enormous amount of variability. This is, no doubt, due to the high level of turbulence in the presence of very fast currents and small-scale topographic features, which will be discussed in the next Chapter. In addition, effects of stratification must be assumed to become important some 5-10 km offshore (see Figures 4.1 to 4.6), say, beyond the 20 m depth contour in Figures 5.4 to 5.21. This has, so far, not been considered because the drogue paths in the present experiments appear to be determined by the flow closer to shore (see Figures 4.7 to 4.25).

6. MODELLING THE CONTAMINANT TRANSPORTS IN THE NIAGARA RIVER PLUME

Most chemicals found in the Niagara River area could probably be traced back to some upstream locations such as effluent discharges or seepage outlets adjacent to waste dump sites. These chemicals are carried by the river currents and eventually enter into Lake Ontario. Increased concern has been expressed as to the destination of the chemicals. Basically, the two physical processes directly affecting the movements of the chemicals are advection and diffusion. The former is the mean translational component and the latter the random fluctuation component. It is due to these two processes that the chemical plume stretches, bends and spreads.

The chemicals may also be subject to other processes such as chemical sedimentation, resuspension, bioturbation, volatilization and hydrolysis. However, the advection and diffusion processes exert the primary influence. Chemicals deposited in sediments conform to the seasonal circulation patterns of the overlying waters; water samples collected outside of the plume may not contain detectable quantities of the chemical; the concentration becomes diluted downstream and cross-stream away from the centre line of the plume. All these are signatures of the two processes. In particular, the dilution and proximity of the chemical plume in relation to water intakes are environmental issues urgently needed to be addressed. Therefore, it is important at the outset to develop the appropriate advection-diffusion model to simulate the transport and dispersion of the contaminants accurately. The other processes can be incorporated at a later stage.

6.1 Computations of Plume Patterns Identified by Lagrangian Tracers

Unlike the conventional Eulerian model in which the governing transport equation is based on a fixed coordinate system, the Lagrangian model is based on a moving frame which follows the parcel of water containing the tracer in question. In other words, the Lagrangian model framework moves in time and space according to some "averaged" current, e.g., the one defined by the movement of the centroid of a group of tracers. The fluctuations of the movement of each tracer with respect to this current provide a description of the randomness of the environmental turbulence, in the simplest sense of the term.

Since many physical and chemical data were collected by using the Lagrangian technique in the Niagara Plume project, we have developed a drogue tracer transport model. The purposes are two-fold: to simulate accurately the plume characteristics defined by the drogues, and to incorporate the results into an existing Eulerian contaminant transport model. The second objective is necessary because the Eulerian model provides a more complete spatial distribution of the concentration at any time than the Lagrangian model. We will elaborate on this subject in Section 6.2. The following are some preliminary results pertaining to the first objective.

6.1.1. The Lagrangian Viewpoints

Mathematically, the Lagrangian description of a two-dimensional flow field consists of defining the pathway of the coordinates $(x(a,b,t,), y(a,b,t))$ at time t of a fluid particle that originates at (a,b) at an earlier time t_o. Thus, $x(a,b,t_o) = a$ and $y(a,b,t_o) = b$. This pathway can be viewed in two ways. The one way is to consider (a,b) as fixed, i.e., for the one chosen particle originated from (a,b) at t_o, so that $(x(a,b,t), y(a,b,t))$ traces out the path of such a particle as time increases. From this viewpoint, the fluid velocity components are (Simpson, 1983):

$$u(x,y,t) = \partial x(a,b,t)/\partial t \tag{6.1}$$

$$v(x,y,t) = \partial y(a,b,t)/\partial t \tag{6.2}$$

The other way is to consider t as fixed so that the Lagrangian functions $(x(a,b,t), y(a,b,t))$ are viewed as a mapping of the region occupied by a patch of fluid in the (a,b) plane at time t_o onto the region now occupied by the same patch in the (x,y) plane at time t. Note that this Lagrangian description differs from the Eulerian description for a fixed time. In this Lagrangian description, the patch has to be small enough to be meaningful; otherwise, a large patch in the (x,y) plane at time t could have been the result of the mapping of several smaller separate patches at one or several earlier points in time. In the Eulerian description, the spatial distribution of all particles frozen at the same time, irrespective of their past history. This Lagrangian description can be used to describe several physical properties conveniently. Okubo et al. (1976) denotes the Jacobian matrix of this mapping by E, i.e.,

$$E = \begin{matrix} \partial x/\partial a & \partial x/\partial b \\ \partial y/\partial a & \partial y/\partial b \end{matrix}_{(a,b,t)} \qquad 6.3$$

whose entries are called the first-order Lagrangian deformations. Its determinant is used in describing the fluid continuity, because the mass of fluid in a vertical column centred on (a,b) is $\rho h(a,b)da\,db$ for a slowly varying depth of $h(x,y)$ and a fluid density of ρ and becomes $\rho h(x,y)dxdy$ at a time t later so that

$$\rho h(a,b)dadb = \rho h(x,y)dxdy \qquad (6.4)$$

or

$$h(a,b) = h(x,y)\left|\det E\right| \tag{6.5}$$

Equation (6.5) is the law of mass conservation under this Lagrangian description.

6.1.2. Computational Techniques with Lagrangian Tracers

Equations (6.1) and (6.2) require continuous descriptions of x,y and t to define u and v, and vice versa. In practice, the information is given as discrete data. For example, the drogue positions are measured at discrete time intervals (Section 3.5), the computed velocities are specified at discrete grid points (Section 5.1). Some form of interpolation is therefore needed to complete the Lagrangian descriptions, particularly (6.1) and (6.2). The simplest way is to use bilinear interpolation for the spatial variables and linear interpolation in time. Other methods include cubic spline interpolation and cubic spline least-squares fit (Simpson, 1983). However, there is no guarantee that these interpolated values obey the mass conservation law (Equation 6.5) or the boundary conditions, unless they are subject to constraints (Lam and Durham, 1984).

With the interpolated data, we are able to compute the pathways of the drogues based on the velocities or estimate the velocities from the drogue paths. We will use the former as an example. Suppose we are given the (interpolated) velocities for all points (x,y) at two given times t_n and t_{t+1}, i.e., $\Delta t = t_{n+1} - t_n$. Typically these velocities may originate from an Eulerian hydrodynamic model (e.g., Section 5.2), but they are assumed to be appropriate also for the Lagrangian mapping discussed in Subsection 6.1.1.

The central differencing approximation to Equations (6.1) and (6.2) are

$$\frac{u(x_{n+1}, y_{n+1}, t_{n+1}) + u(x_n, y_n, t_n)}{2} = \frac{x_{n+1} - x_n}{\Delta t} \tag{6.6}$$

$$\frac{v(x_{n+1}, y_{n+1}, t_{n+1}) + v(x_n, y_n, t_n)}{2} = \frac{y_{n+1} - y_n}{\Delta t} \tag{6.7}$$

From Equations (6.6) and (6.7), the new position for the drogue can be computed by solving iteratively the following system of algebraic equations:

$$x_{n+1} = x_n + \frac{\Delta t}{2} (u(x_{n+1}, y_{n+1}, t_{n+1}) + u(x_n, y_n, t_n)) \tag{6.8}$$

$$y_{n+1} = y_n + \frac{\Delta t}{2} (v(x_{n+1}, y_{n+1}, t_{n+1}) + v(x_n, y_n, t_n)) \tag{6.9}$$

Functional iteration is required because the unknowns x_{n+1}, y_{n+1} appear as arguments of the functions u and v on the right-hand side of the equations. A convenient initial guess is to put $x_{n+1} = x_n$ and $y_{n+1} = y_n$ on the right-hand side to start the iteration.

Alternately, Bennett et al. (1983) proposed to approximate the velocities at time t_{n+1} by the velocities and velocity gradients at time t_n by using the truncated Taylor's series,

$$u(x_{n+1}, y_{n+1}, t_{n+1}) = u(x_n, y_n, t_n) + \left(\frac{\partial u}{\partial x}\right)_n (x_{n+1} - x_n) + \left(\frac{\partial u}{\partial y}\right)_n (y_{n+1} - y_n) \tag{6.10}$$

$$v(x_{n+1}, y_{n+1}, t_{n+1}) = v(x_n, y_n, t_n) + \left(\frac{\partial v}{\partial x}\right)_n (x_{n+1} - x_n) + \left(\frac{\partial v}{\partial y}\right)_n (y_{n+1} - y_n) \tag{6.11}$$

so that the new position of the drogue can be expressed as

$$x_{n+1} = x_n + \Delta t \left[u(x_n, y_n, t_n) + \frac{1}{2}\left(\frac{\partial u}{\partial x}\right)_n (x_{n+1} - x_n) + \frac{1}{2}\left(\frac{\partial u}{\partial y}\right)_n (y_{n+1} - y_n)\right] \tag{6.12}$$

$$y_{n+1} = y_n + \Delta t \; [v(x_n, y_n, t_n) + \frac{1}{2} (\frac{\partial v}{\partial x})_n (x_{n+1} - x_n)$$

$$+ \frac{1}{2} (\frac{\partial v}{\partial y})_n (y_{n+1} - y_n)] \qquad (6.13)$$

Equations (6.12) and (6.13) can be rearranged and solved directly for the unknowns x_{n+1}, y_{n+1} from the resulting system of two linear equations with the two unknowns.

Both systems (Equations 6.8-6.9 and 6.12-6.13) are second order accurate and are superior than first order accurate methods such as using only the velocities at t_n to extrapolate the drogue positions.

6.1.3. Randomness in a Drogue Path

Drogue paths observed in the lake such as those reported in Section 3.2 are instantaneous measurements, i.e., the drogues are carried by the instantaneous current. In practice, particularly in model predictions, the information necessary to duplicate the paths exactly is not always available and is often impossible to obtain. For example, as pointed out in the previous section, the velocities that can be measured, or computed, or even derived from the drogue data themselves are obtainable at discrete points in time and space only. The continuous description necessary to reconstruct the drogue path has to be based on some form of interpolation. This ad hoc technique of treating the subgrid details is quite acceptable in transport modelling, provided that the details or noises that have been filled in can be accounted for by some turbulence model.

The literature on the turbulence characteristics of Lagrangian tracers is limited; they are mainly centred on the deformation tensor and eddy diffusivities based on statistical variances (Okubo et al., 1976). In the case of the Niagara River plume, the observed instantaneous path can be considered in a simple way as a composite of a mean path and a random displacement. The quantification of the random component is difficult, not only because of the grid spacing problem but also because there are three distinct turbulence regimes that need to be discerned. At the river itself, in the high speed areas, the turbulence is dominated by the momentum induced eddies. A common example of modelling such turbulence is the k-ε model. In the lake portion, in the so-called far-field of the coastal zone, the turbulence has been empirically characterized by a length-scale dependent diffusivity (Murthy and Kenny, 1974). In the open lake regime, yet another diffusivity concept has to be used. These three turbulence models, however, have not been jointly used in a Lagrangian transport model, although some attempts have been made in the Eulerian sense (Lam and Durham, 1984).

With such a limited background, both in terms of theories and empirism, we do not feel we are in a position to develop an elaborate turbulence model. Since the Niagara plume is mostly characterized by the river jet turbulence, which is small compared to the high advective flow, we feel that a simple model suffices. An example is the one which adds on a random displacement after the advective step is computed by, for example, Equations (6.8) and (6.9). This random displacement will be based on a set of normally distributed random lengths whose maximum would not exceed 10% of the advective displacement in each step. It is also recommended that the cross-stream random displacement should be less than that in the streamline direction to maintain a smooth path.

6.1.4 Model Results

From a simulation point of view, reconstruction of the drogue paths by using the above Lagrangian transport model can be considered as a prediction, if none of the information from the observed drogues are used except for comparison purposes. Since the hydrodynamic currents have been computed (Section 5.5), they can be used as the mean velocities of the drogues. In particular, the top layer currents from the multilayer hydrodynamic model is most appropriate for computing the drogue positions, because the drogues are maintained at a constant depth of 3 m, i.e., within the model layer. These computed currents are based on the Eulerian system over a 1 km x 1 km grid for the lake portion and a 0.2 km x 0.2 km grid for the river portion. The Stokes effects (Murthy, 1973) and the vertical velocity components are ignored, whereas the horizontal components are interpolated in space and bilinearly and in time linearly as discussed in Subsection 6.1.2.

We find that the Equations (6.8–6.9) offer a more convenient way to compute the drogue positions than Equations (6.12–6.13), because the velocity gradients are not required and the values at both present and advanced time levels are used. Given the loss of subgrid details because of the grid spacings, it is not possible to start the simulation with the exact locations at the drogue release and to expect perfect reconstruction of the paths. Instead, an appropriate location is chosen as the initial position and ten to thirty drogues are assumed to be released simultaneously. These drogues will proceed to slightly different positions after the first advective step (i.e., Equations 6.8–6.9) because of the random perturbation (Subsection 6.1.3).

Figures 6.1–6.6 show the observed and computed drogue positions for the dates indicated (the time given in GMT is the starting time). The drogues are computed over the same period as the experiment at ten-minute intervals for the first half-hour and then at half-hourly intervals for the remaining time. The results compare quite well as far as the plume shape and direction are concerned.

These plume characteristics are found to be mainly affected by the river discharges and the wind driven currents (cf. wind records provided in Figures 5.4 - 5.21 for the corresponding dates). For example, when the wind is moderate and from the north, as on May 27, 1982, the drogues are conveyed by the river jet to the lake in a northerly direction (Figure 6.1). With a stronger and north-easterly wind, as on June 25, 1982, the drogues carried by the river are met with a strong eastward current and bent accordingly (Figure 6.2). Sometimes, the drogues do not conform to the shape of one single plume but manifest some degree of bifurcation, particularly when the winds are strong and alter rapidly in direction. Such is the case for August 12, 1982 with strong winds changing from the north-east to south-east and then to north-east again. Both the observed and the computed drogue paths show bifurcated plume shapes. A better example of the response of drogue paths to changes in wind direction is found in the three-day period of November 8 to 10, 1982. The wind blows strongly from the south-west in the first day with the drogues completely deflected to the east as a result (Figure 6.4); the second day sees a weaker wind from the north-east and the plume is predominantly carried by the river discharge flowing toweards the north (Figure 6.5); the wind strengthens again on the third day from the east this time, deflecting the plume to the west (Figure 6.6).

These are, of course, limitations with this simple Lagrangian model. It depends on the availability of an accurate hydrodymic model or some form of information about the circulation for defining the advective steps (Equations 6.8–6.9). Whereas the general direction of the drogue paths is correct, the distances travelled by the drogues have been somewhat underestimated. This deficiency is due to the use of the computed currents which are integrated over a layer of 5 to 10 m thick, as opposed to the use of the exact currents at 3 m deep. The randomness treatment plays only a secondary role: it is more important to obtain an accurate advective prediction first than to develop an overly elaborate turbulence model at this stage. On the whole, however, considering that these predictions are based only on the wind record and river discharge rates, plume calculations are satisfactory in terms of reproducing the plume directions and shapes.

6.1.5 Sensitivity Analysis

Figure 6.7 shows the results of a sensitivity test on the choice of randomness in affecting the calculation of the pathway of a cloud of floating objects (e.g., a spill). Using the computed currents of October 6, 1982 and the methods outlined above, we obtain the results depicted on the left-hand side of the figure. If we magnify the initial cloud to twice the original size and allow the random perturbation to cover up to a maximum of 30% of the advective distance determined by Equations (6.8–6.9), see discussions of Subsection 6.1.3), then the cloud will spread wider as it drifts along with the current, as shown on the right-hand side of the figure. These results demonstrate the effects of drastically changing the turbulence submodel (by a factor of three). Further study on turbulence is, therefore, required when the advective calculation is deemed reasonably reliable.

6.2. <u>**Simulation of Contaminant Plumes by an Eulerian Transport Model**</u>

The above discussions on Lagrangian modelling pertain to floatable objects and their pathways from the viewpoint of an observer who moves along with them. This approach helps to focus on the local characteristics of the plume. One advantage that emerges is that chemical sampling apparatus may be attached to these floatables to ensure that the concentrations are measured within the plume. The disadvantage, however, is that the concentration measurements are localized, i.e., grouped together according to whichever way these floatables may travel. In order to complete the description of the spatial distribution of the concentrations at any given time, it is necessary to see them from the perspective of an observer at a fixed position, i.e, from an Eulerian view.

6.2.1. The Coastal Zone Transport Model

The Eulerian approach to coastal zone contaminant transport modelling has been developed (Lam et al., 1984). The application of this model to the Niagara River plume is straightforward and can be summarized as follows. The calculations are performed on the 1 km grid (Figure 5.1) and use the hydrodynamic currents computed on this grid. The governing equation for the depth integrated model in finite-difference notations, is

$$\frac{\partial}{\partial t} = (HC)_{i,j} = X_{i,j} - X_{i+1,j} + Y_{i,j} - Y_{i,j+1} - W_{i,j} C_{i,j} + S_{i,j} \tag{6.14}$$

where H is the depth (cm), C is the concentration of the pollutant (g/cm^3), S is the source per unit area ($g\ cm^{-2}\ s^{-1}$), W is the settling velocity (cm/s), and X and Y are the transport components through the sides of the grid square with labels i indicating the left, i+1 for the right, j for the bottom, j+1 for the top, so that $X_{i,j}$ is at the left side of the square, $Y_{i,j}$ is at the bottom side, but $H_{i,j}$ and $C_{i,j}$ are assumed to be at the centre of the grid squre. Furthermore,

$$X_{i,j} = \frac{U_{i,j}}{DS}(C_{i-1,j} \text{ or } C_{i,j}) + \frac{A}{DS^2}\frac{H_{i,j-1} + H_{ij}}{2}(C_{i-1,j} - C_{i,j}) \tag{6.15}$$

$$Y_{i,j} = \frac{V_{i,j}}{DS}(C_{i,j-1} \text{ or } C_{i,j}) + \frac{A}{DS^2}\frac{H_{i,j-1} + H_{i,j}}{2}(C_{i-1,j} - C_{i,j}) \tag{6.16}$$

where U and V are components of the vertically integrated current (cm/s), DS is the length of the sides of the grid square (cm) and A is the horizontal eddy diffusivity (cm^2/s).

The decision to use $C_{i-1,j}$ or $C_{i,j}$ is based on the upstream differencing scheme (UDS), in which only upstream values are assumed to be essential in advective processes. This will add a numerical diffusion in the order of $U_{i,j} \cdot DS/H_{i,j}$ and $V_{i,j} \cdot DS/H_{i,j}$ to the physical diffusivity A. Thus, for systems where high accuracy of the physcial diffusion is required, the grid spacing must be reduced to offset this numerical effect. On the other hand, averaged concentrations $(C_{i-1,j} + C_{i,j})$ and $(C_{i,j-1} + C_{i,j})/2$ can be used throughout the computation, if a central differencing scheme (CDS) is used. However, spatial instability may occur in such a scheme, if $U_{ij}DS/H_{ij}A$ exceeds 2, or at locations with strong sources or sinks. More numerical methods such as the finite element methods (Lam et al., 1984) can also be used by are beyond the scope of discussion here.

As in the case of the hydrodynamic model, explicit time differencing is used for the left-hand side of (Equation 6.14). The following time stability criteria, however, must be satisfied:

$$\frac{U_{i,j}}{H_{i,j}} \frac{\Delta t}{DS} < 1$$

and (6.15)

$$\frac{A\Delta t}{DS^2} < \tfrac{1}{2}$$

The above conditions on numerical spatial dispersion and time stability may be modified somewhat if more than one variable of contaminants, which react kinetically with each other, are used.

6.2.2. Results

The model represented by (Equation 6.14) is appropriate for homogeneous lake conditions; for stratified conditions, a multi-layer model has to be used (Lam, 1978). As discussed in Chapter 4, the stratified effects are limited to the summer months and away from the immediate areas of the river mouth. To demonstrate the homogenous model, we choose the episodes in November 8 to 10, 1982, which are all under fully mixed conditions. The upstream differencing scheme (Equations 6.15-6.16) is used, which accounts for the open boundary conditions in a straight forward manner: for contaminant leaving the region through an open boundary, only the upstream values are used, but for contaminant entering the region through the same boundary, the concentration at the previous time step is used. The time step is taken to be 100 s. At the river inlet, a constant concentration of 10 mg/L is assumed to be maintained. Several eddy diffusivities have been used and the numerical diffusion is found to be small if A is greater than 10^3 cm^2/s. However, from our experience with the Lagrangian transport model (Subsection 6.1.3 and Figure 6.7), the eddy diffusivity required to simulate the spread of the drogue plume is rather small. Therefore, the value of 10^3 cm^2/s is used.

As seen in Figures 6.4-6.5, the period of November 8 to 10, 1982 contains three distinct wind episodes which, together with the effect of the river discharge, influence the direction and shape of the drogue plume. To examine each of these episodes, we design four hypothetical cases of contamination by a conservative pollutant. In the first three cases, the transports computed by the hydrodynamic model at 1700 GMT on each of the three days are assumed to prevail throughout the computation, i.e., each of the three cases is based on steady-state currents. Approximately, November 8 corresponds to a south-westerly wind; November 9, north-easterly; and November 10, easterly. Shown in Figures 6.8(a)-(c) are these wind directions (detailed wind records shown in Chapter 5) and the concentration contours after a continuous release with a source concentration of 10 mg/L for sixty hours. The contaminant plume responds to these steady current episodes differently: it travels more to the east with the November 8 currents, centres around the river mouth with the November 9 currents, and clearly more towards the west with the November 10 currents.

If the dynamic currents are used (i.e., if the currents are allowed to change in time for the same period of sixty hours starting on 1700 GMT, November 8, 1982), the resulting concentration contours are obtained as shown in Figure 6.8(d). This latter contour picture can be considered as a composite of the previous three pictures and, therefore, represents a more realistic one as far as the actual wind record and hence the hydrodynamic currents are concerned.

This series of figures is designed to offer a comparison between the different probable routes the Niagara River plume could have taken as it enters Lake Ontario. As illustrated above, in a matter of three days the wind and current change substantially and affect the course of the contaminant transport significantly.

6.2.3. Future Work

Based on the model results presented so far, it is clear that the Niagara River plume should be characterized by meteorological episodes. On one hand, the modelling of episodic events as demonstrated above should be pursued with the existing grid with more data, particularly those of the toxic substances. On the other hand, the long-term toxic effects should be addressed with a coarser grid to allow more variables in the model. This coarser grid system must reflect some of the seasonally averaged circulation patterns in its design. At present, both attempts have been made. The extent to which these models can be developed, e.g., how many variables (benthos, planktons, etc.) and compartments (water, sediment, etc.), depends very much on the availability of data and scientific knowledge of the contaminants found in the river plume.

ACKNOWLEDGEMENTS

The field work was organized and supervised by the Technical Operations Division, and the resourcefulness and persistence of the personnel assigned to this project was mainly responsible for the success of the experiments.

REFERENCES

Lam, D.C.L., C.R. Murthy and R.B. Simpson, 1984. Effluent transport and diffusion models for the coastal zone, Lecture Notes Series on Coastal and Estuarine Studies, Vol. 5, Springer-Verlag Publishers, N.Y., 168 p.

Lam, D.C.L., 1978. Simulation of water circulation and chloride transports in Lake Superior for summer 1973. J. Great Lakes Research, 4, 343-349.

Lam, D.C.L. and R.W. Durham, 1984. Finite element analysis of a radioactive tritium patch and a waste heat plume observed near the Pickering Nuclear Power Generating Station, Lake Ontario. J. Great Lakes Research, 10, 59-67.

Murthy, C.R., 1969. Large scale diffusion studies in the Niagara River mouth, Lake Ontario. Proc. 12th Conf. Great Lakes Res., Int. Ass. Great Lakes Res., pp 635-651.

Murthy, C.R., 1973. A comparison of Lagrangian and Eulerian current measurements in coastal waters of Lake Ontrario. Proc. 16th Conf. Great Lakes Res., 1034-1037.

Murthy, C.R. and B.C. Kenny, 1974. Diffusion in coastal currents of large lakes. Rapp. P.-V. Revn. Const. Int. Expolor. Mer, 167, 111-120.

Okub, A., C.C. Ebbesmeyer and J.M. Helseth, 1976. Determination of Lagragian deformations from analysis of current followers. J. Phys. Ocean., 6, 524-527.

Simpson, R.B., 1983. Lagrangian data analysis of Niagara River outflow data. OSS/NWRI Interim Contract Report 02SE.KW405-3-0093. 13 p.

w MOTION PACKAGE
▲ METEOROLOGICAL STATION
● TIDE GAUGE
* FIXED TEMPERATURE PROFILER
x CURRENT METER - PL10m, GEO 1m off bottom
o CURRENT METER - GEO at 30 and 50m.
+ WAVE RIDER

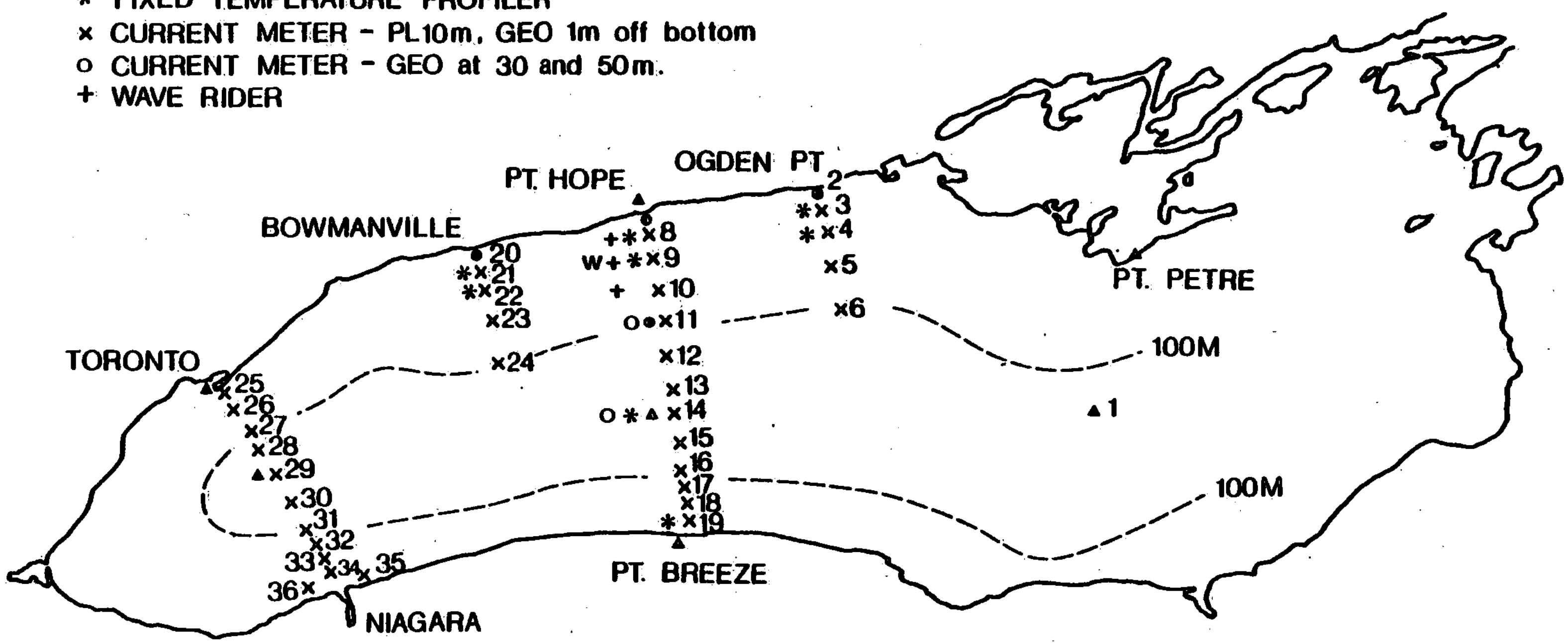

TOTAL REQUIRMENTS

1 MOTION PACKAGE
8 METEOROLOGICAL STATIONS
4 TIDE GAUGES
8 TEMPERATURE PROFILERS
33 PLESSEY CURRENT METERS
32 GEODYNE CURRENT METERS
3 WAVE RIDERS

LAKE ONTARIO - 1982 MOORING LOCATIONS

- • P12m, Gb-1
- * G12m, G50m, Gb-1
- + G12m, P50m, Gb-1
- ▲ METEOROLOGICAL STATION
- W WAVE RIDER
- B BBA
- M MOTION PACKAGE

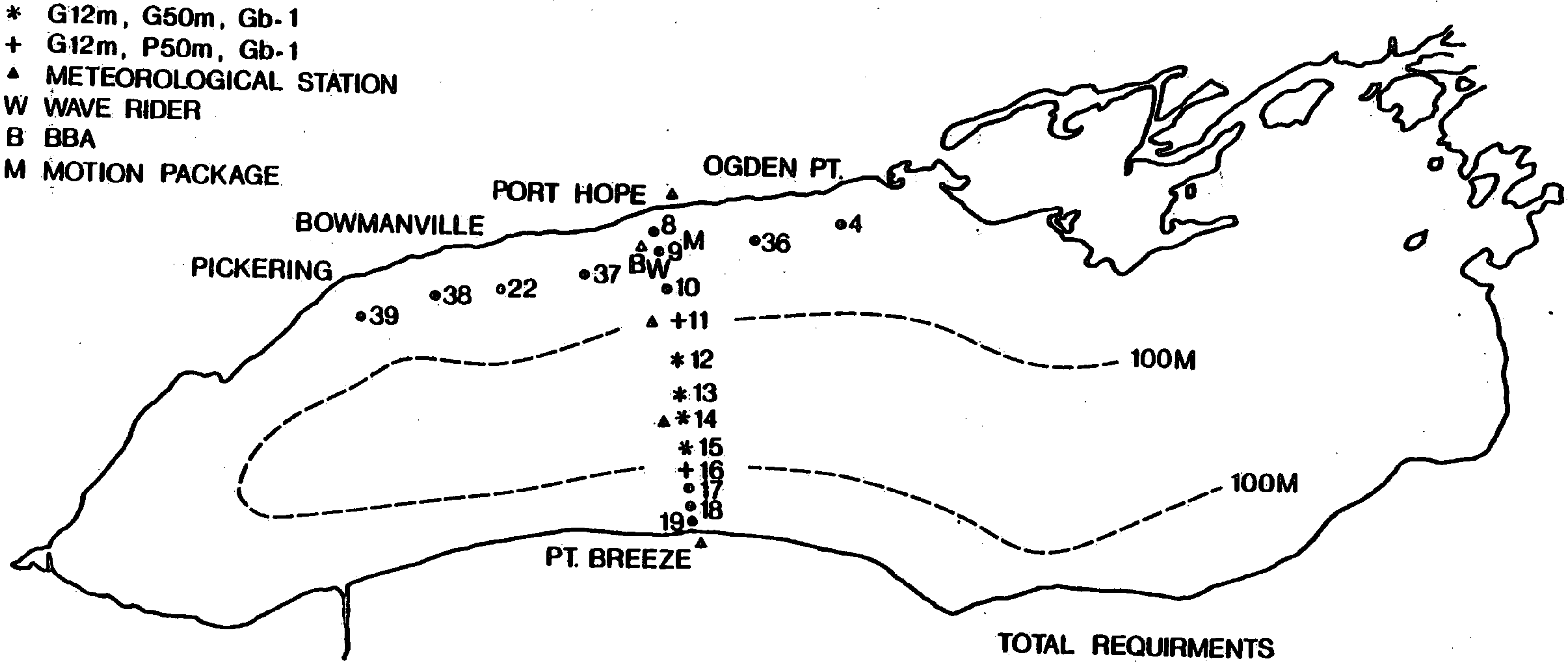

NOTE;
STATION 9 IS THE STUDY AREA FOR AN INTENSIVE MEASUREMENT PERIOD (IP) FROM NOV. 3 TO NOV. 24 1982.

TOTAL REQUIRMENTS

	28	GEODYNE CURRENT METERS
	4	PLESSEY CURRENT METERS
	2	METEOROLOGICAL STATIONS
(IP)	2	WAVE RIDERS
(IP)	1	MOTION PACKAGE
(IP)	1	BBA (M CATS)
(IP)	1	METEOROLOGICAL STATION

LAKE ONTARIO FALL / WINTER 1982/83 FIELD MEASUREMENT STATIONS

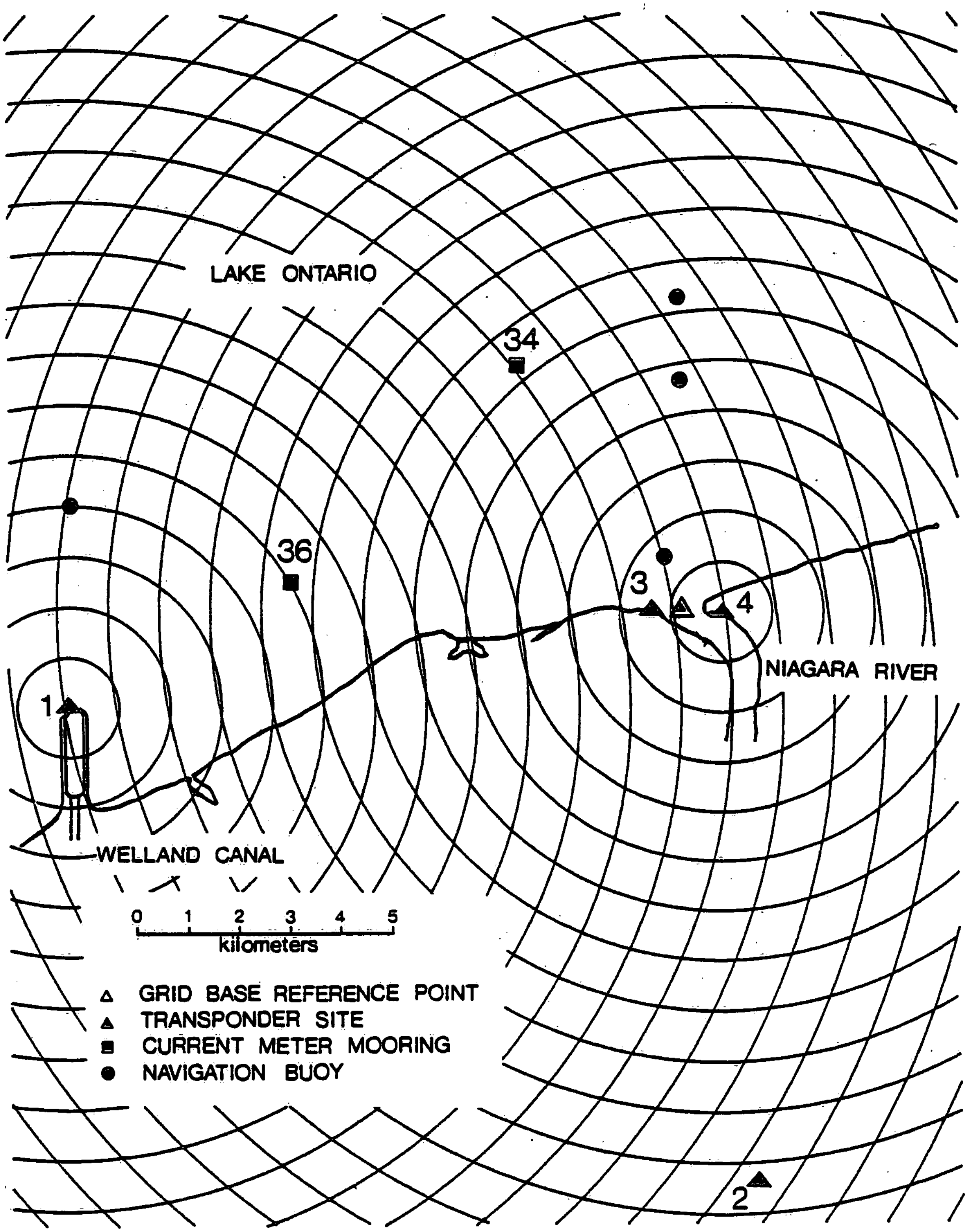

NIAGARA STUDY AREA WITH RANGE RINGS FOR TRANSPONDERS 1 AND 4

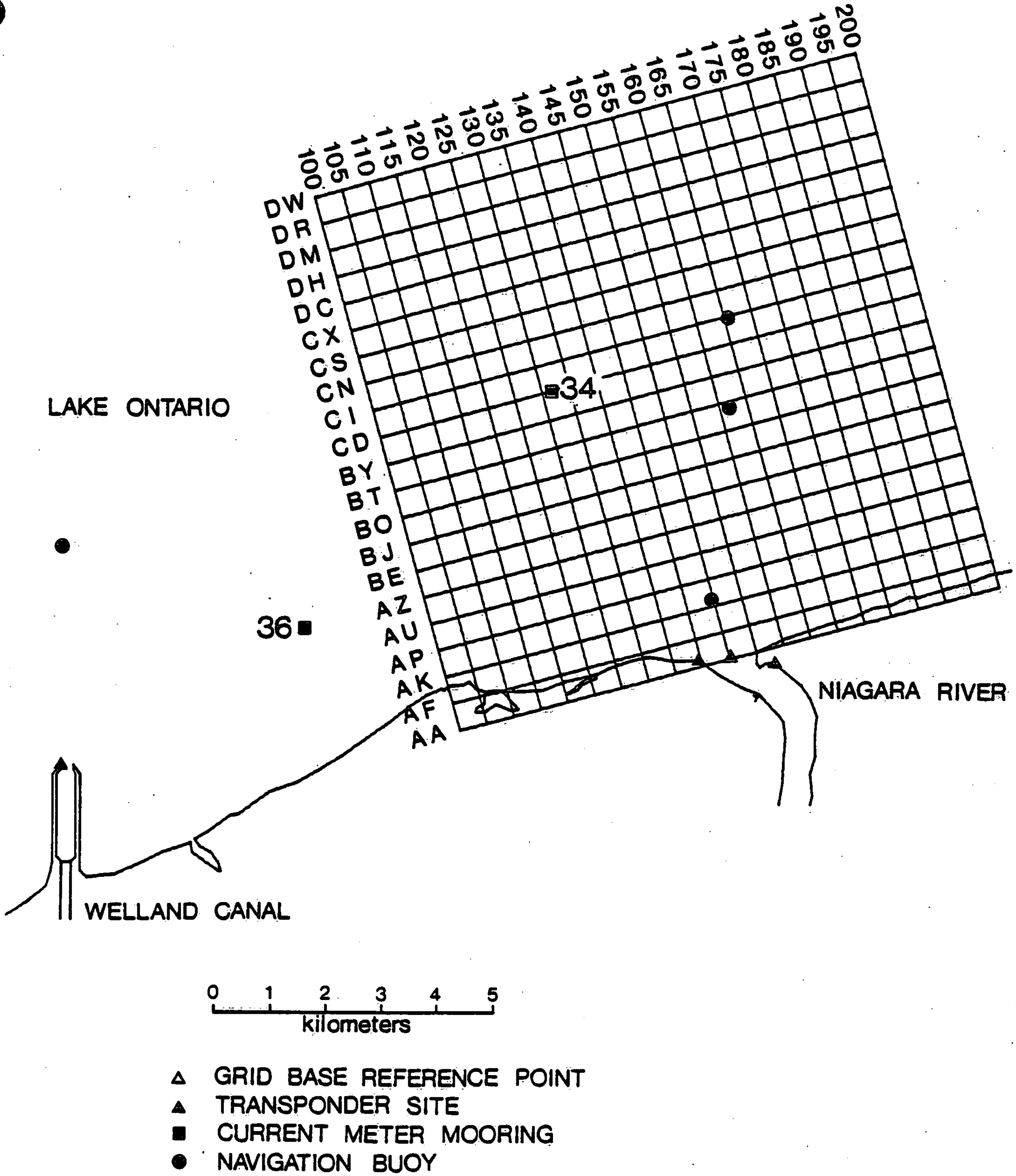

NIAGARA STUDY AREA WITH TEMPERATURE STATION GRID

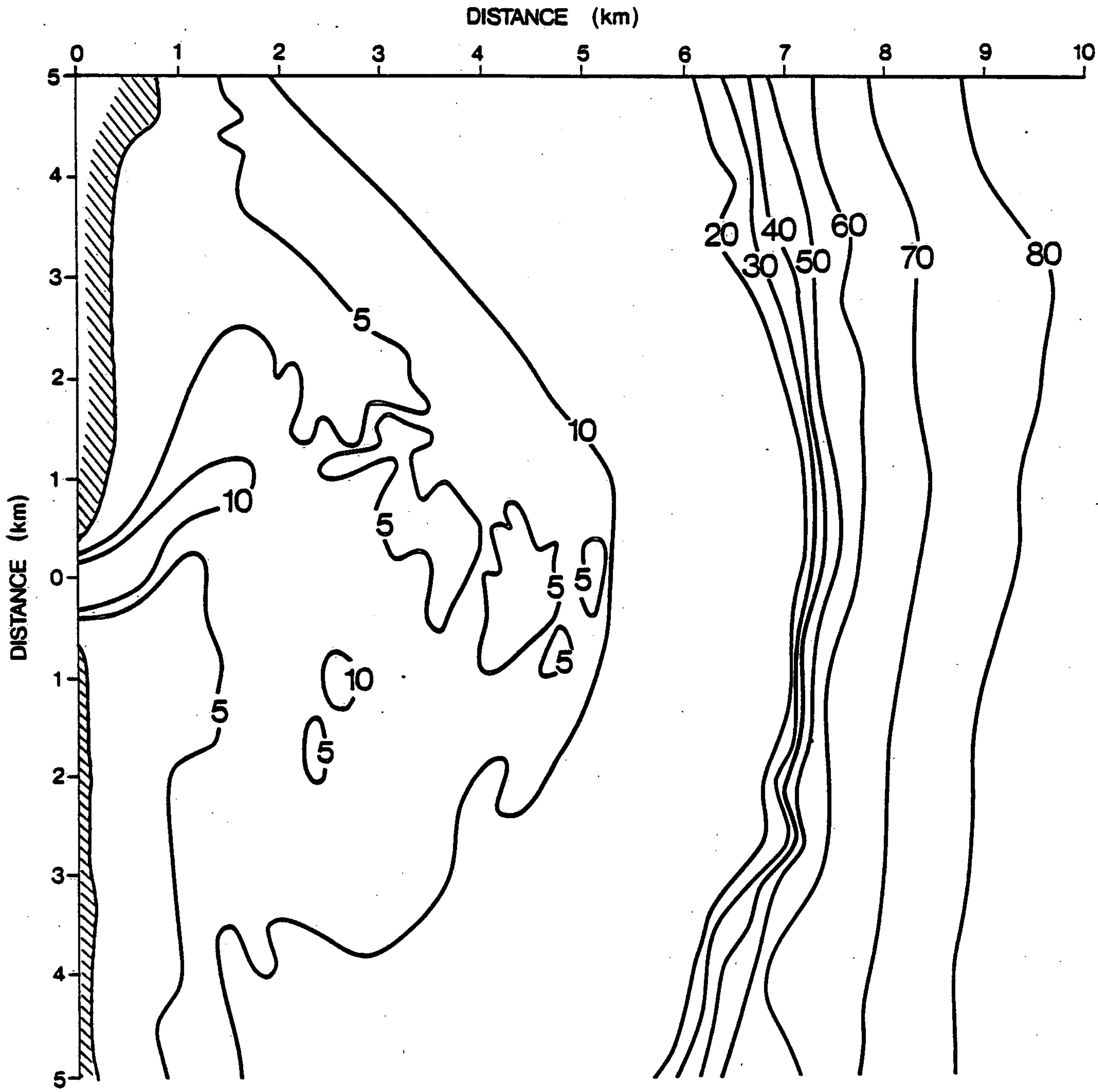

Fig. BATHYMETRY OF THE NIAGARA RIVER GRID

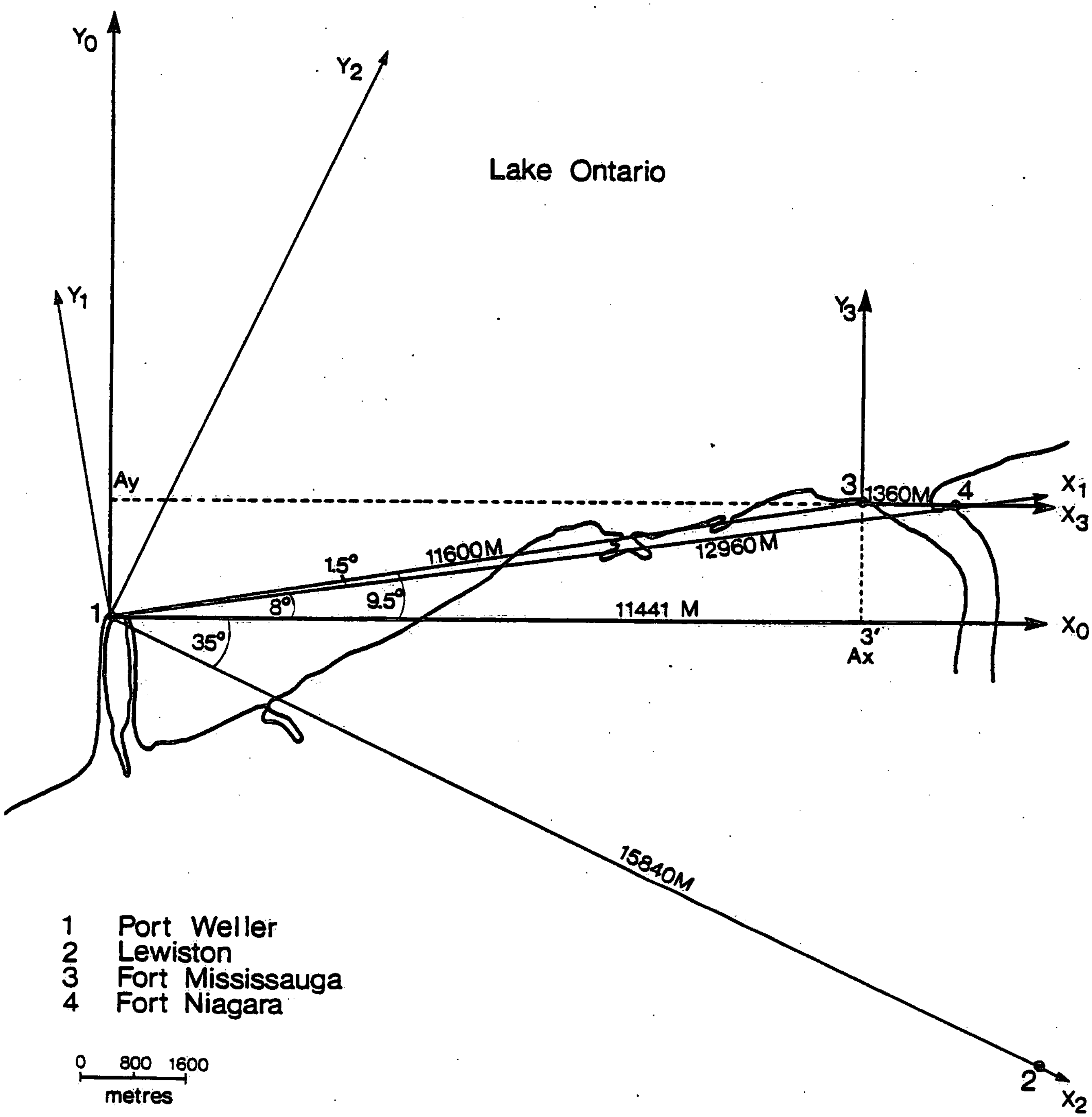

1 Port Weller
2 Lewiston
3 Fort Mississauga
4 Fort Niagara

Fig. 3.2 THE SYSTEM OF CO-ORDINATES

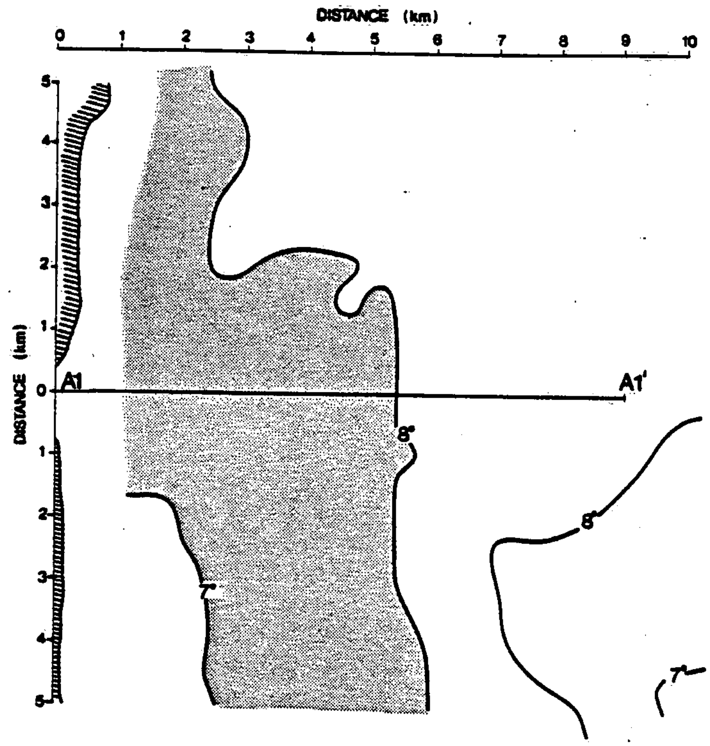

Fig. HORIZONTAL DISTRIBUTION OF AVERAGED TEMPERATURES: NIAGARA RIVER PLUME, UPPER LAYER, 26-28 MAY 1982.

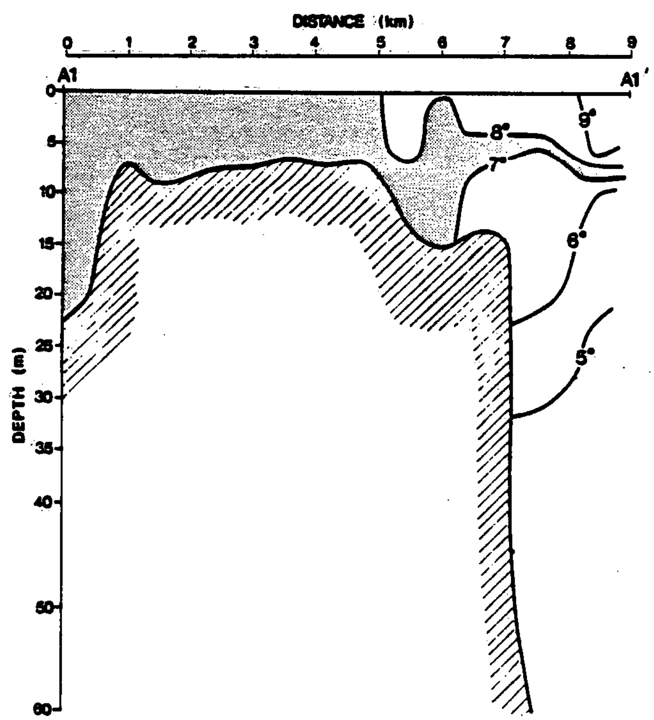

Fig. AVERAGED TEMPERATURES IN THE VERTICAL CROSS-SECTION A1 - A1', 26 - 28 MAY, 1982

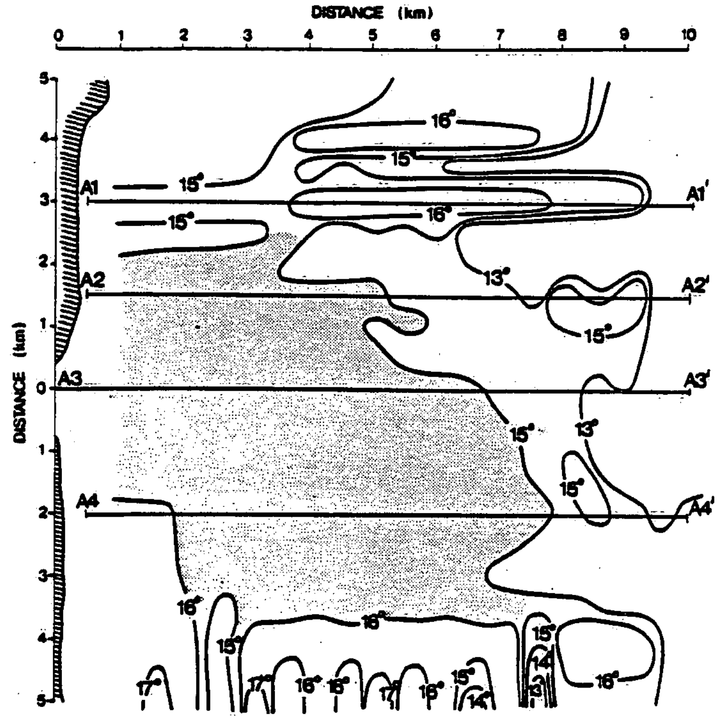

Fig. HORIZONTAL DISTRIBUTION OF AVERAGED TEMPERATURES: NIAGARA RIVER PLUME, H = 1m, 21-25 JUNE, 1982.

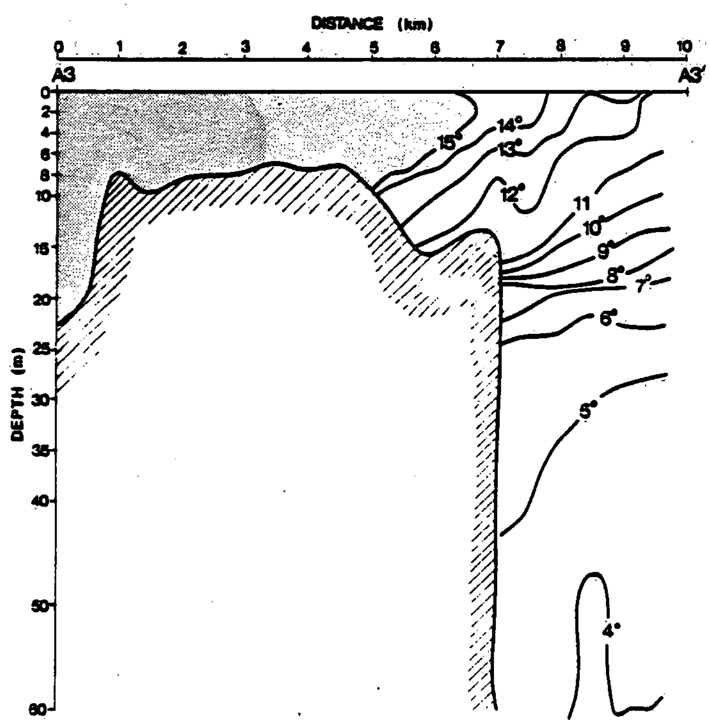

Fig. AVERAGED TEMPERATURES IN THE VERTICAL CROSS-SECTION A3 - A3', 21-25 JUNE, 1982.

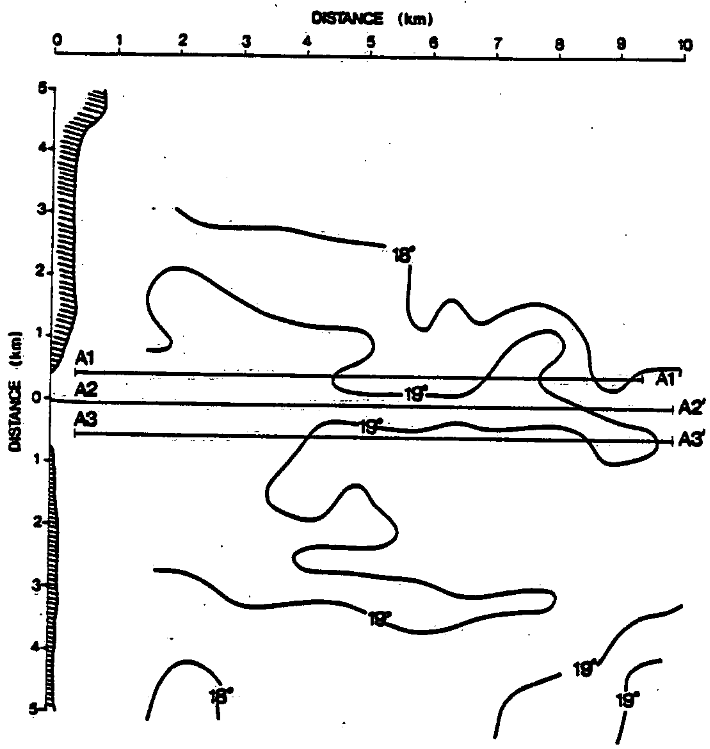

Fig. HORIZONTAL DISTRIBUTION OF AVERAGED TEMPERATURES: NIAGARA RIVER PLUME, (H = 1m) 6-8 JULY, 1982.

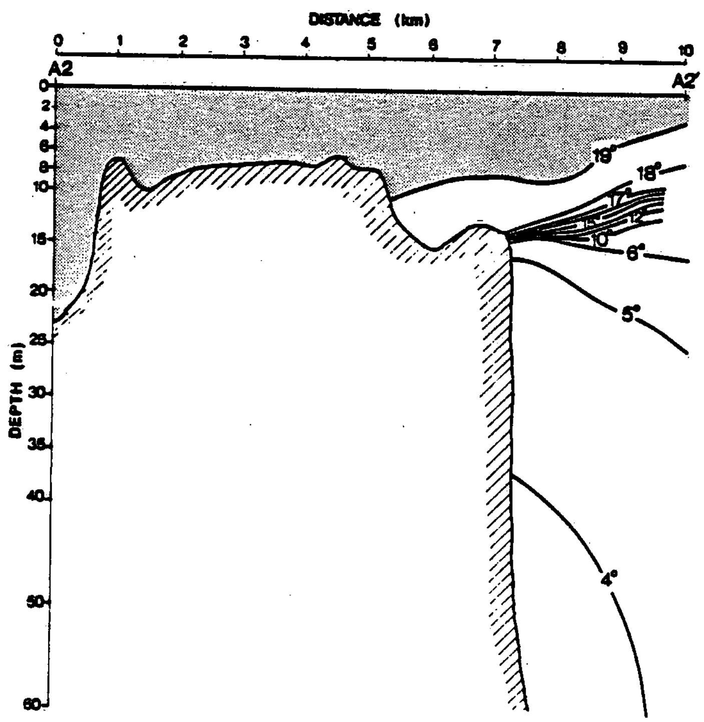

Fig. AVERAGED TEMPERATURES IN THE VERTICAL CROSS - SECTION A2 - A2', 6 - 8 JULY, 1982.

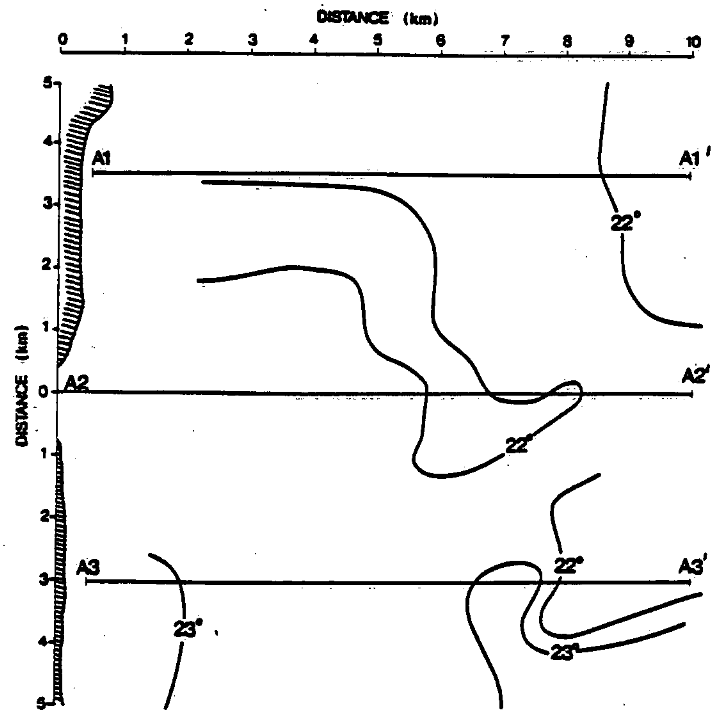

Fig. HORIZONTAL DISTRIBUTION OF AVERAGED TEMPERATURES: NIAGARA RIVER PLUME, (H = 1m) 10-12 AUGUST, 1982.

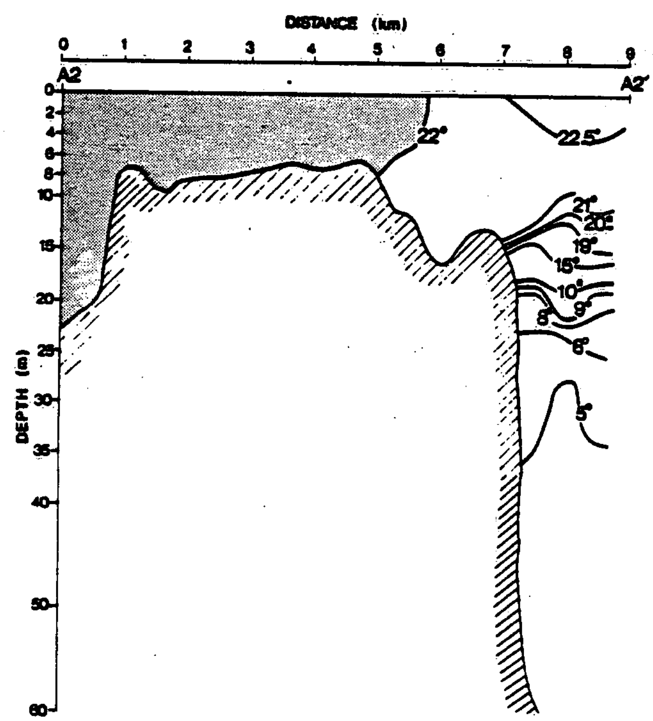

Fig. AVERAGED TEMPERATURES IN THE VERTICAL CROSS-SECTION A2-A2', 10-12 AUGUST, 1982

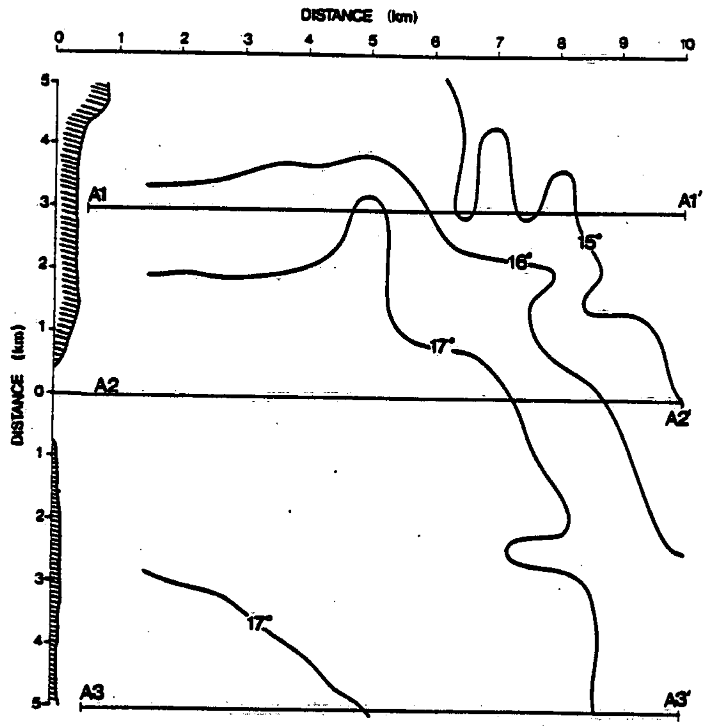

Fig. HORIZONTAL DISTRIBUTION OF AVERAGED TEMPERATURES: NIAGARA RIVER PLUME, UPPER LAYER (10m of thickness), 5-7 OCTOBER, 1982.

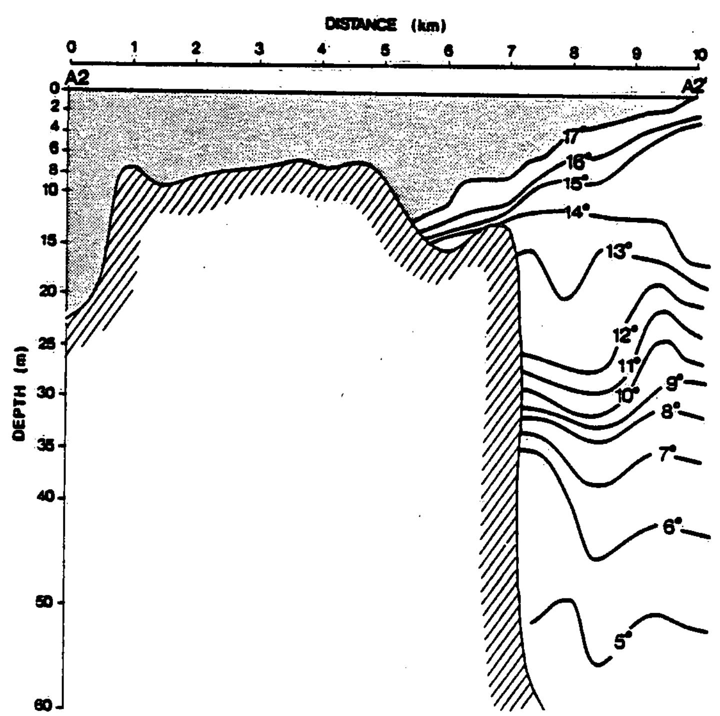

Fig. AVERAGE TEMPERATURES IN THE VERTICAL CROSS-SECTION A2-A2' 5-7 OCTOBER 1982.

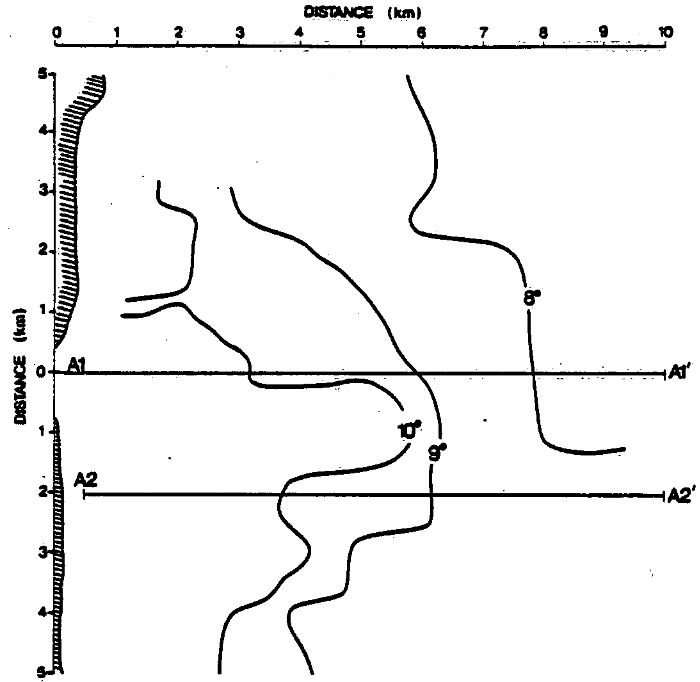

Fig. HORIZONTAL DISTRIBUTION OF AVERAGED TEMPERATURES: NIAGARA RIVER PLUME, UPPER LAYER, 8-10 NOVEMBER, 1982.

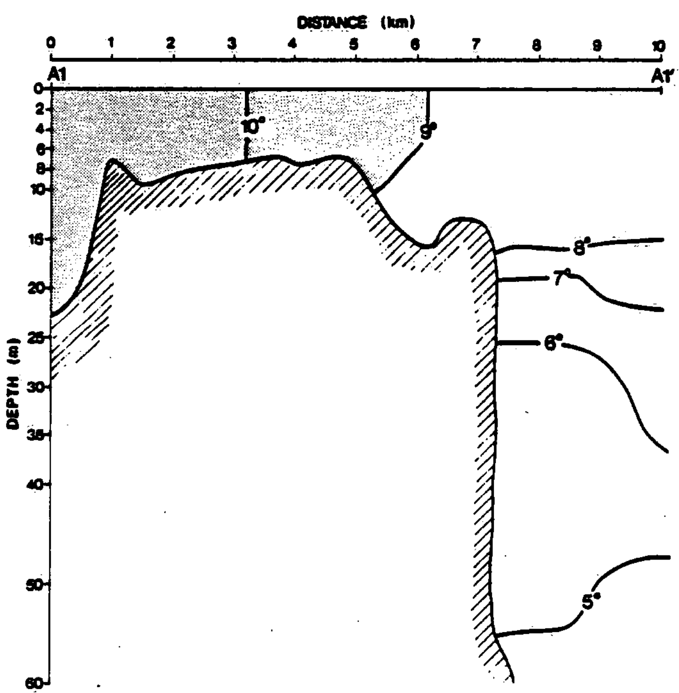

Fig. AVERAGED TEMPERATURES IN THE VERTICAL CROSS-SECTION A1-A1', 8-10, NOVEMBER 1982.

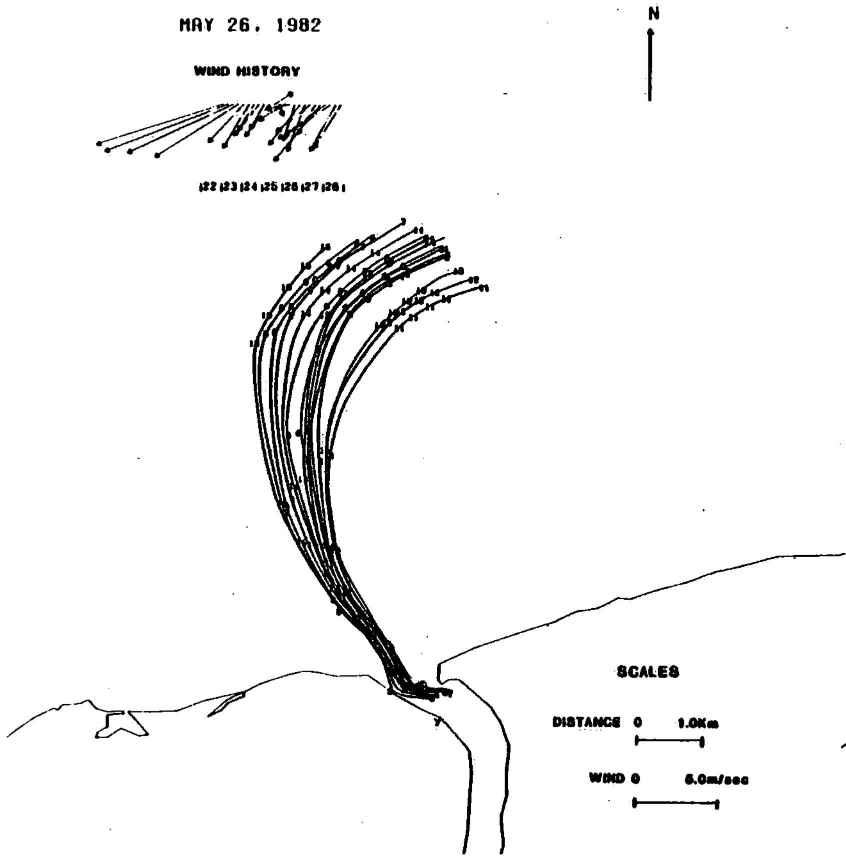

LAGRANGIAN TRAJECTORY

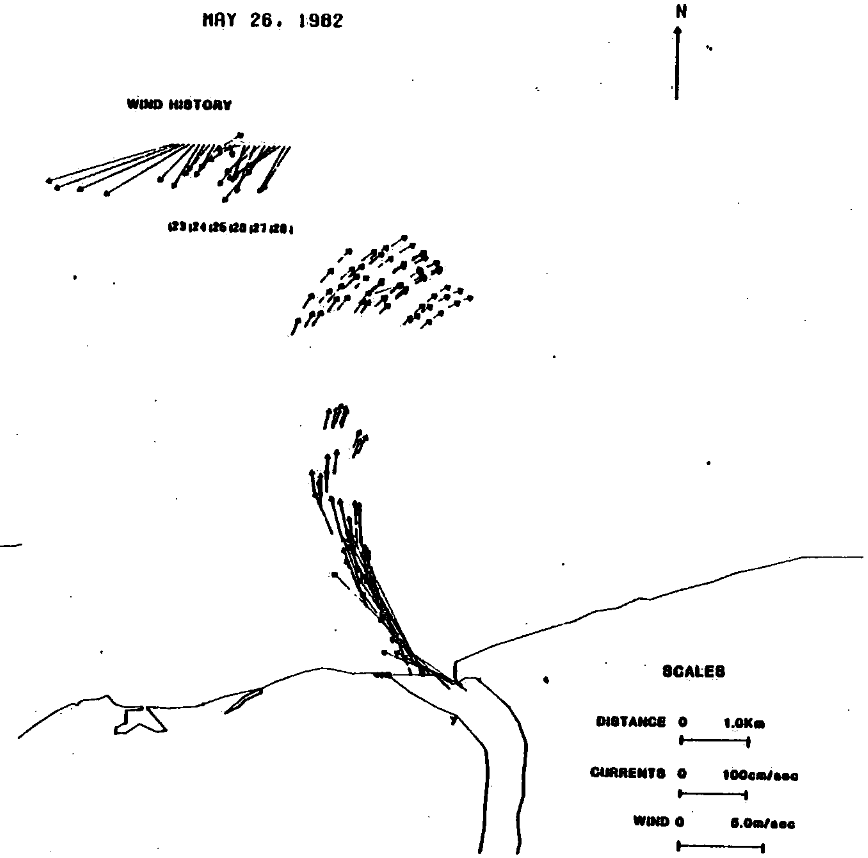

HORIZONTAL VELOCITY FIELD

4.7

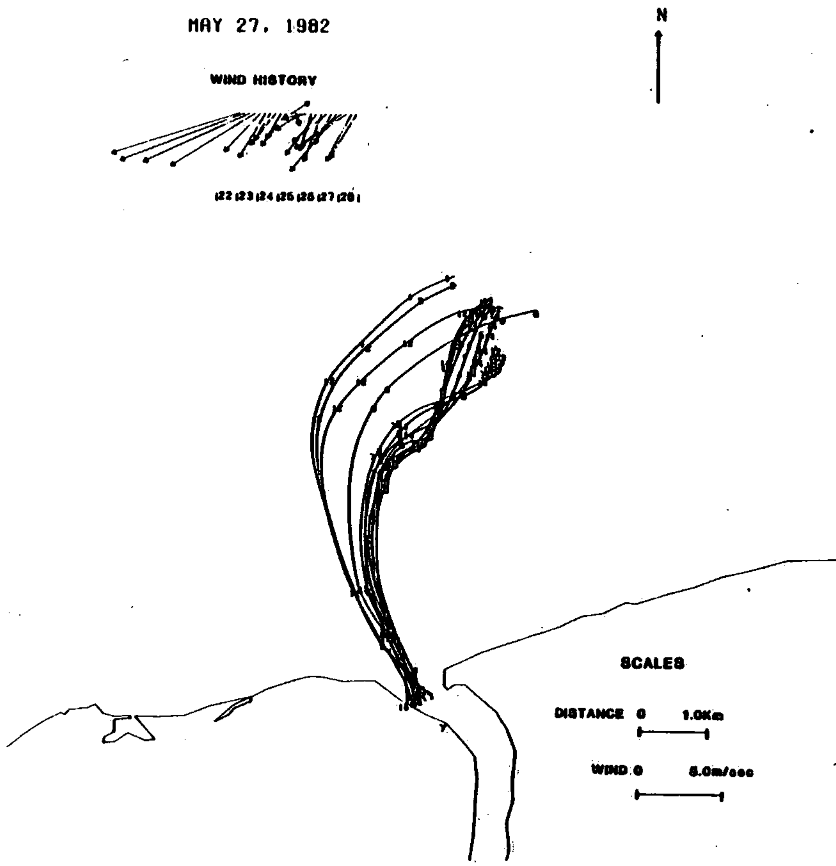

LAGRANGIAN TRAJECTORY

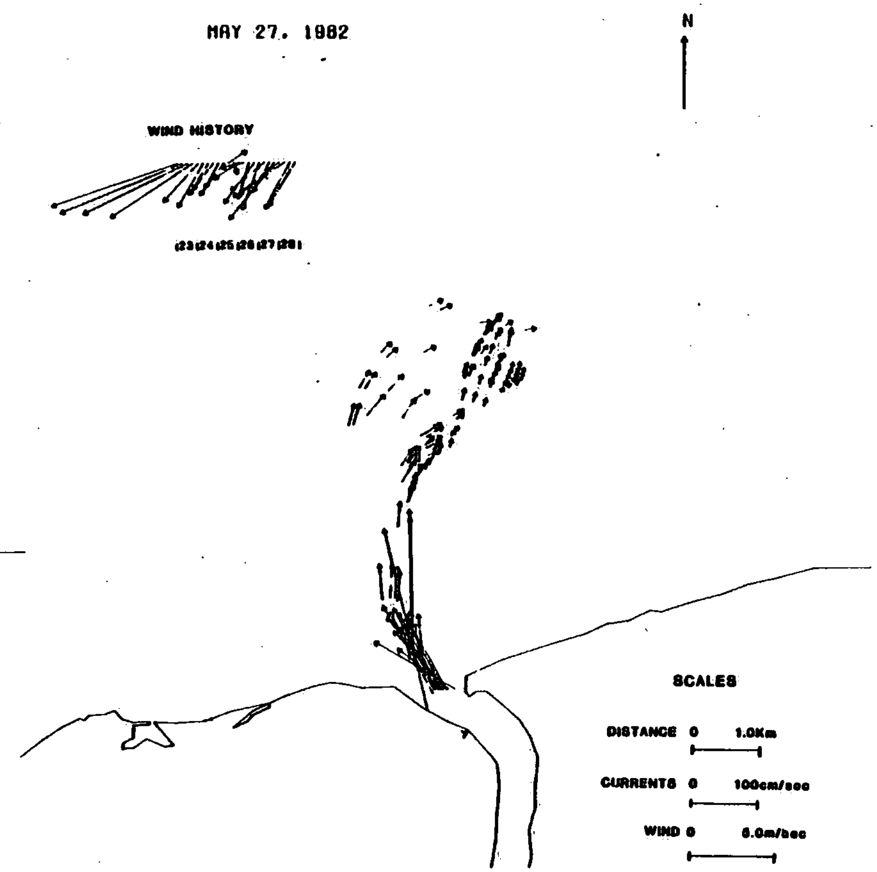

HORIZONTAL VELOCITY FIELD

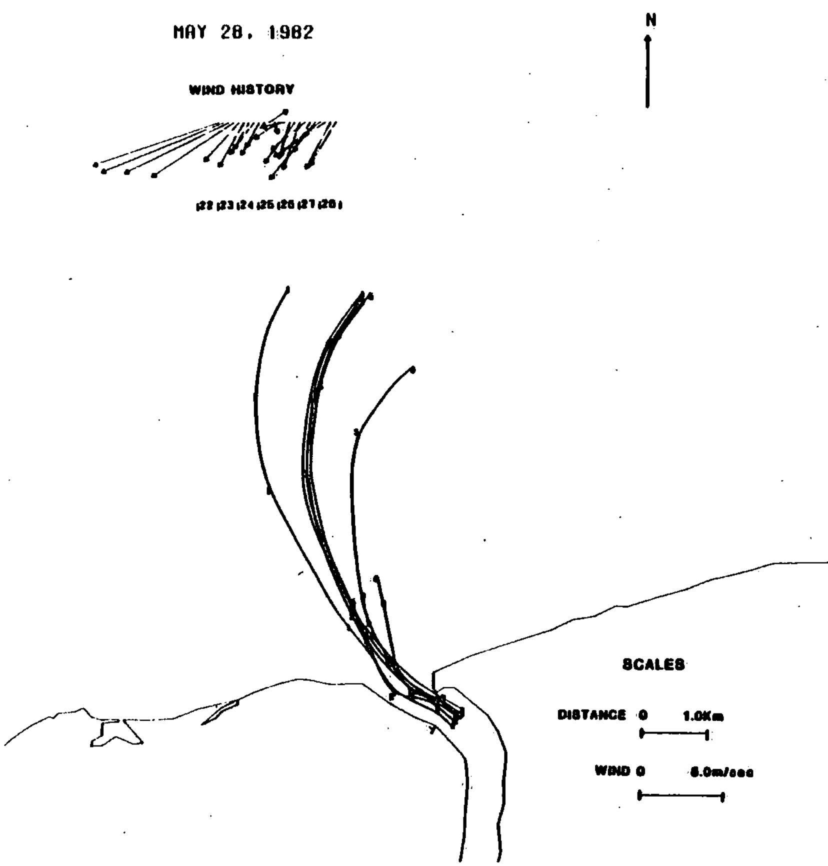

LAGRANGIAN TRAJECTORY

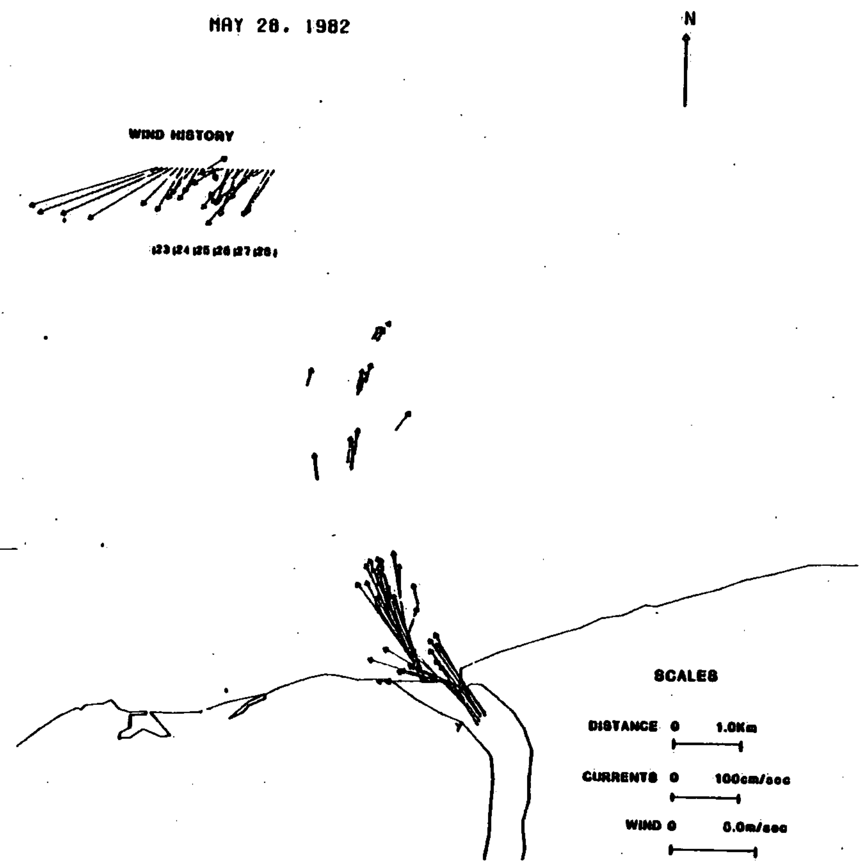

HORIZONTAL VELOCITY FIELD

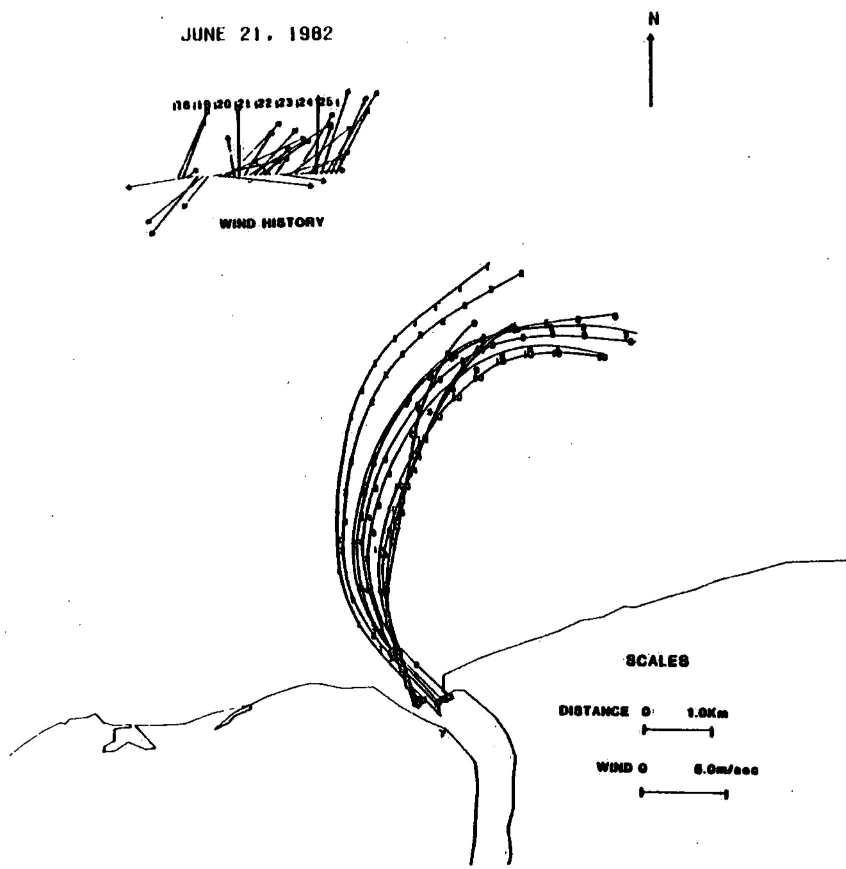

LAGRANGIAN TRAJECTORY

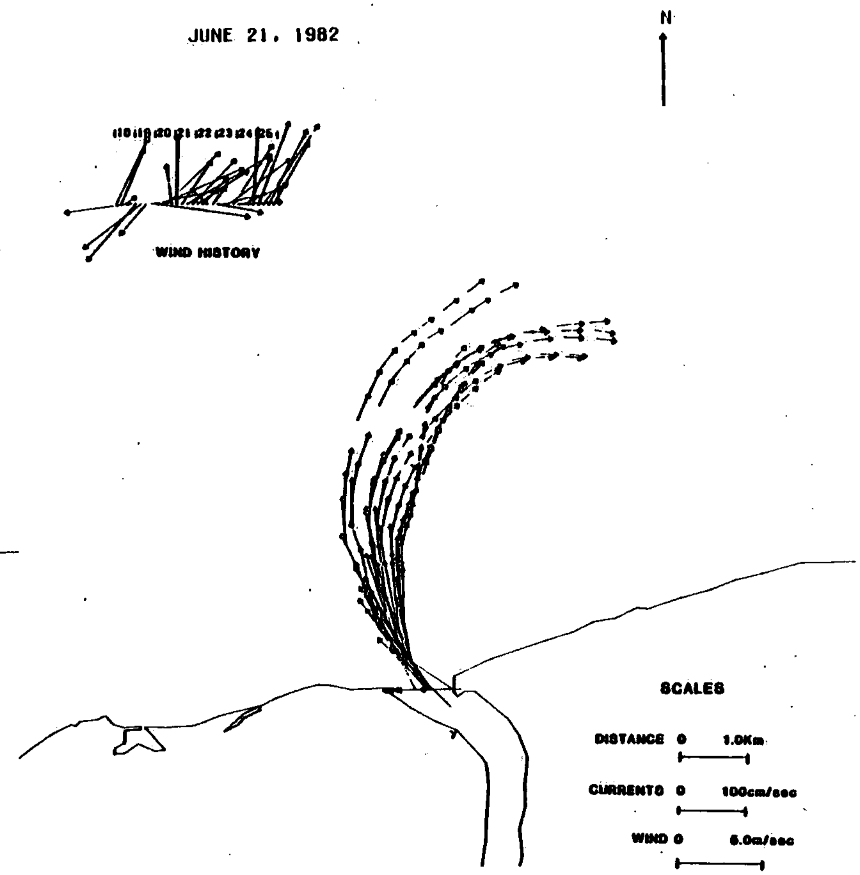

HORIZONTAL VELOCITY FIELD

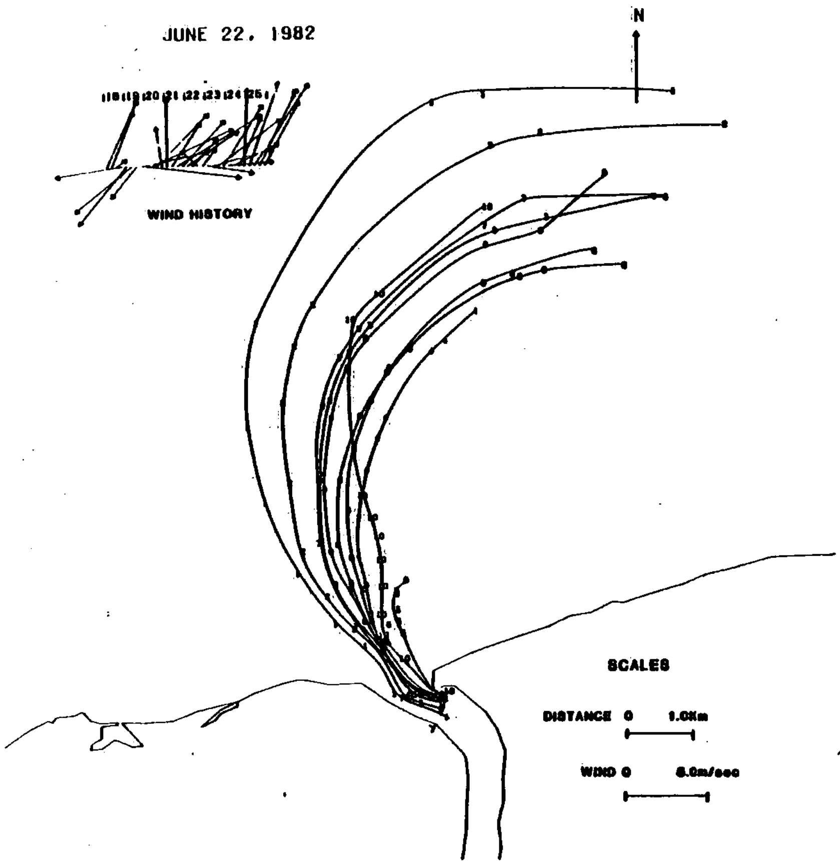

LAGRANGIAN TRAJECTORY

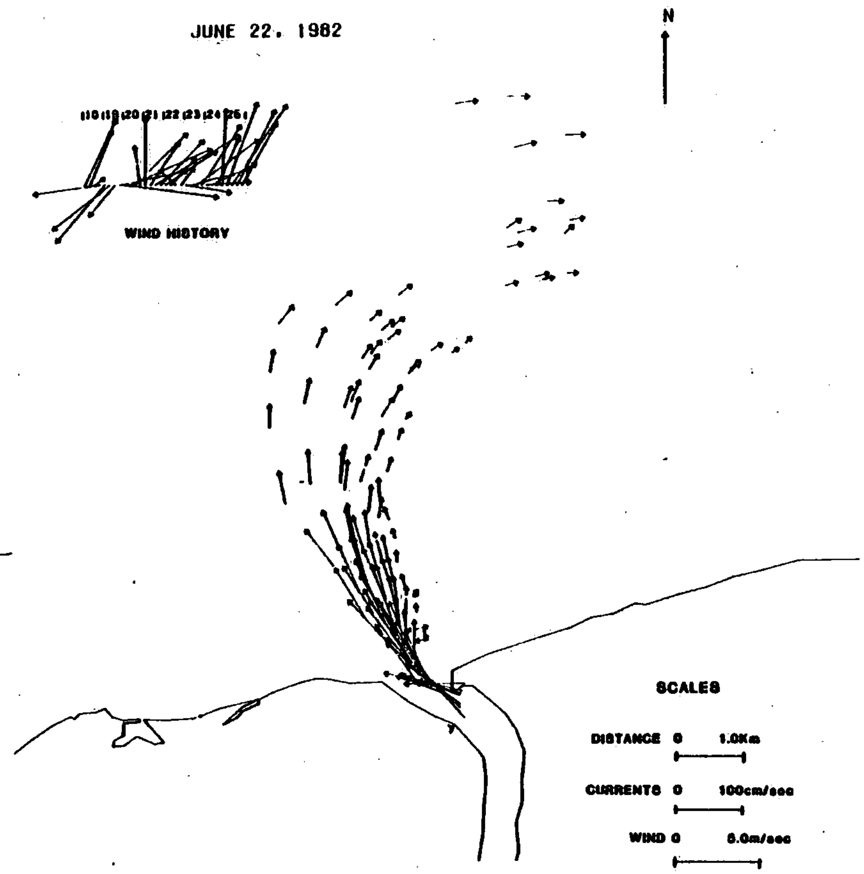

HORIZONTAL VELOCITY FIELD

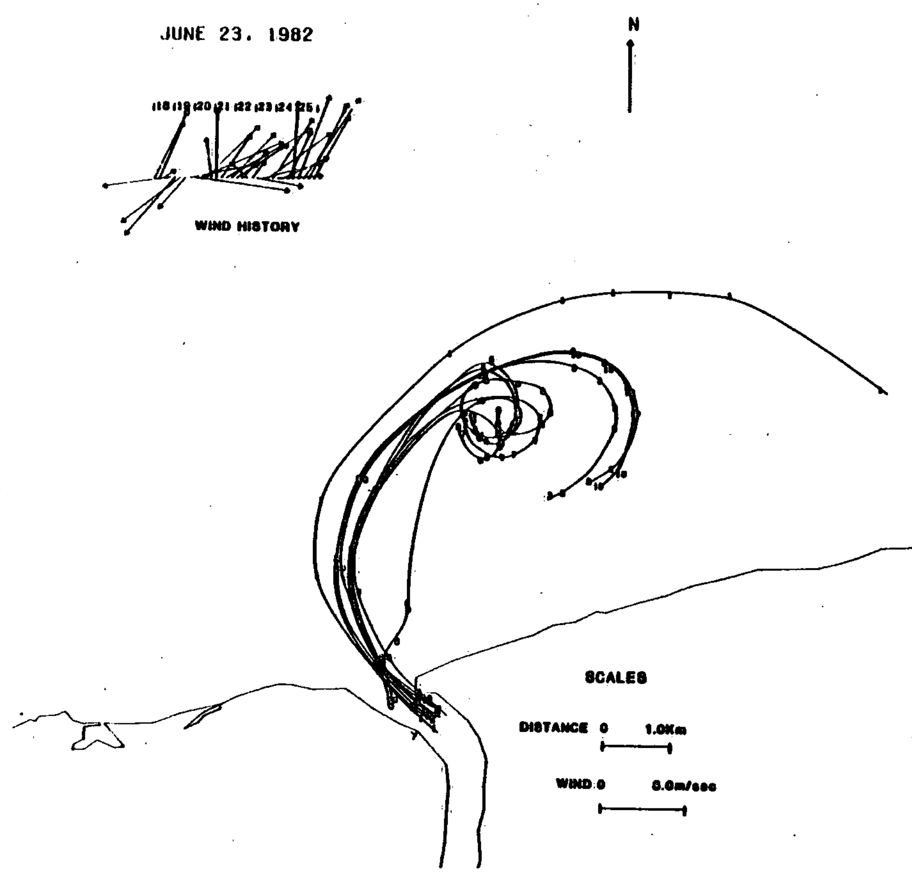

LAGRANGIAN TRAJECTORY

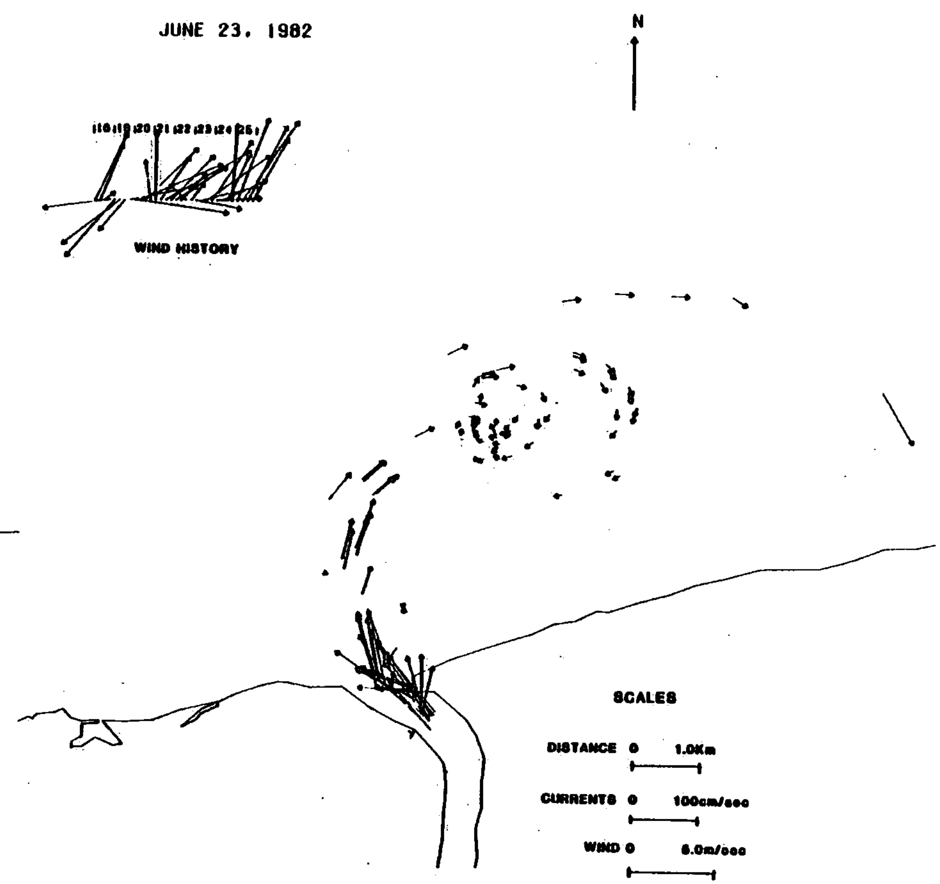

HORIZONTAL VELOCITY FIELD

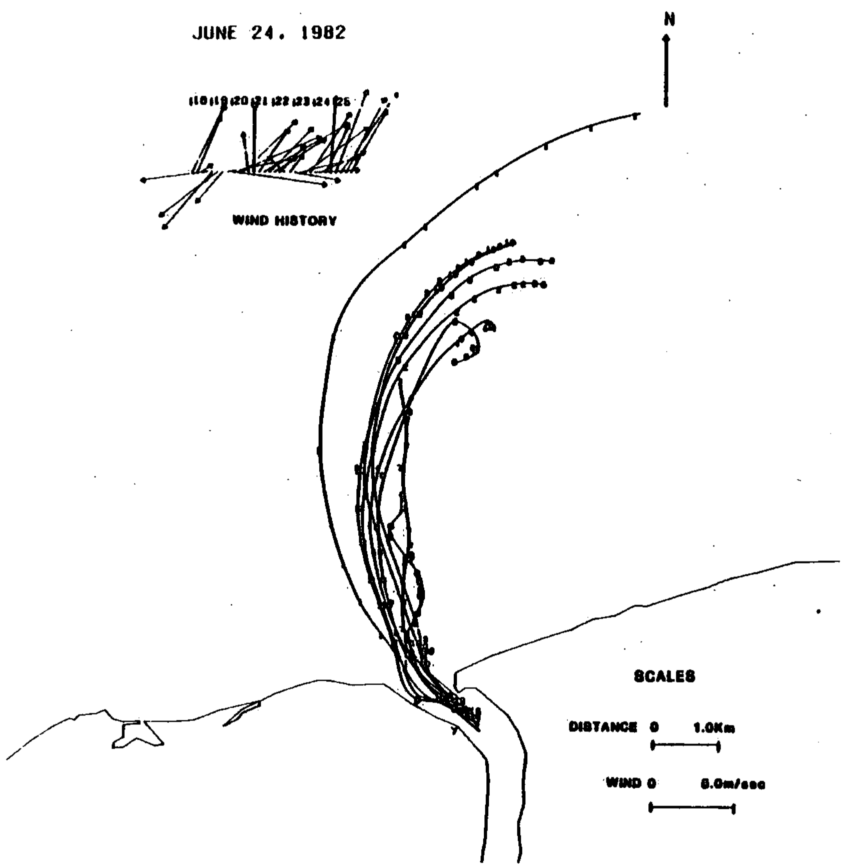

LAGRANGIAN TRAJECTORY

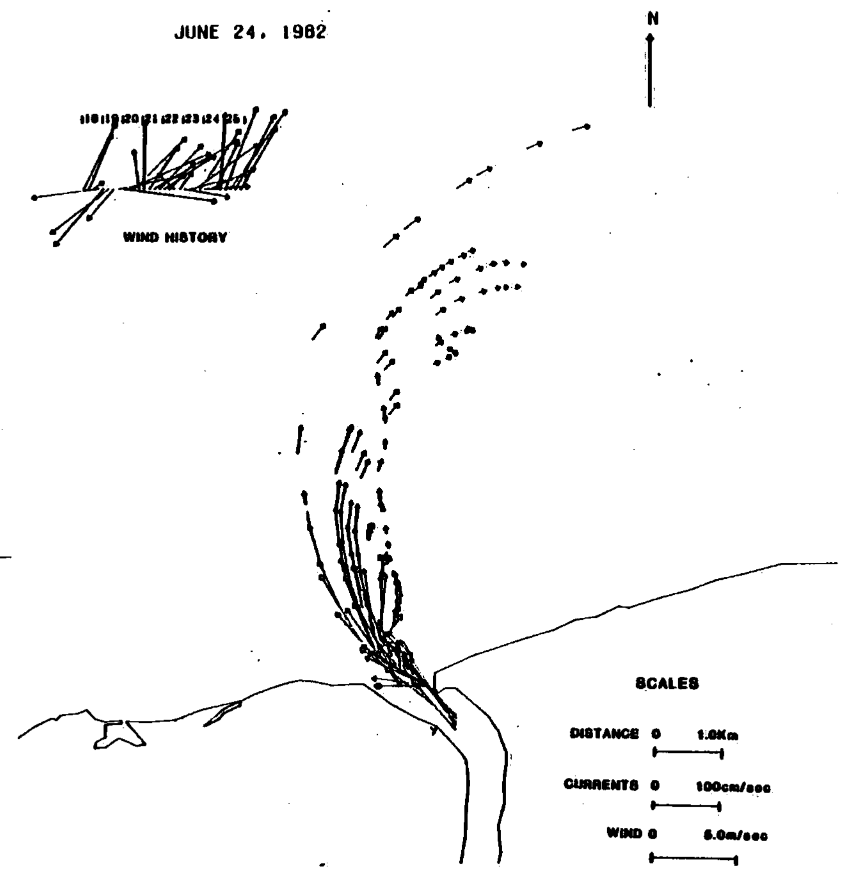

HORIZONTAL VELOCITY FIELD

4.13

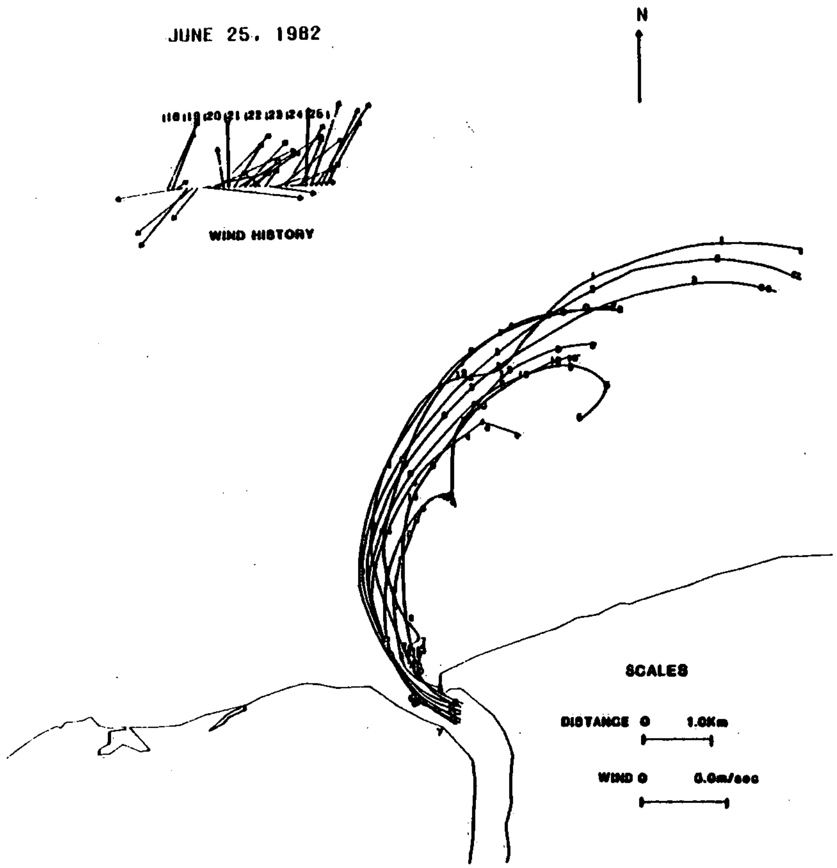

LAGRANGIAN TRAJECTORY

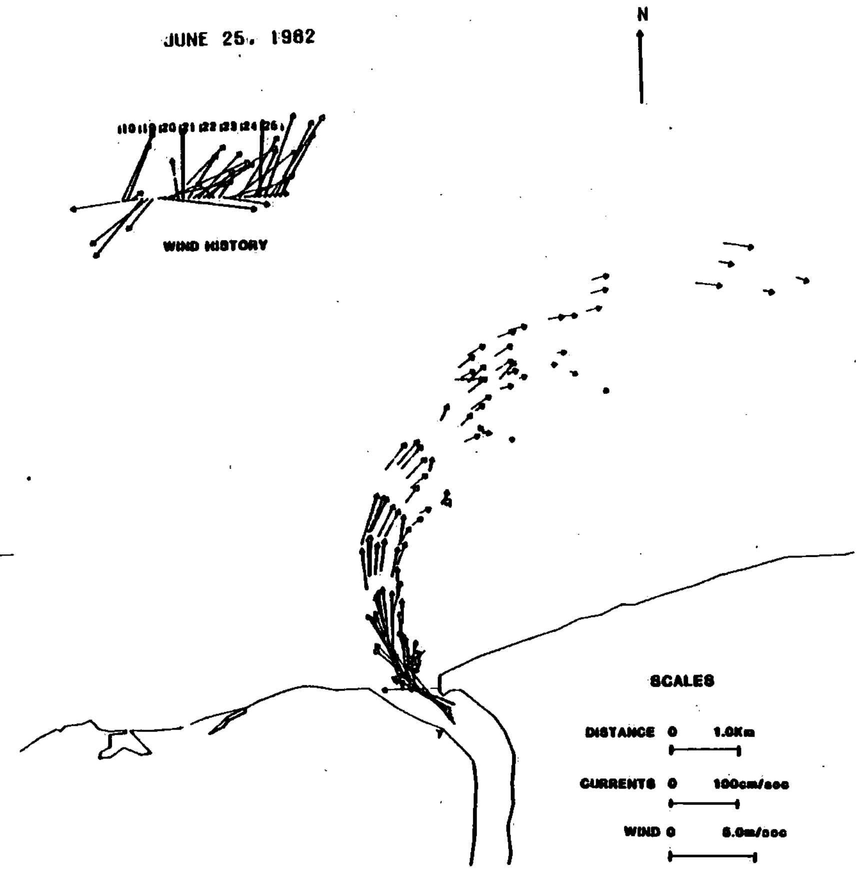

HORIZONTAL VELOCITY FIELD

4.14

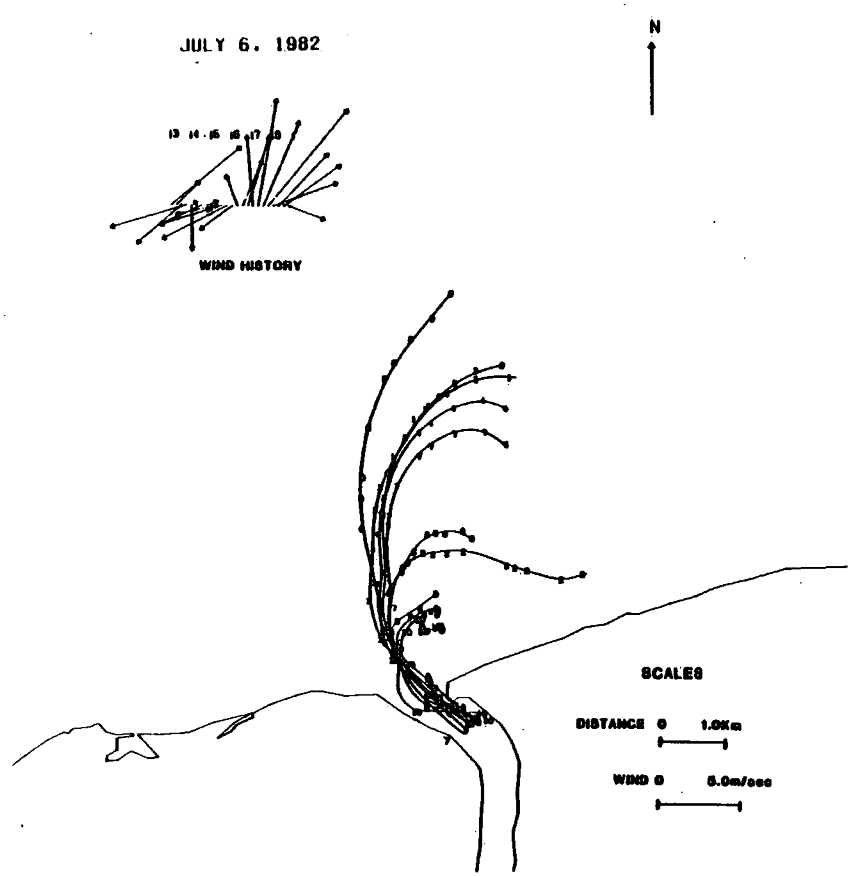

LAGRANGIAN TRAJECTORY

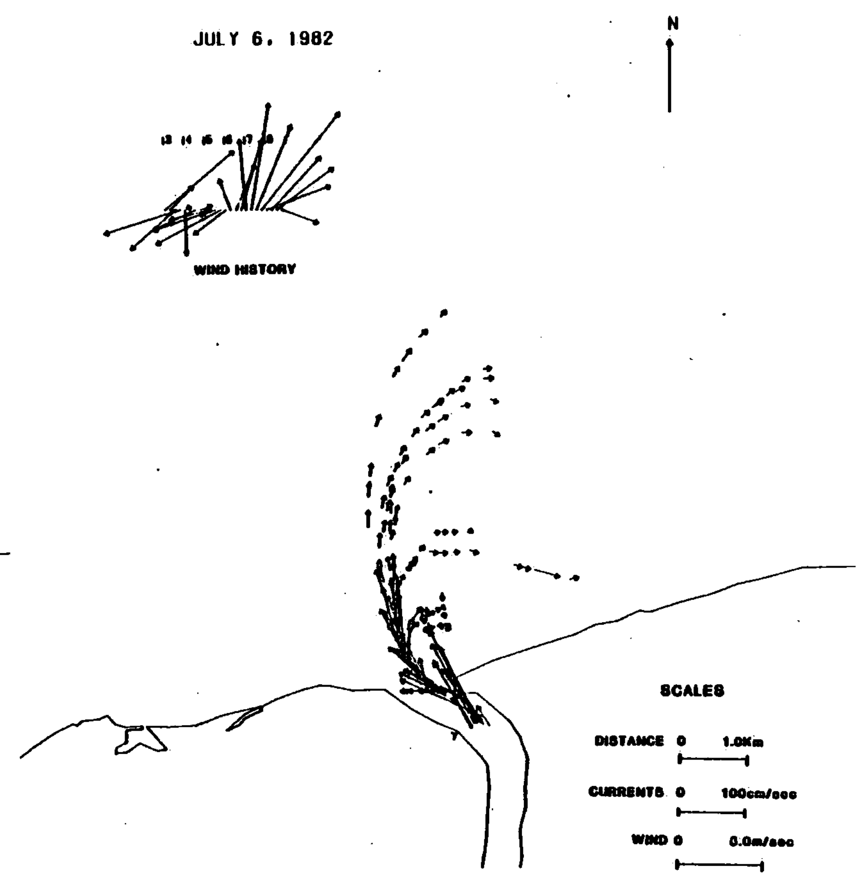

HORIZONTAL VELOCITY FIELD

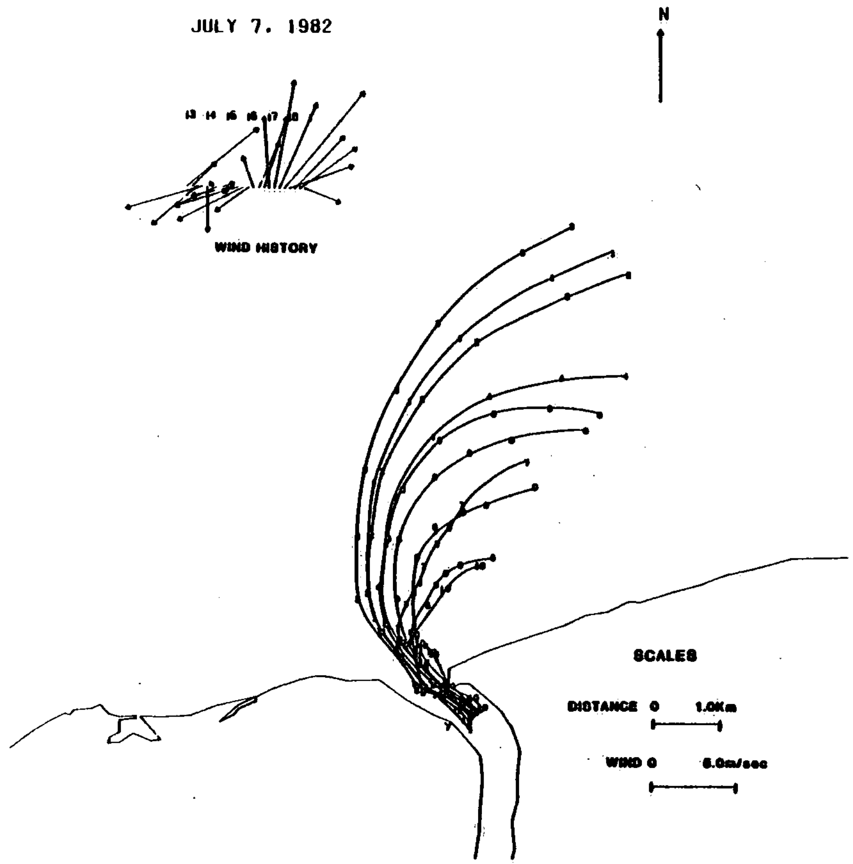

LAGRANGIAN TRAJECTORY

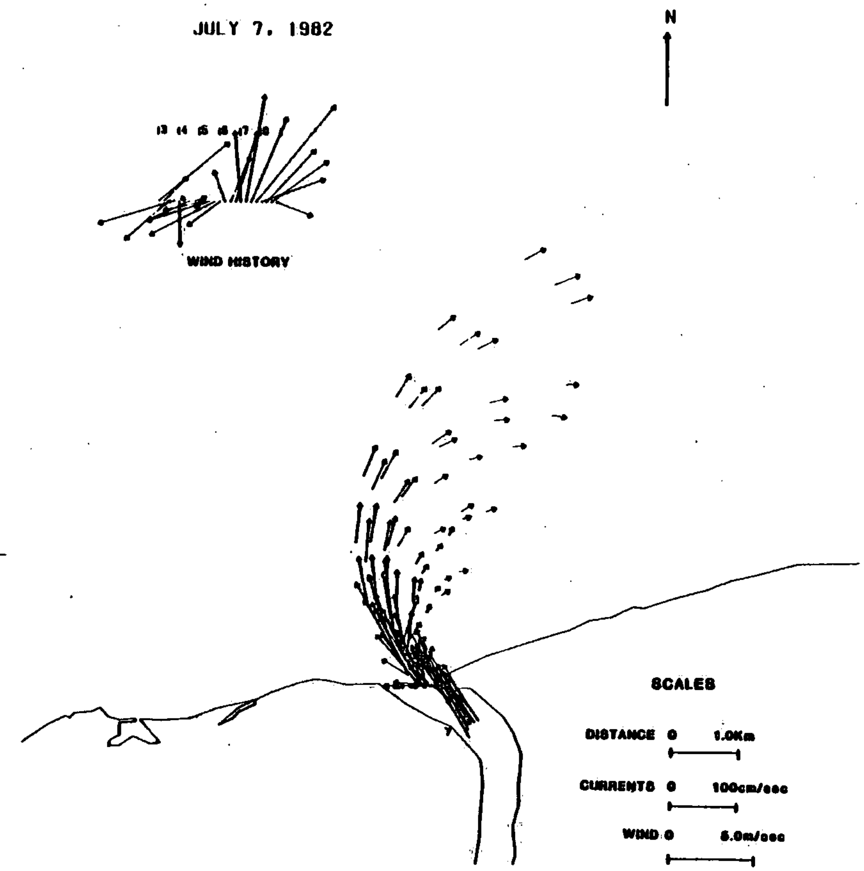

HORIZONTAL VELOCITY FIELD

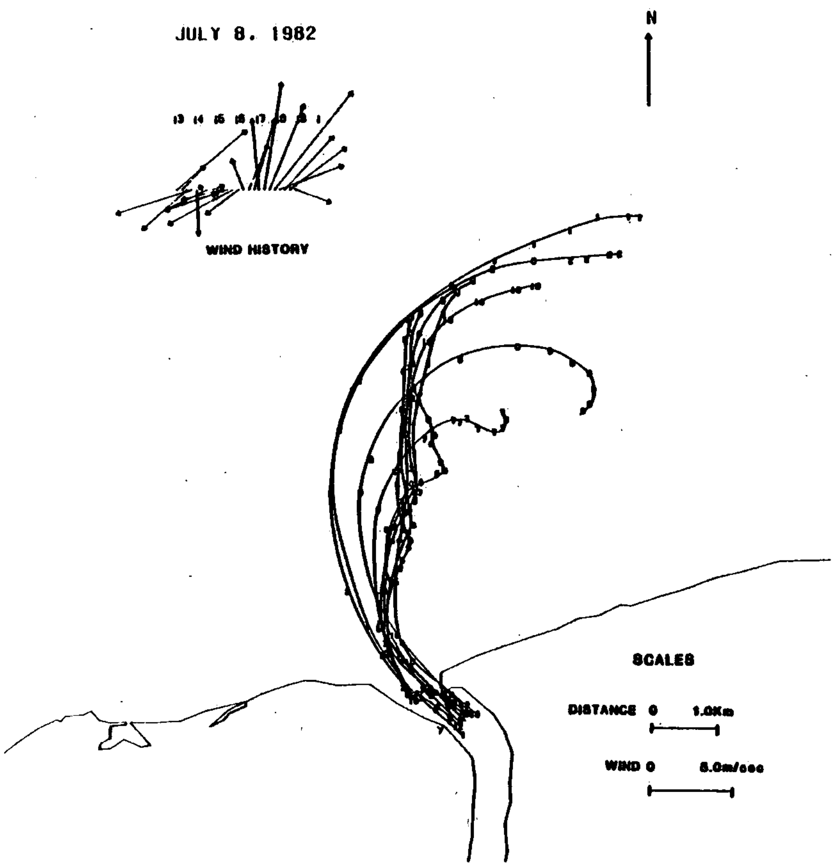

LAGRANGIAN TRAJECTORY

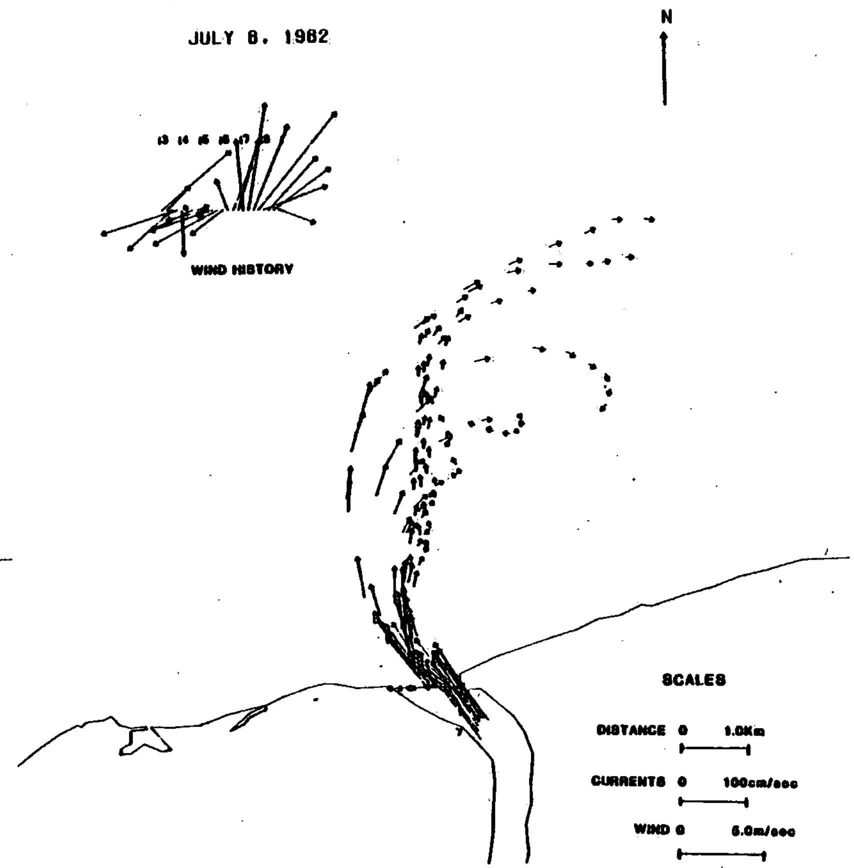

HORIZONTAL VELOCITY FIELD

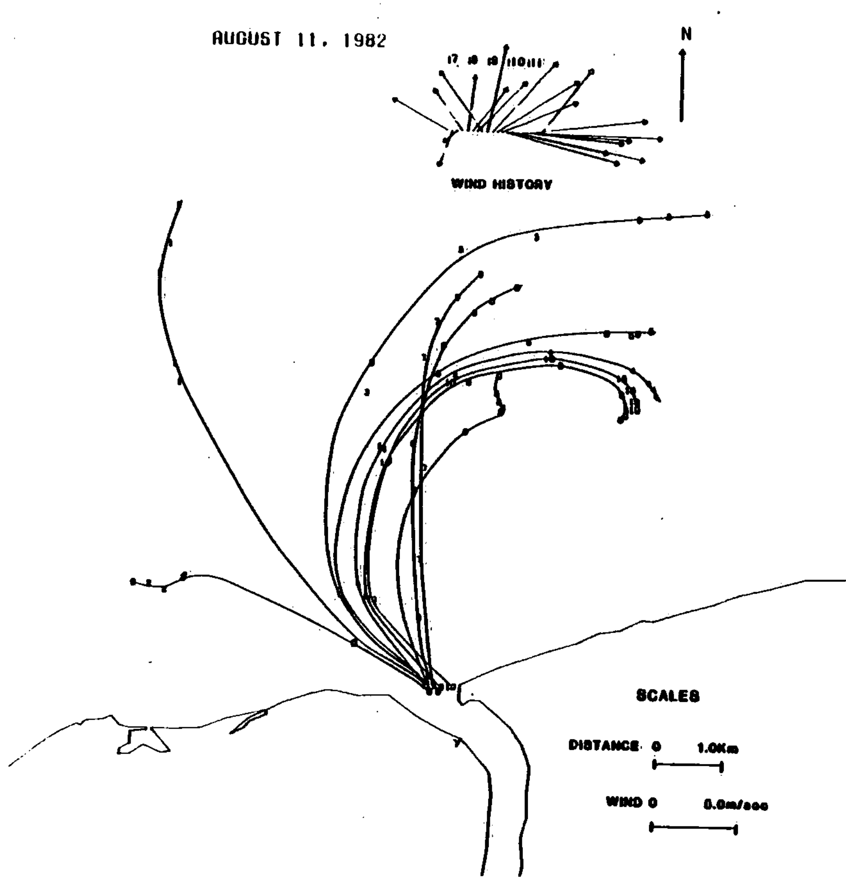

LAGRANGIAN TRAJECTORY

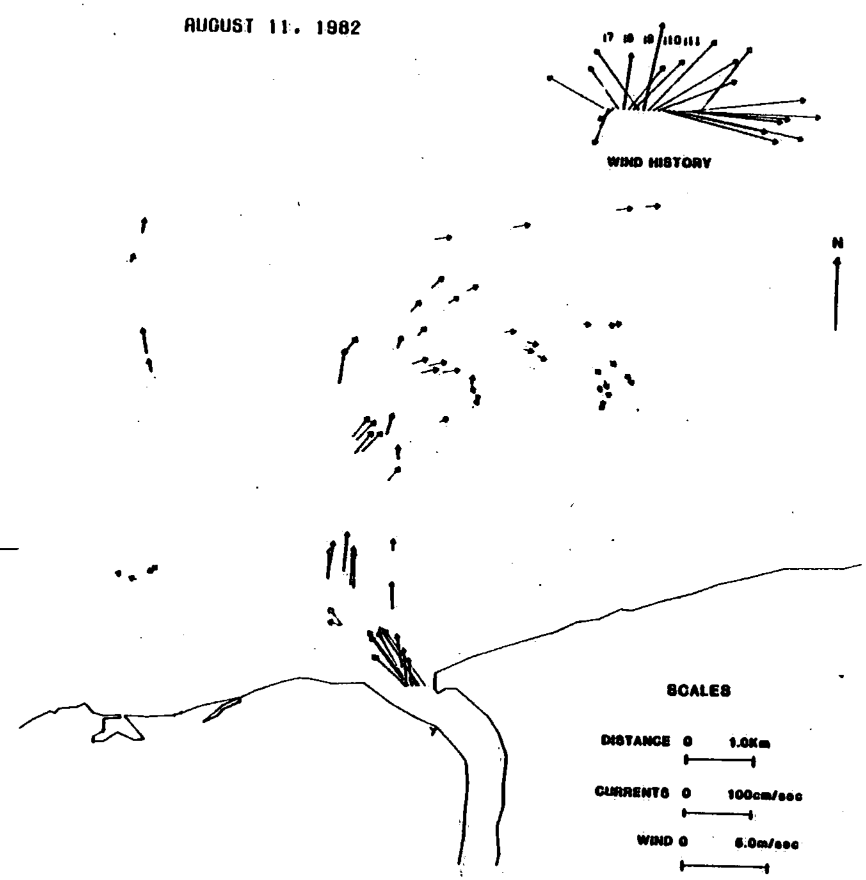

HORIZONTAL VELOCITY FIELD

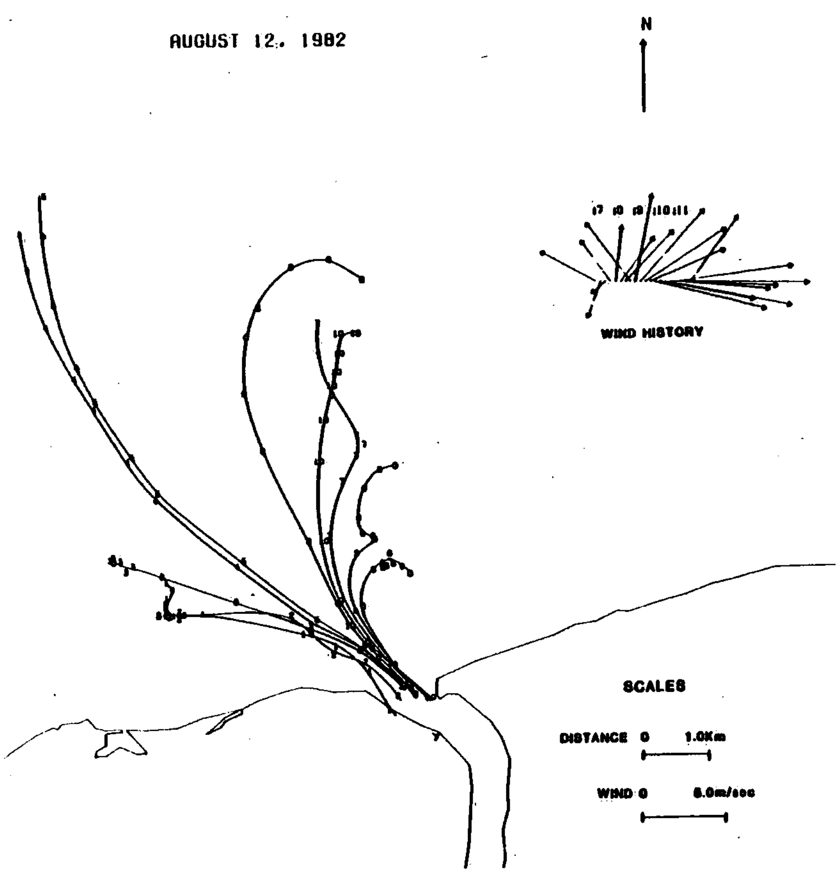

LAGRANGIAN TRAJECTORY

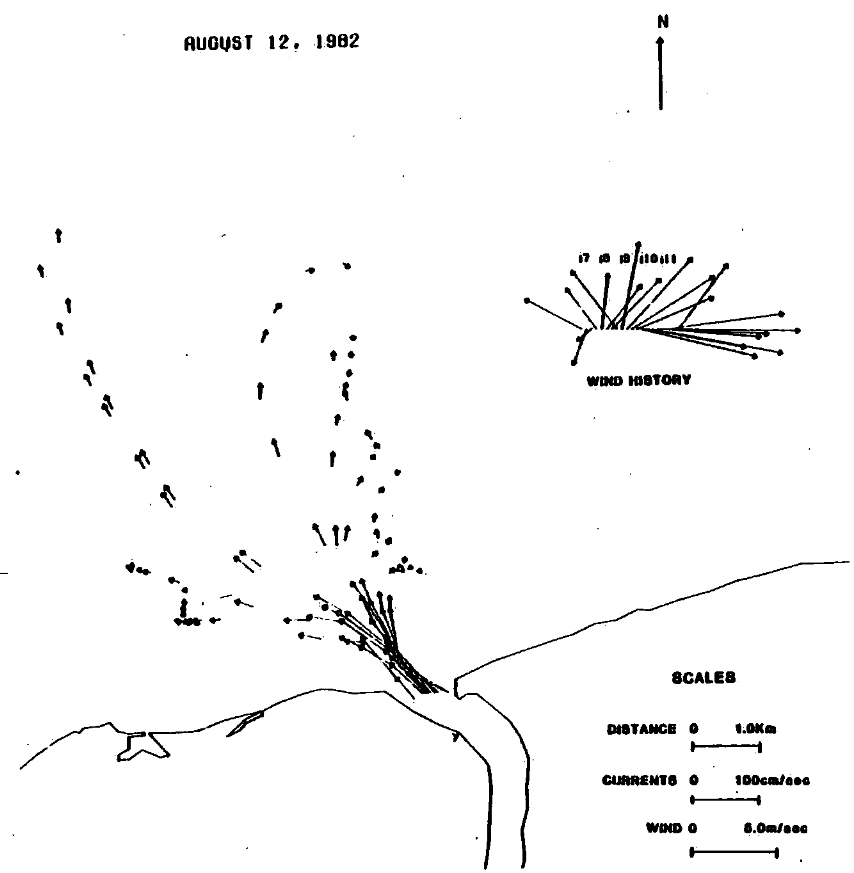

HORIZONTAL VELOCITY FIELD

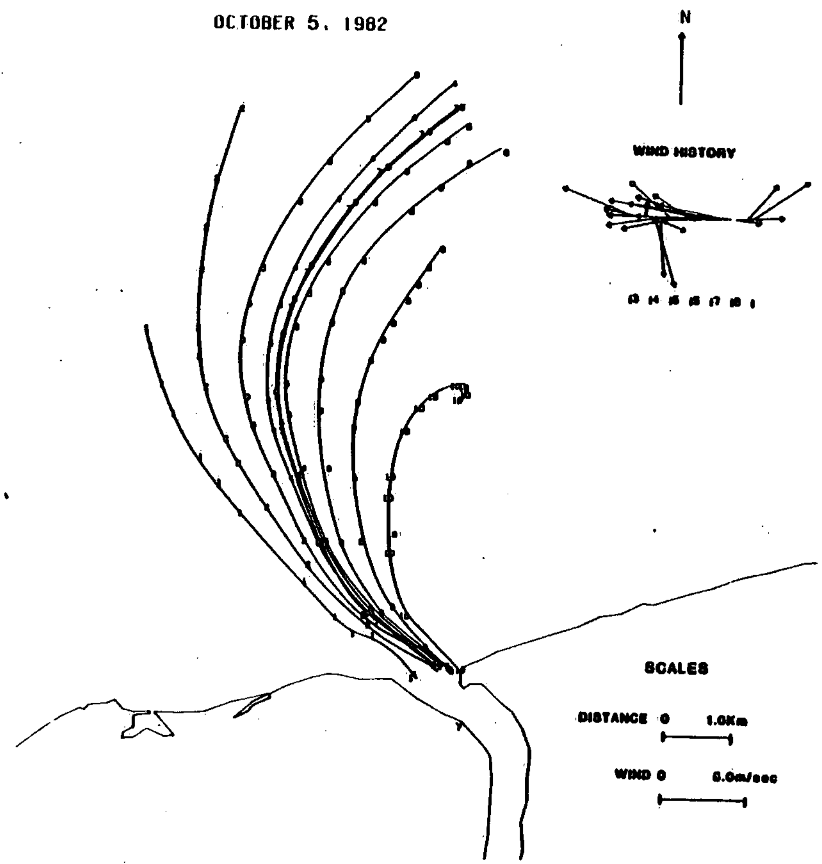

LAGRANGIAN TRAJECTORY

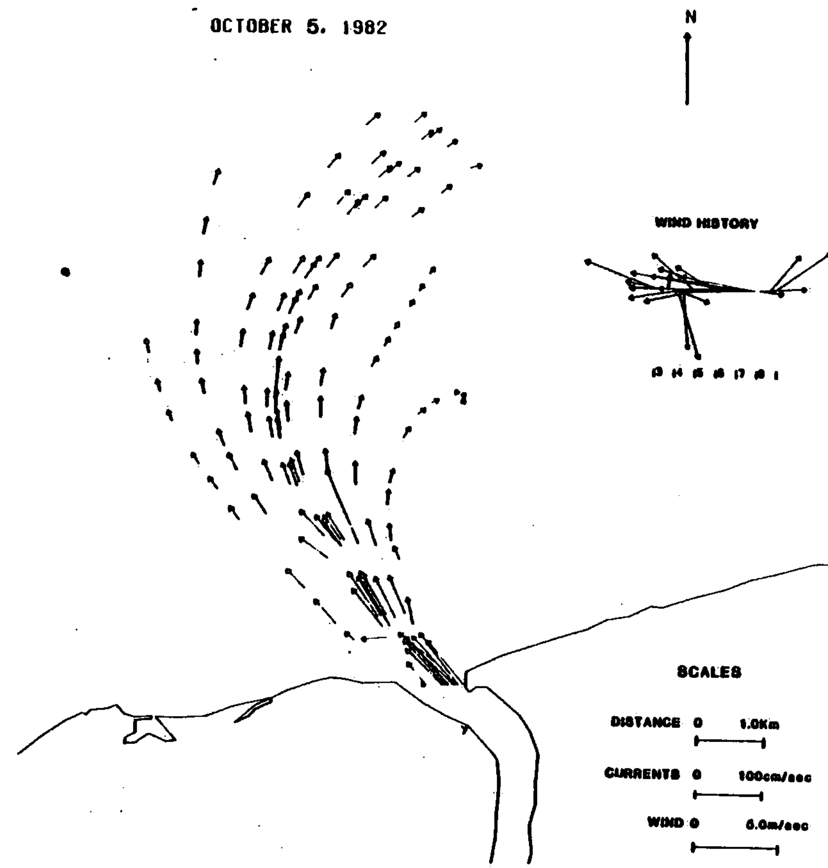

HORIZONTAL VELOCITY FIELD

4.20

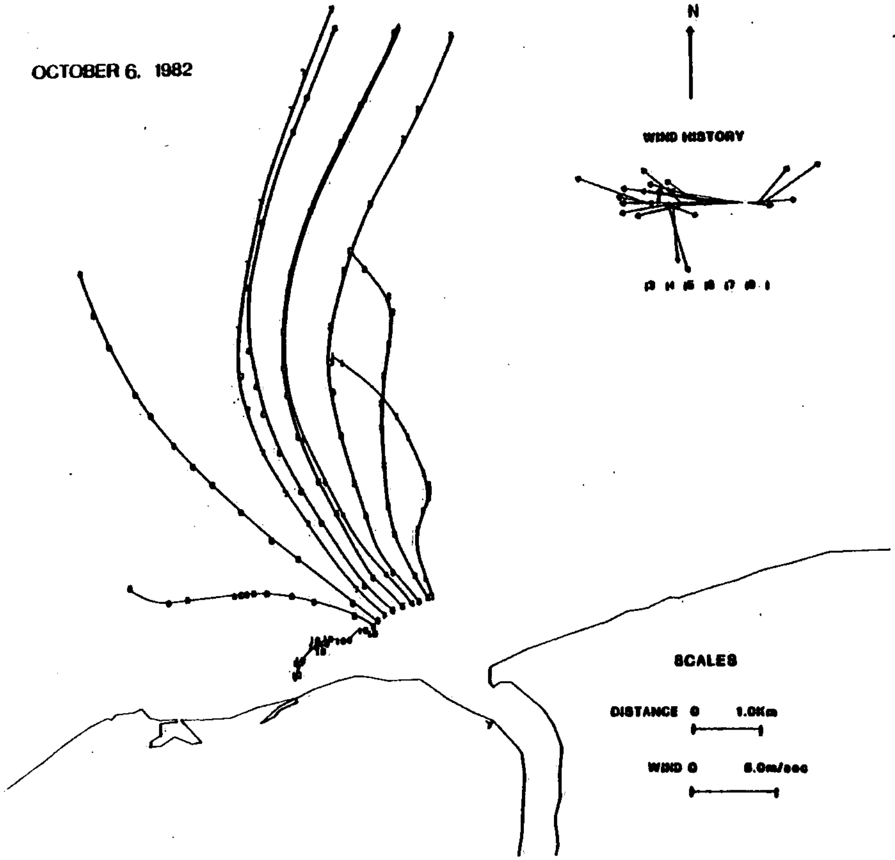

LAGRANGIAN TRAJECTORY

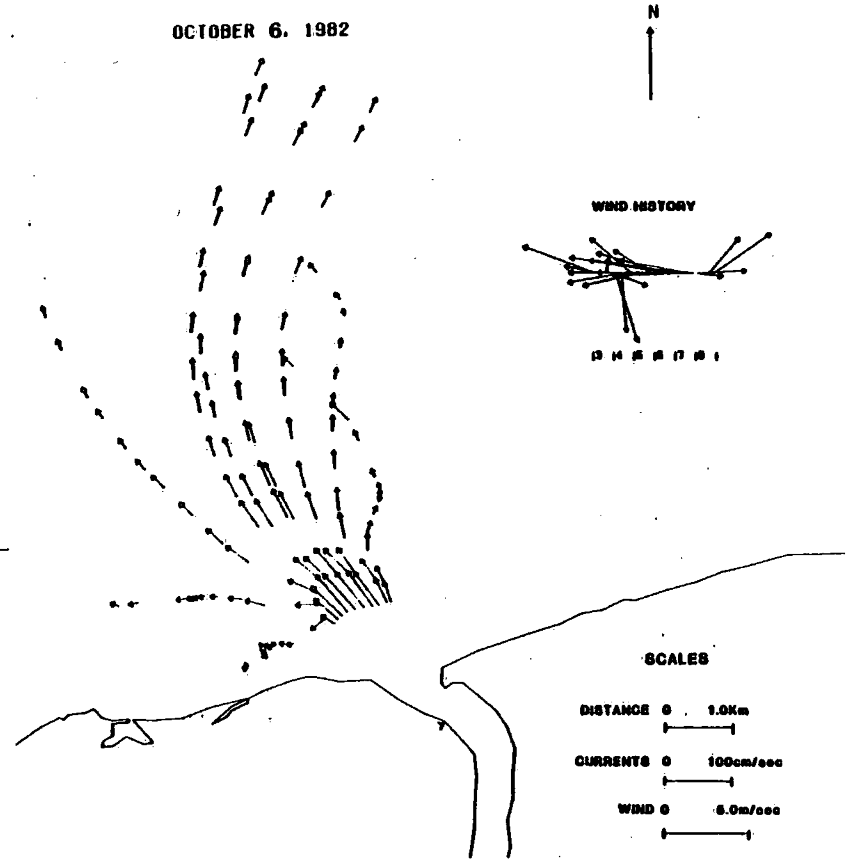

HORIZONTAL VELOCITY FIELD

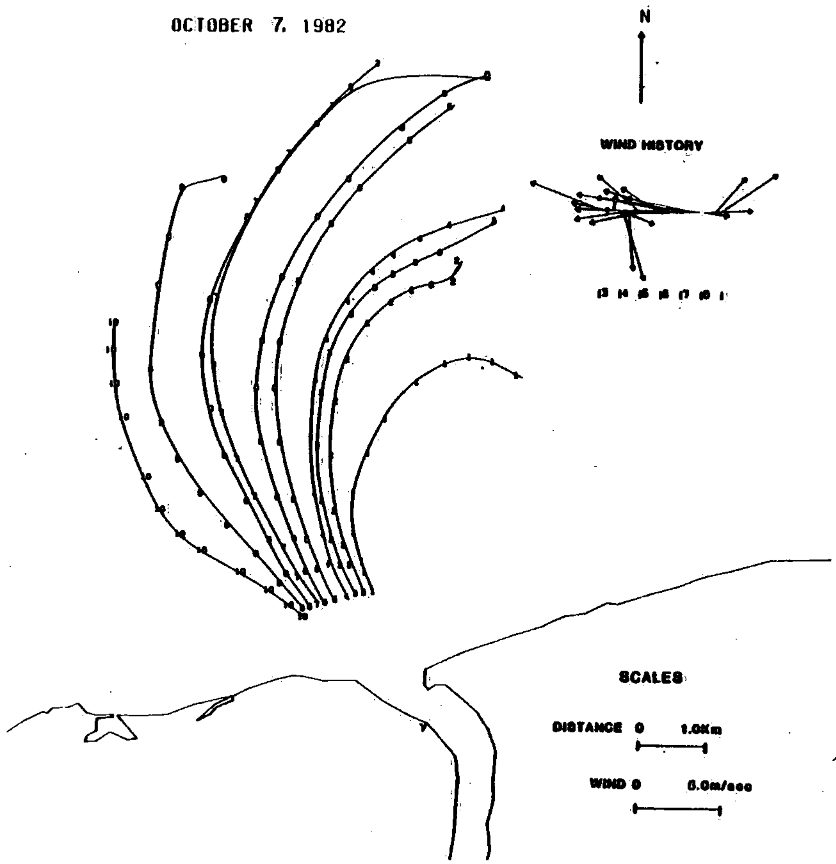

LAGRANGIAN TRAJECTORY

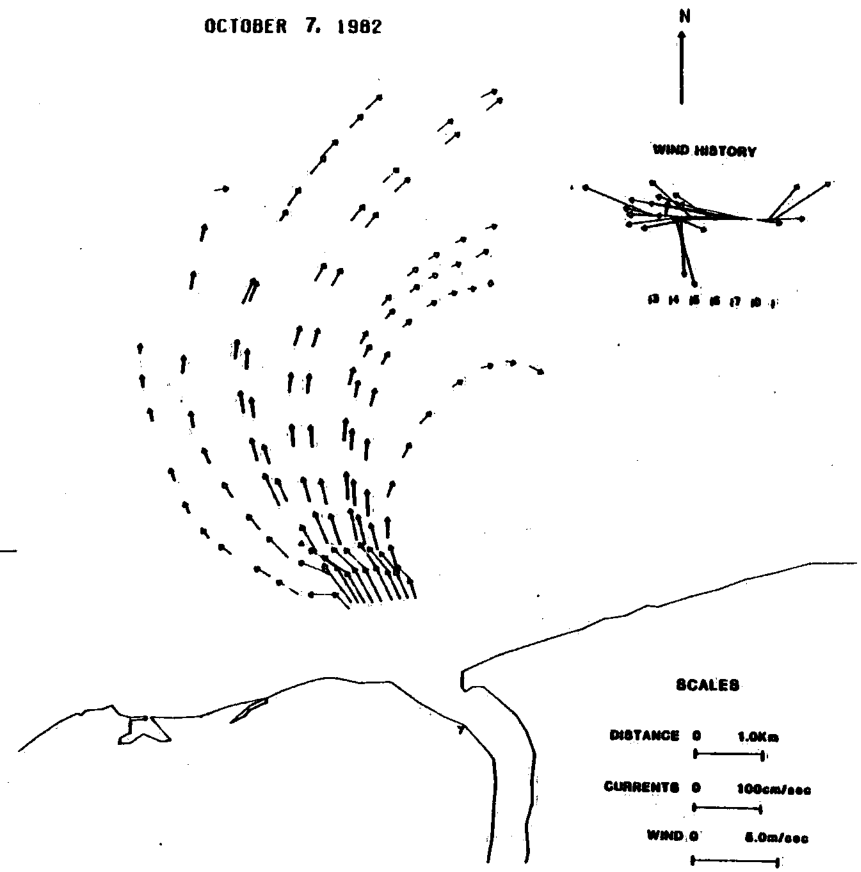

HORIZONTAL VELOCITY FIELD

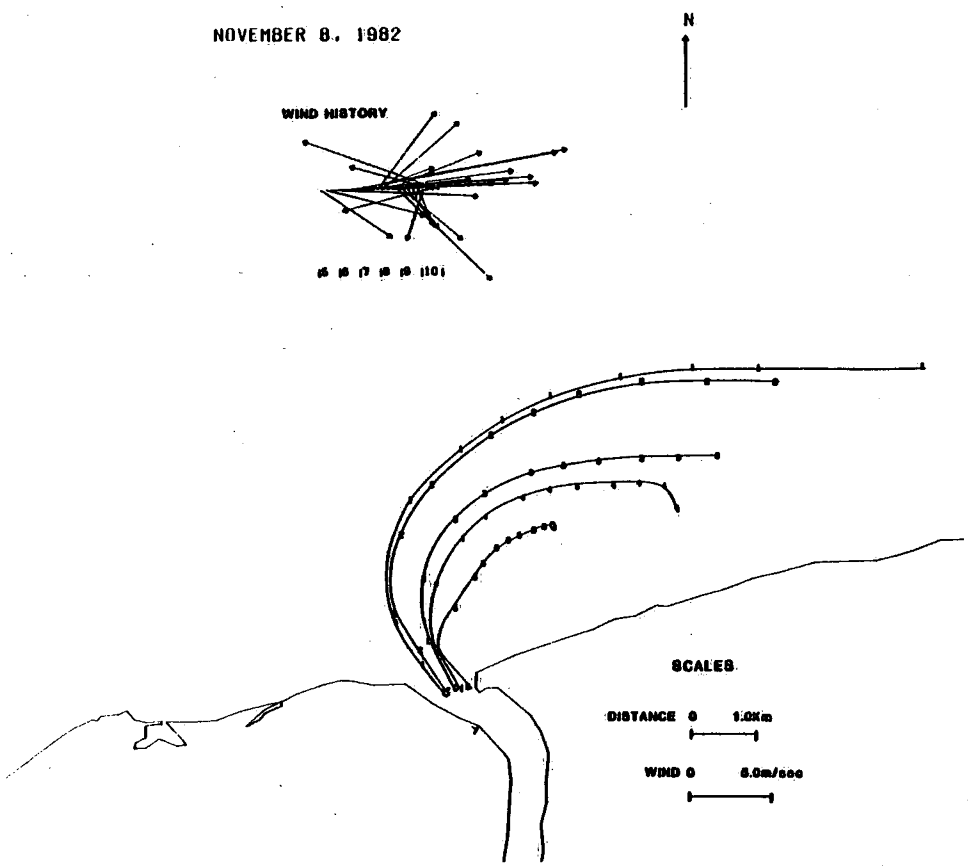

LAGRANGIAN TRAJECTORY

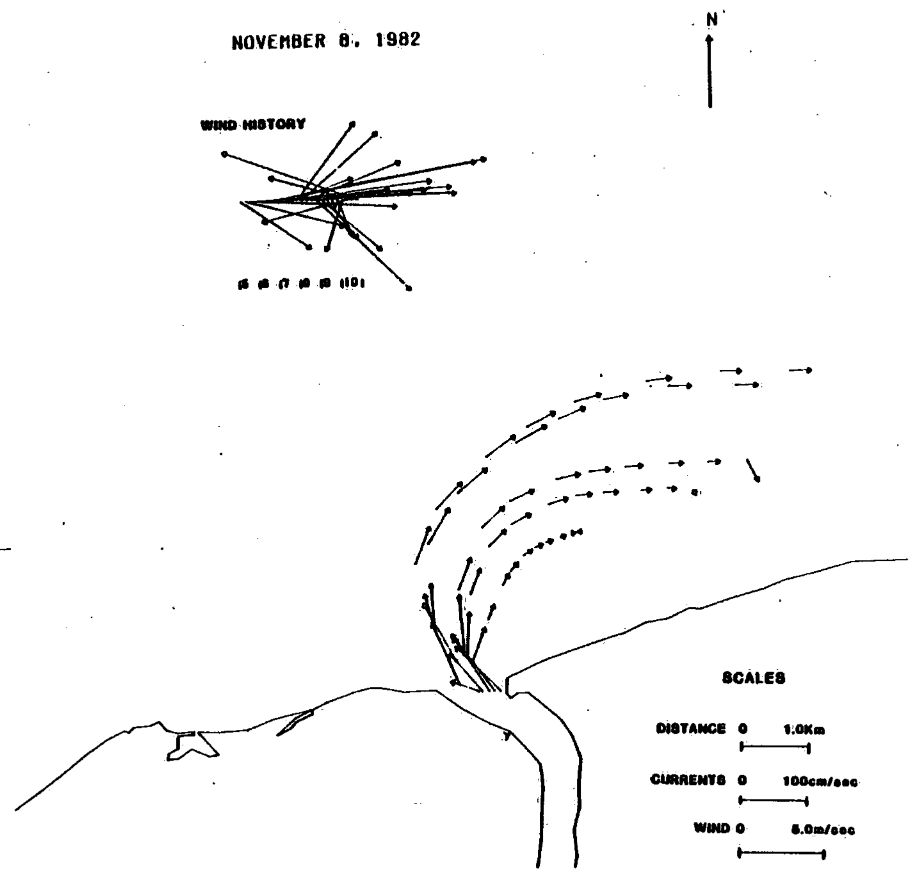

HORIZONTAL VELOCITY FIELD

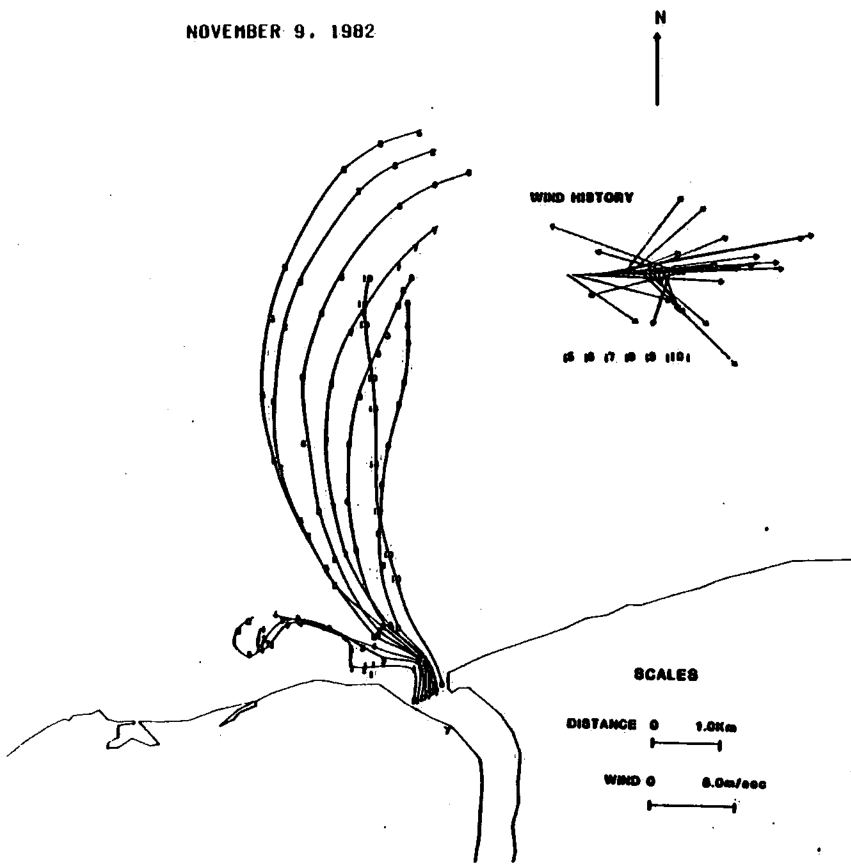

LAGRANGIAN TRAJECTORY

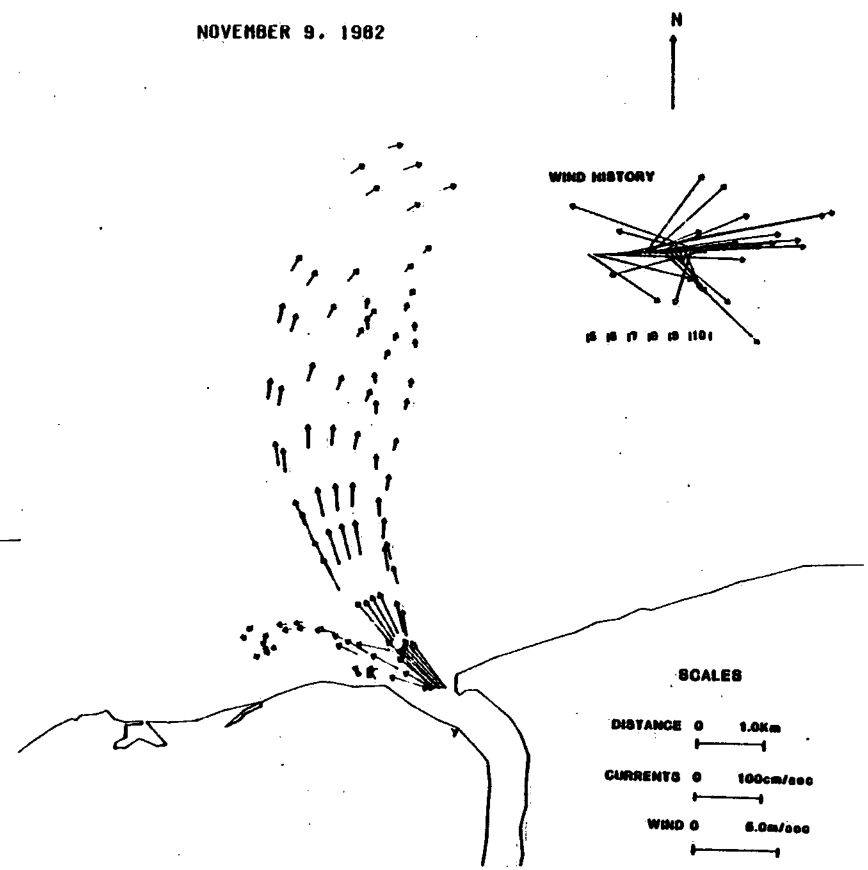

HORIZONTAL VELOCITY FIELD

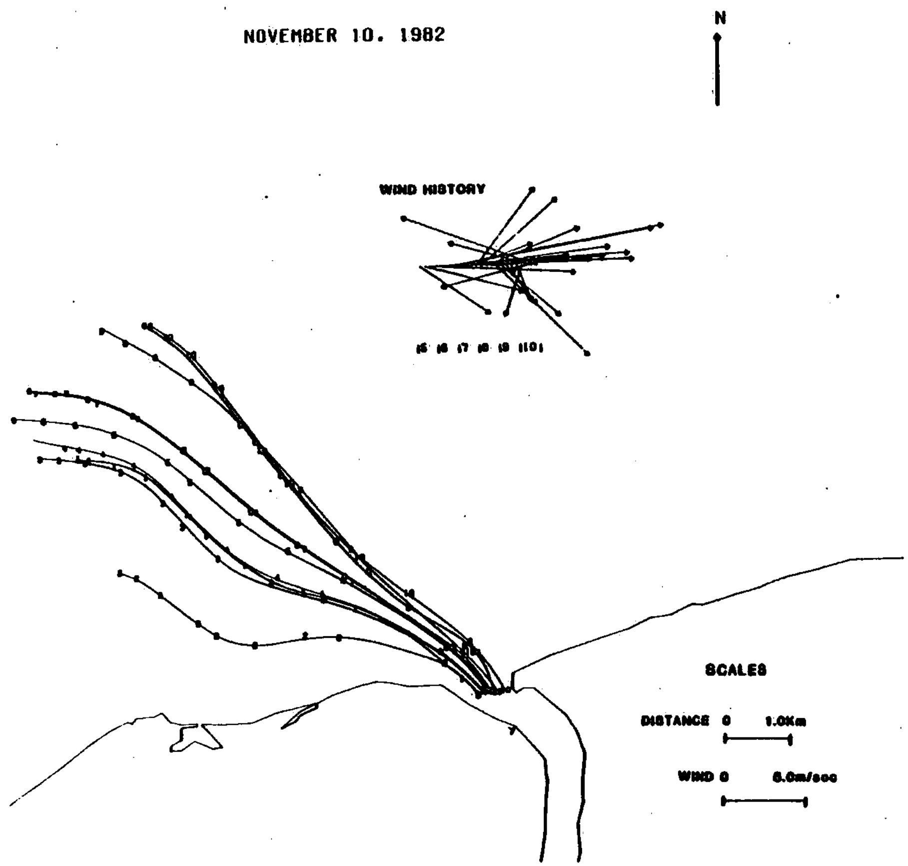

LAGRANGIAN TRAJECTORY

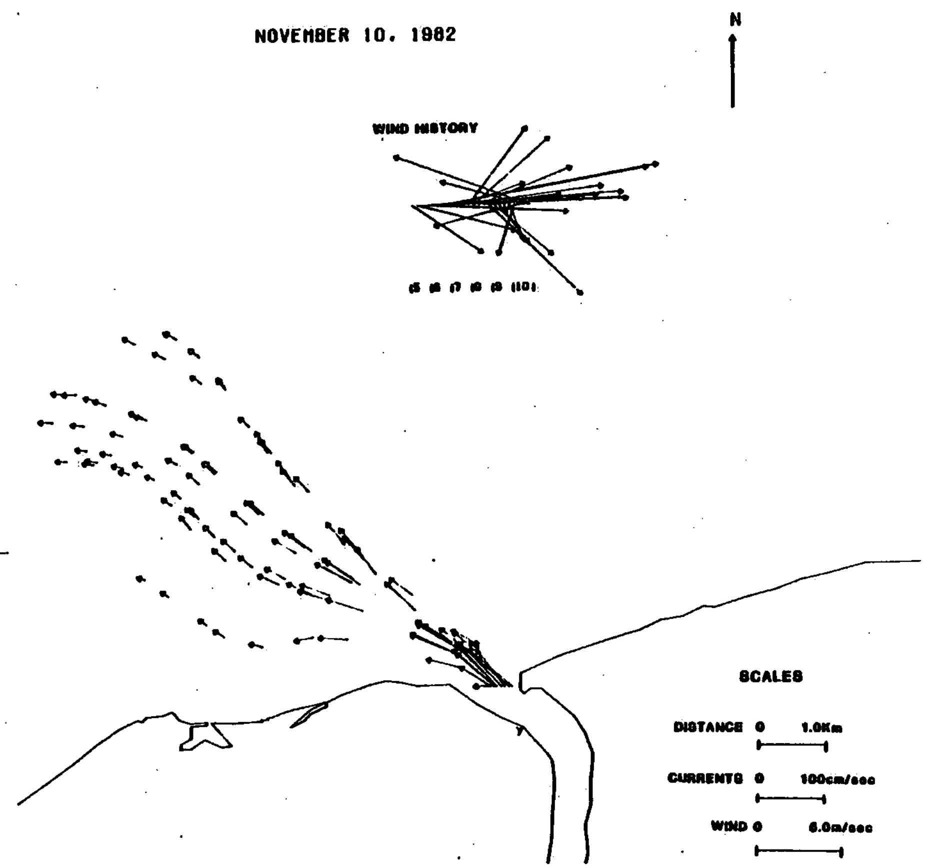

HORIZONTAL VELOCITY FIELD

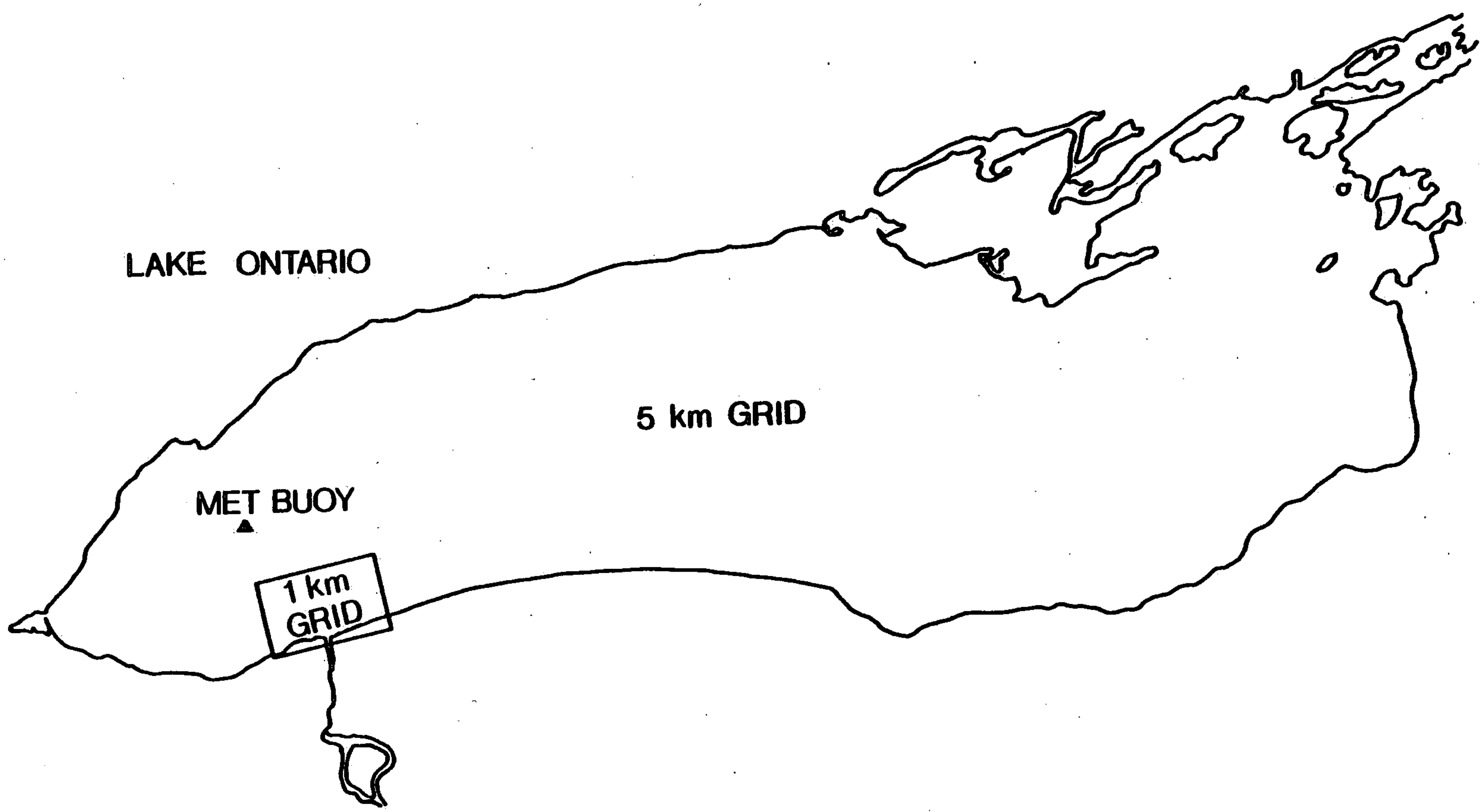

5.1

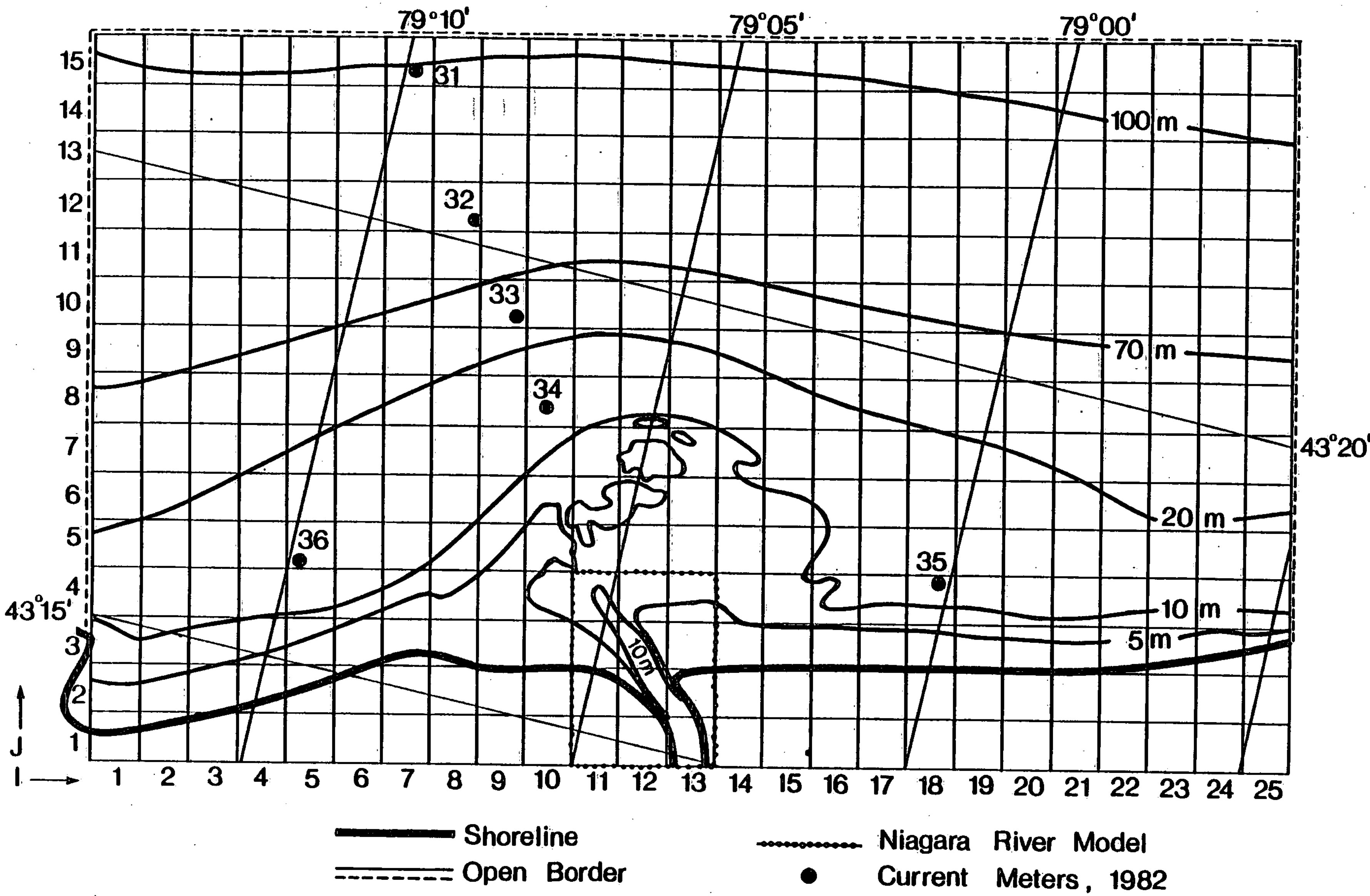

LAKE ONTARIO NEAR NIAGARA RIVER, 1-KM GRID, ROTATED 13.5°

Large numbers = Grid indices of 1 km grid of Lake Ontario near Niagara

Numbers in parentheses = Grid indices on output file flowmap

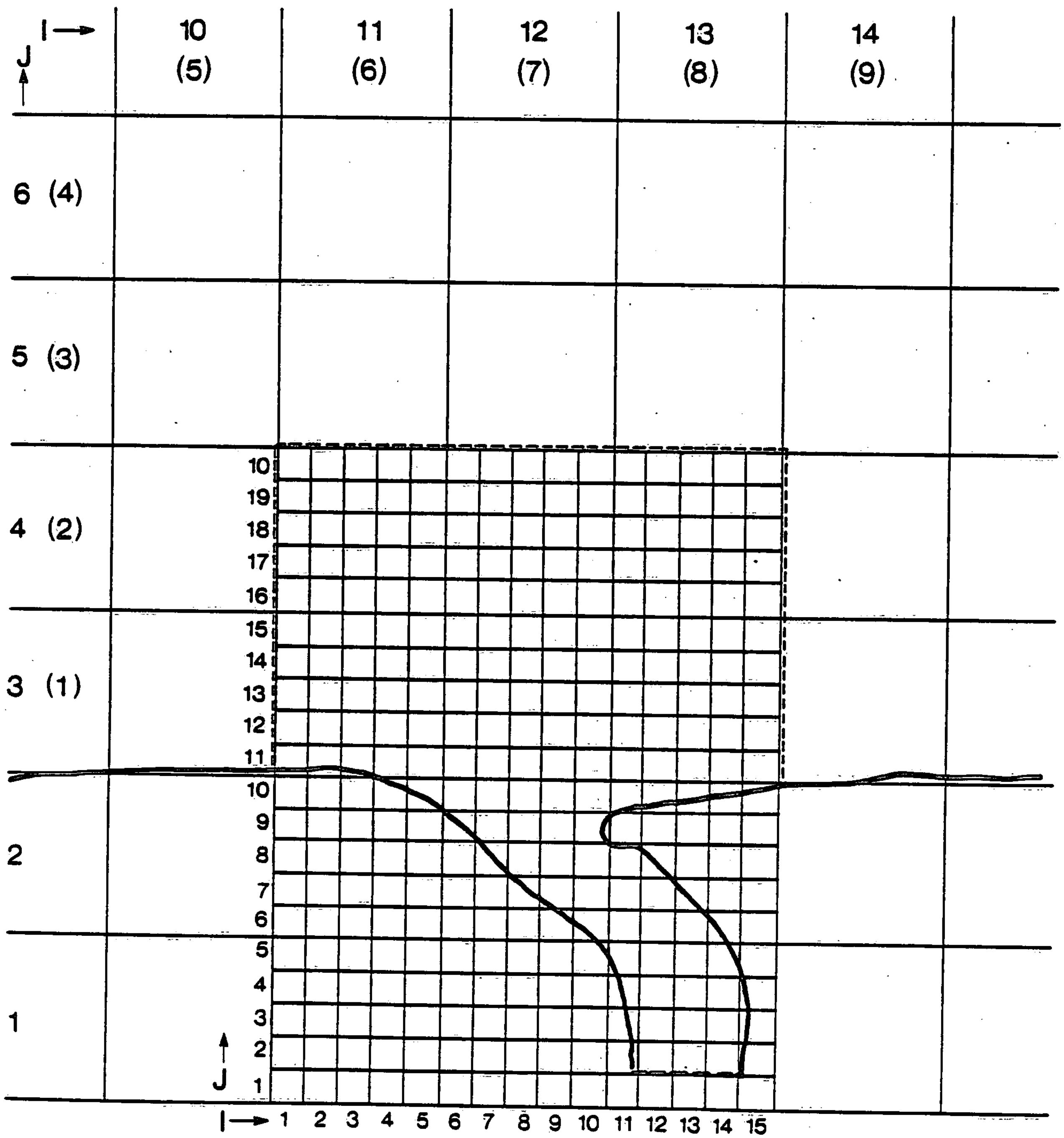

NIAGARA RIVER MODEL, 200 m GRID, IMBEDDED IN 1 KM GRID
OUTPUT FILE RIVMAP. ----- open border

MAY 27, 1982 (14:00 GMT)

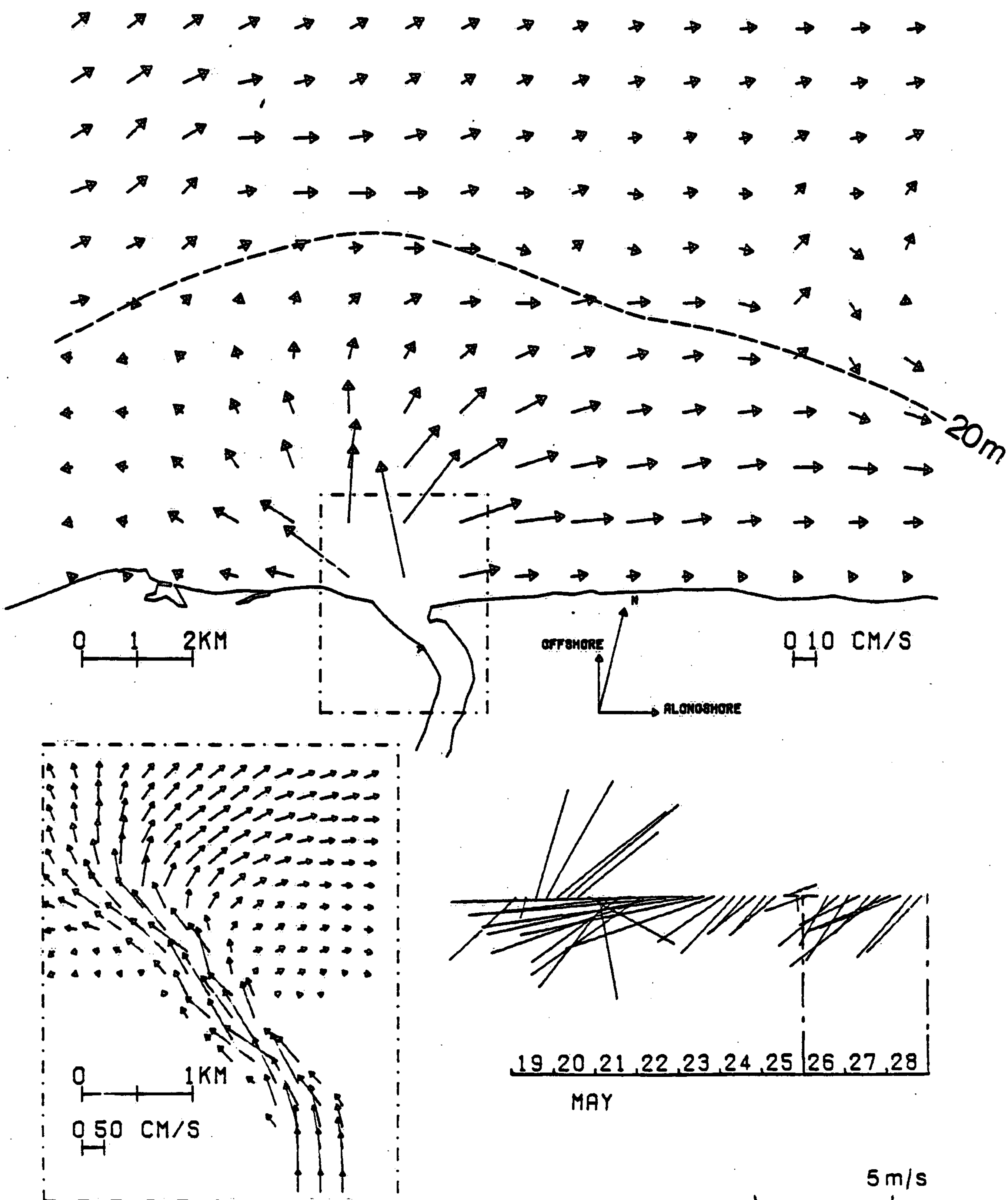

MAY 28, 1982 (14:00 GMT)

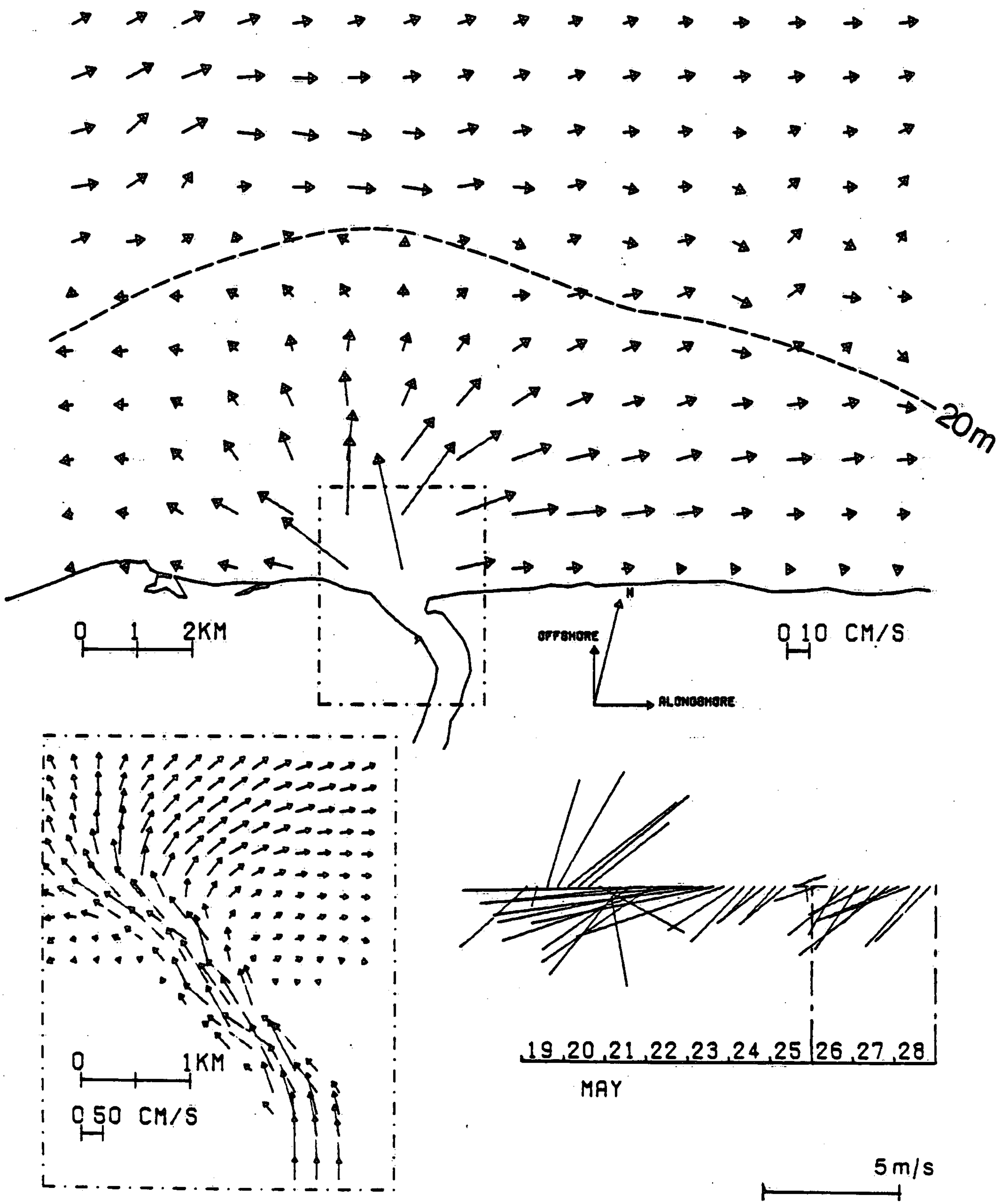

JUN 22, 1982 (14:00 GMT)

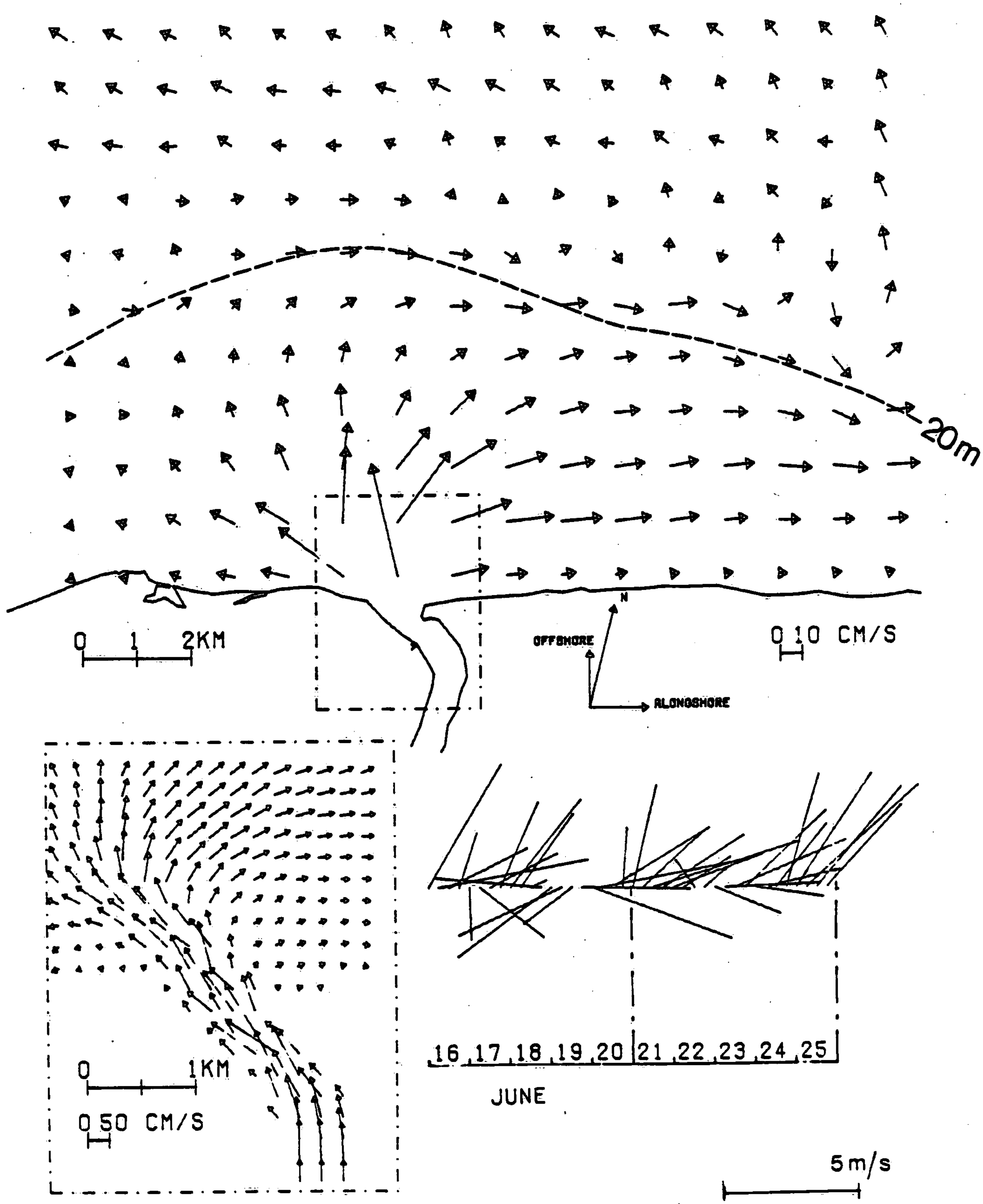

JUN 23, 1982 (14:00 GMT)

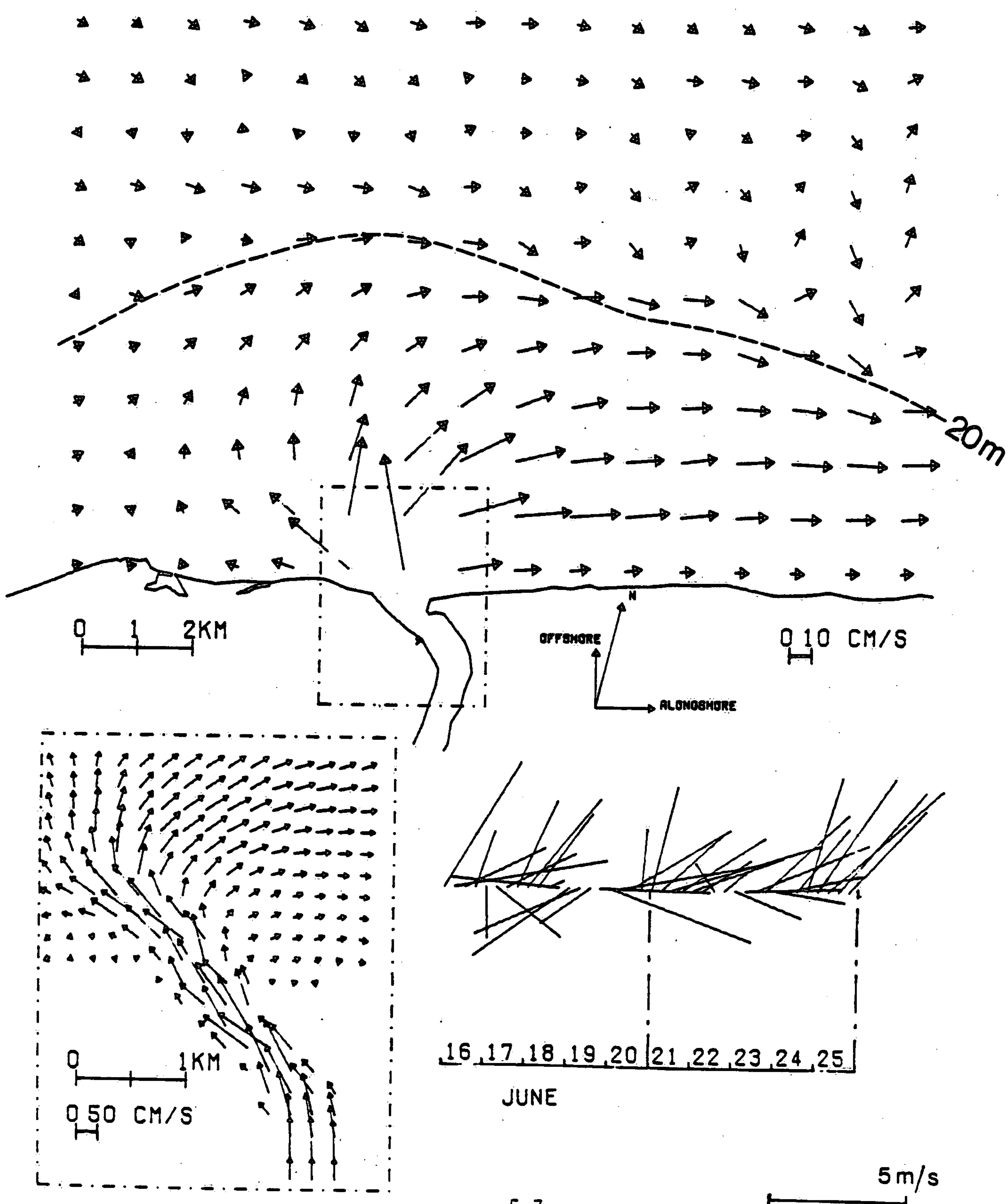

JUN 24, 1982 (14:00 GMT)

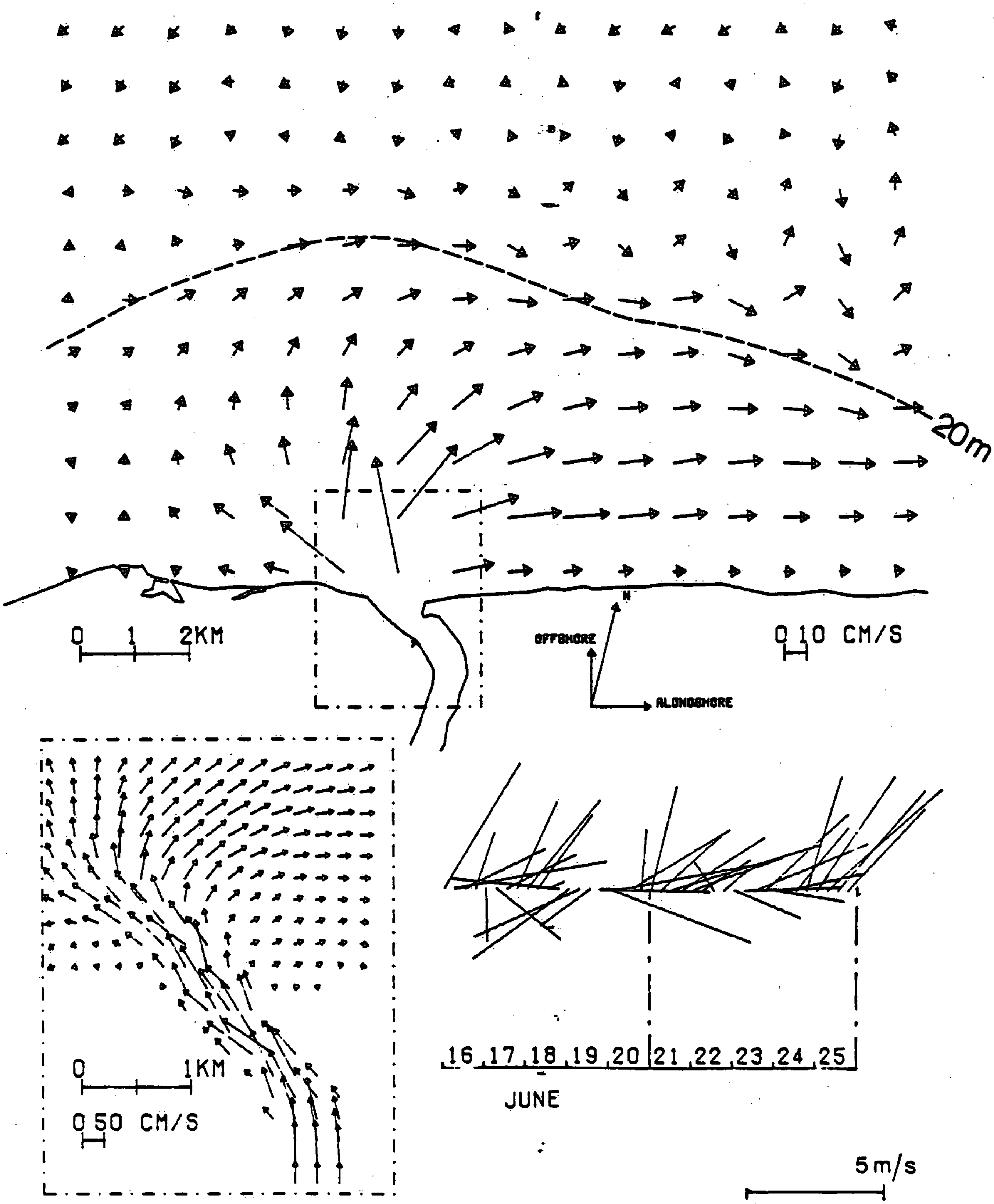

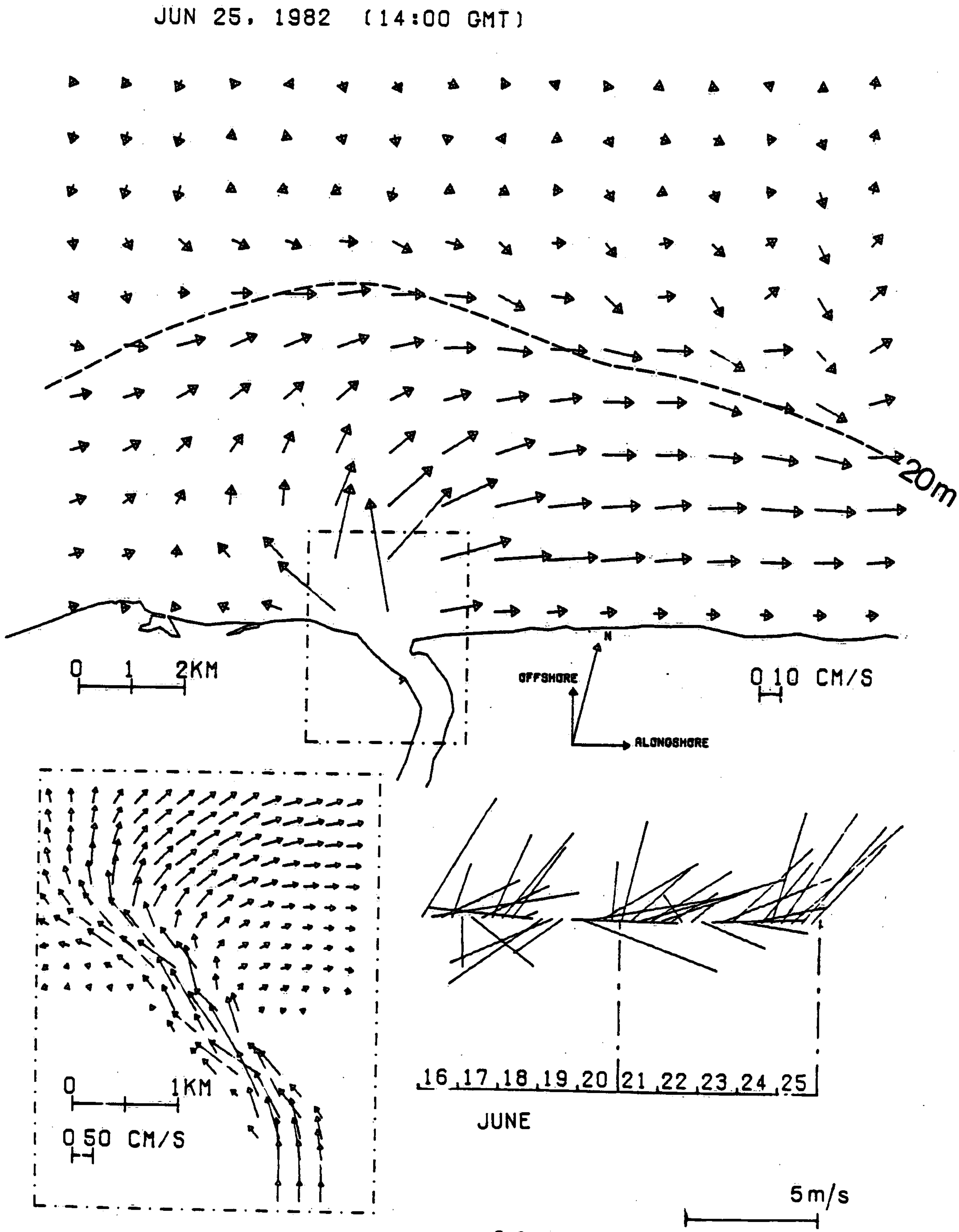
JUN 25, 1982 (14:00 GMT)
20m
0 1 2KM
N
OFFSHORE
ALONGSHORE
0 10 CM/S
0 1KM
0 50 CM/S
16 17 18 19 20 21 22 23 24 25
JUNE
5m/s

JUL 6, 1982 (14:00 GMT)

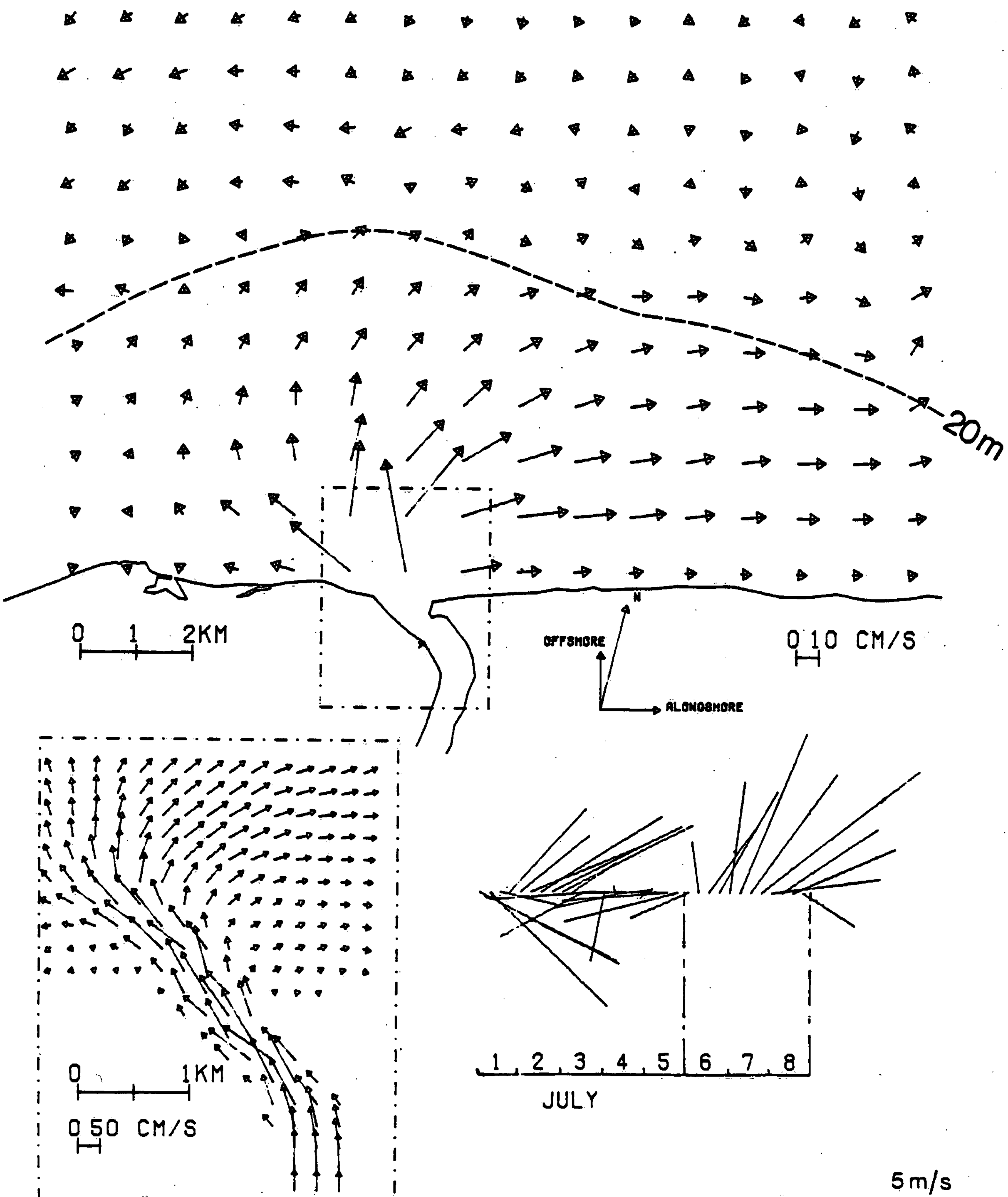

JUL 7, 1982 (14:00 GMT)

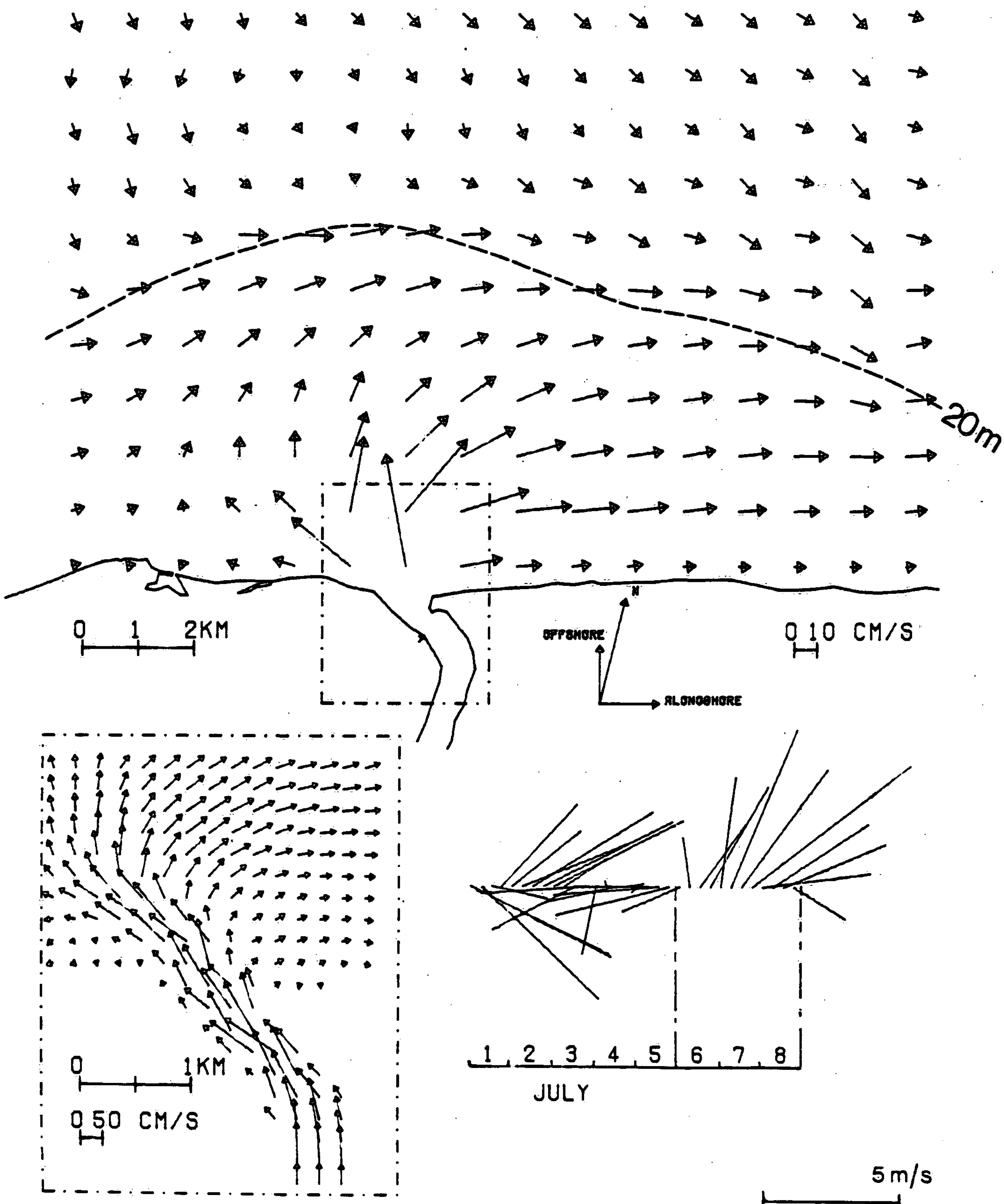

JUL 8, 1982 (14:00 GMT)

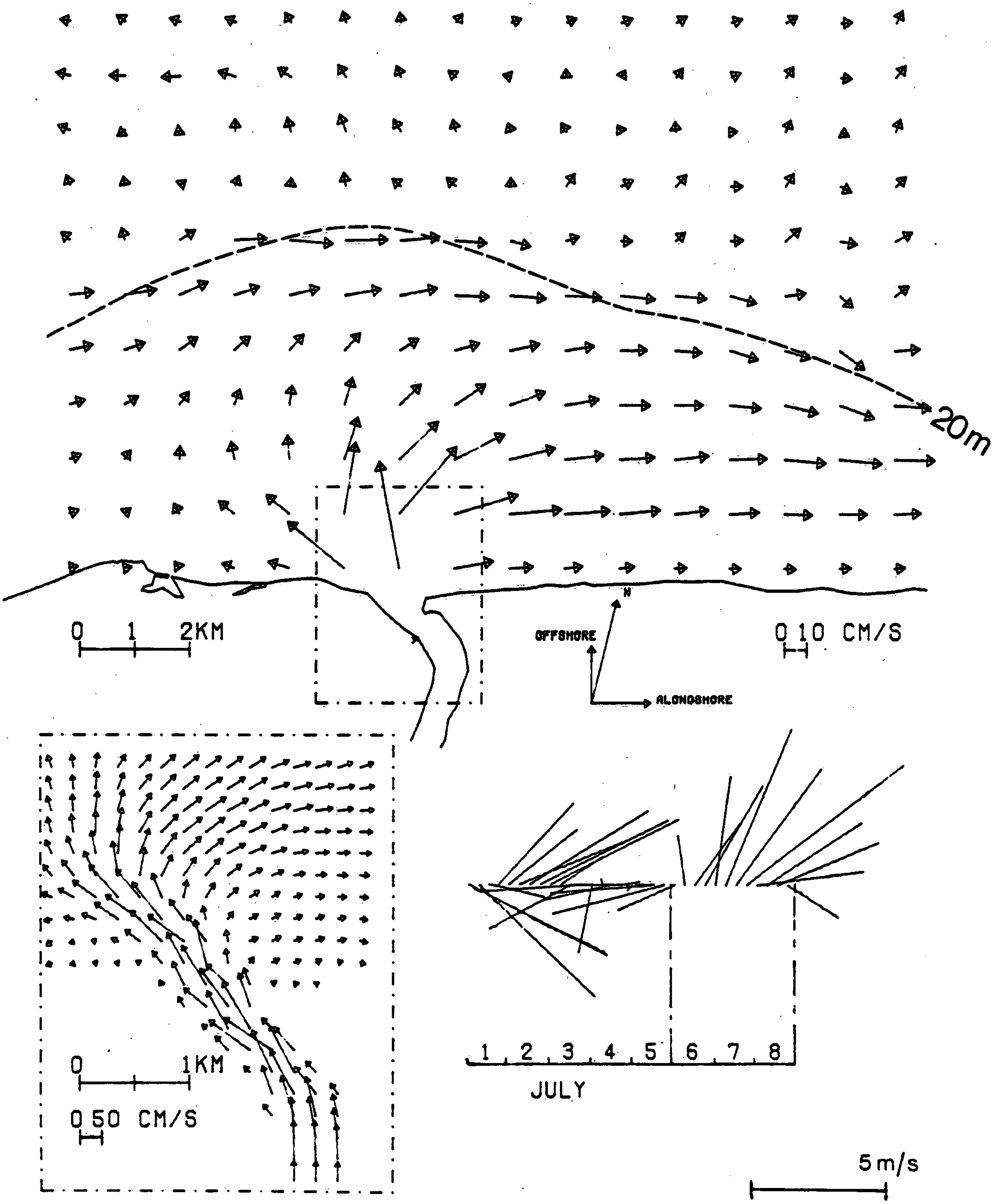

AUG 11, 1982 (14:00 GMT)

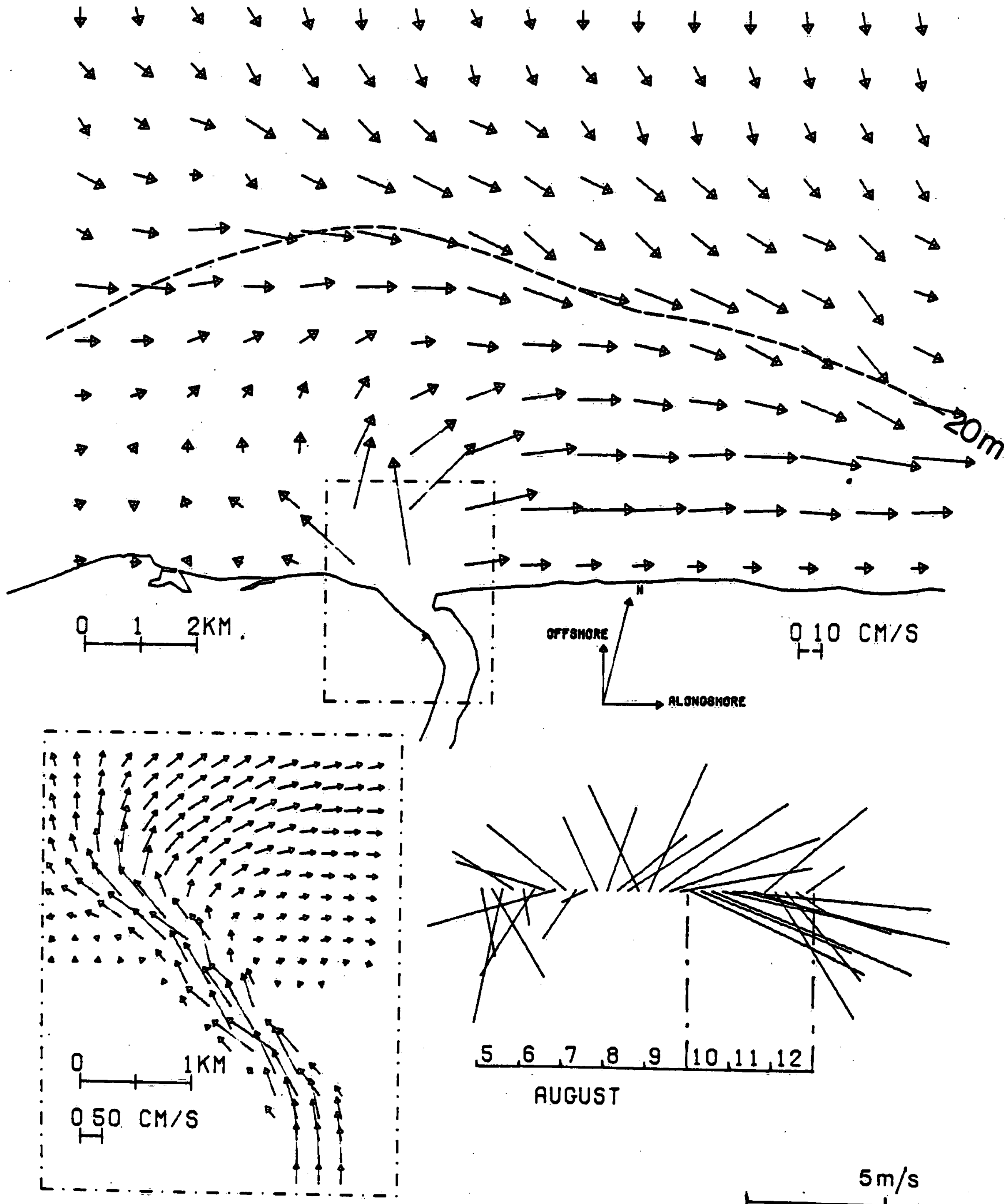

AUG 12, 1982 (14:00 GMT)

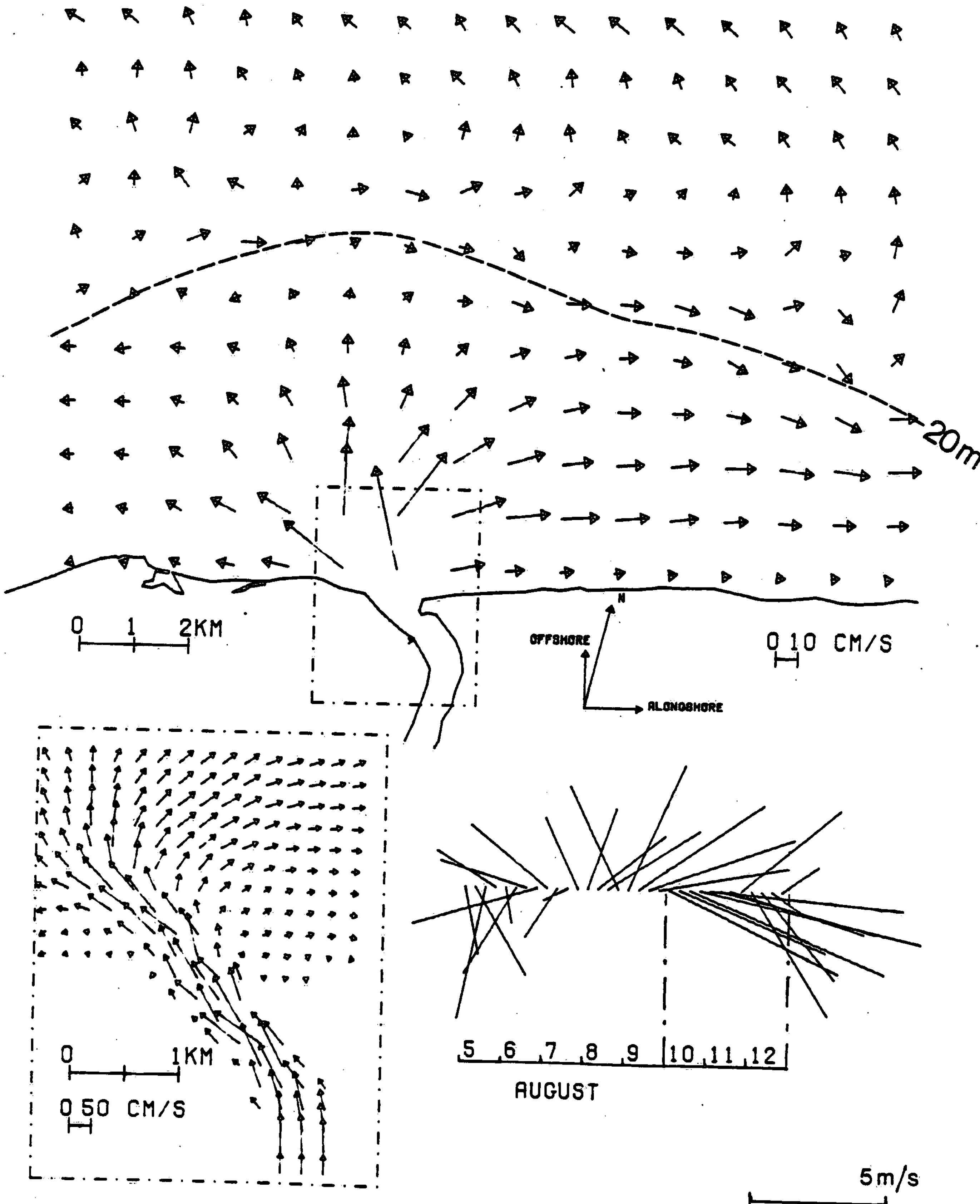

OCT 5, 1982 (14:00 GMT)

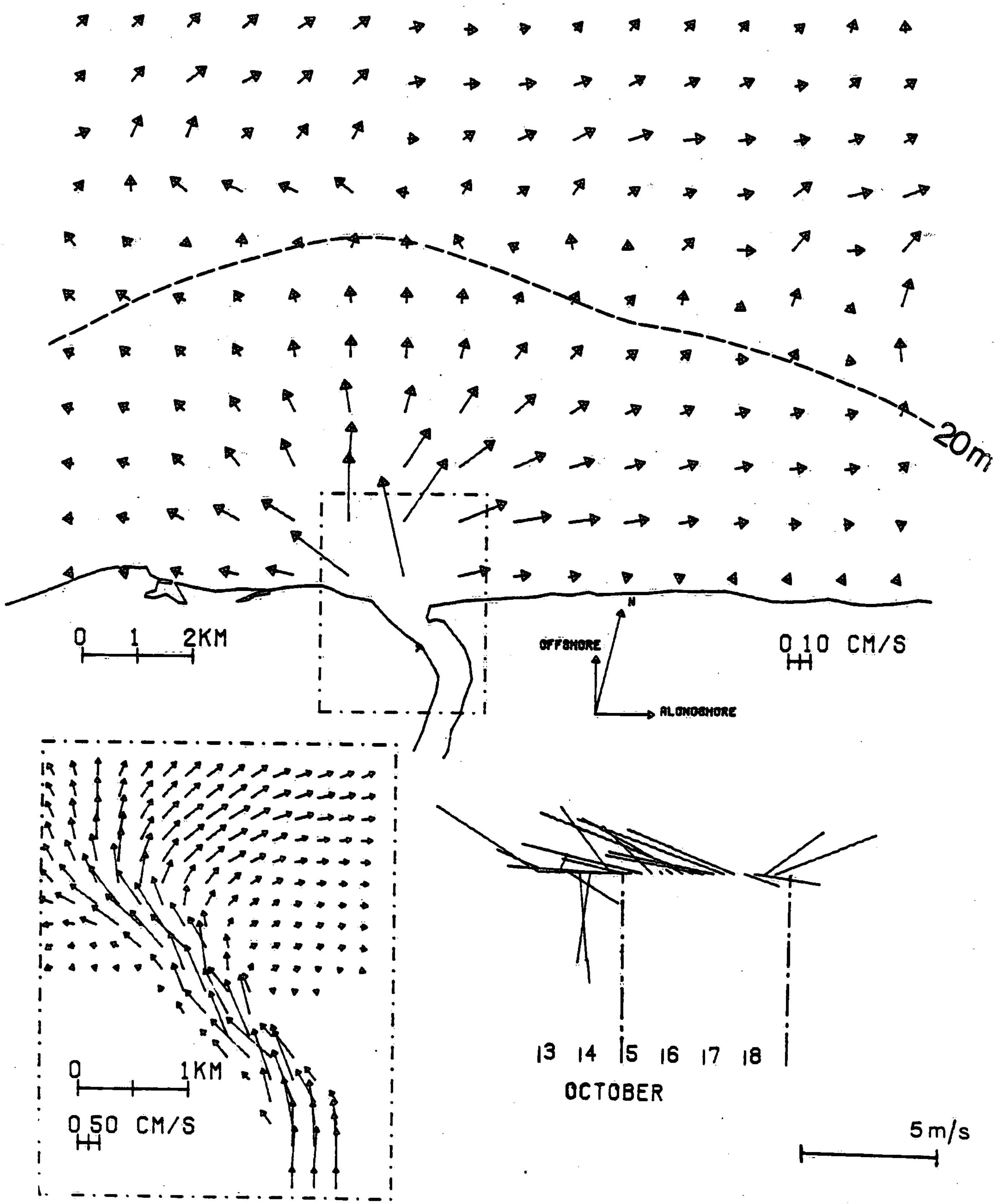

OCT 6, 1982 (14:00 GMT)

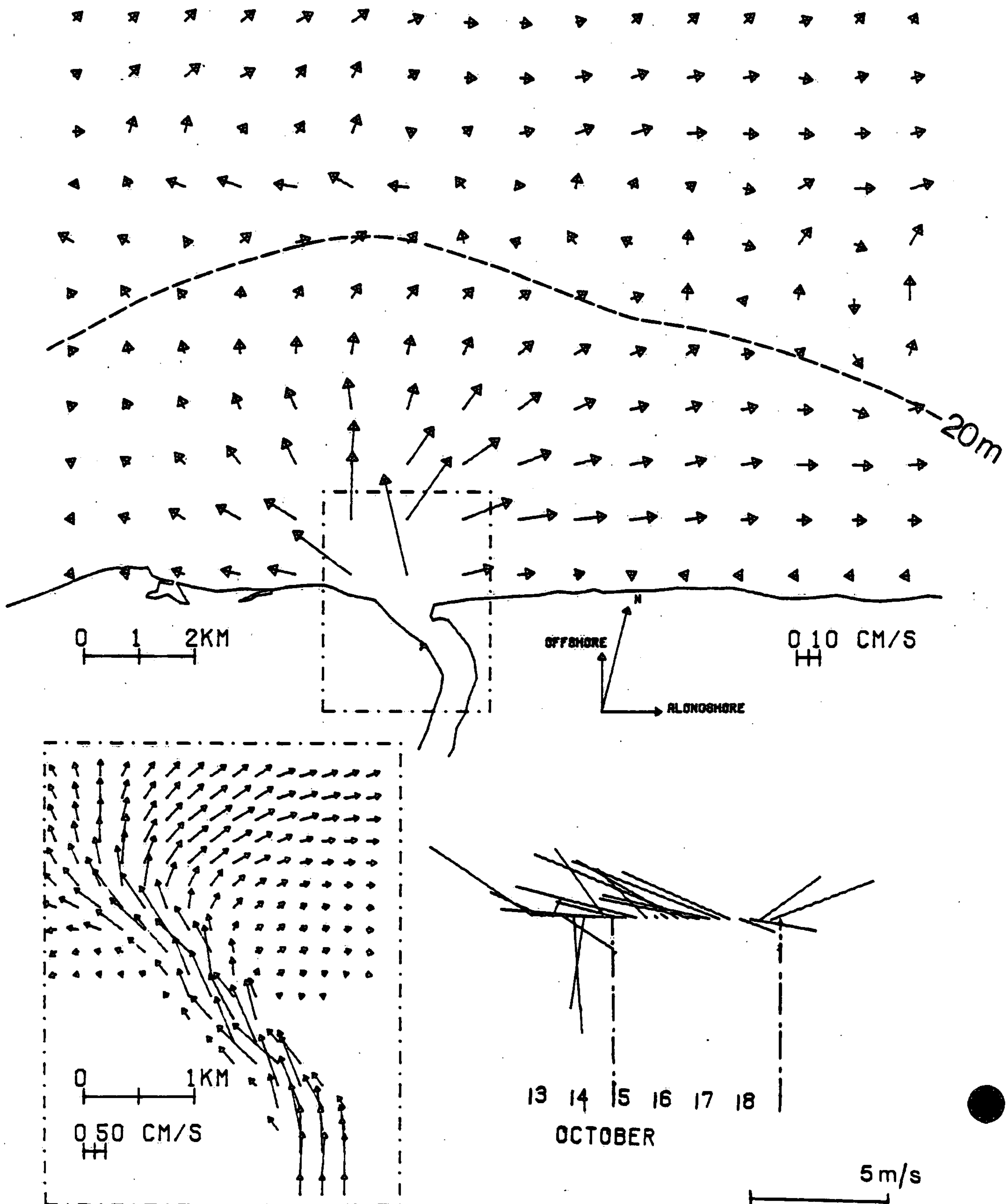

OCT 7, 1982 (14:00 GMT)

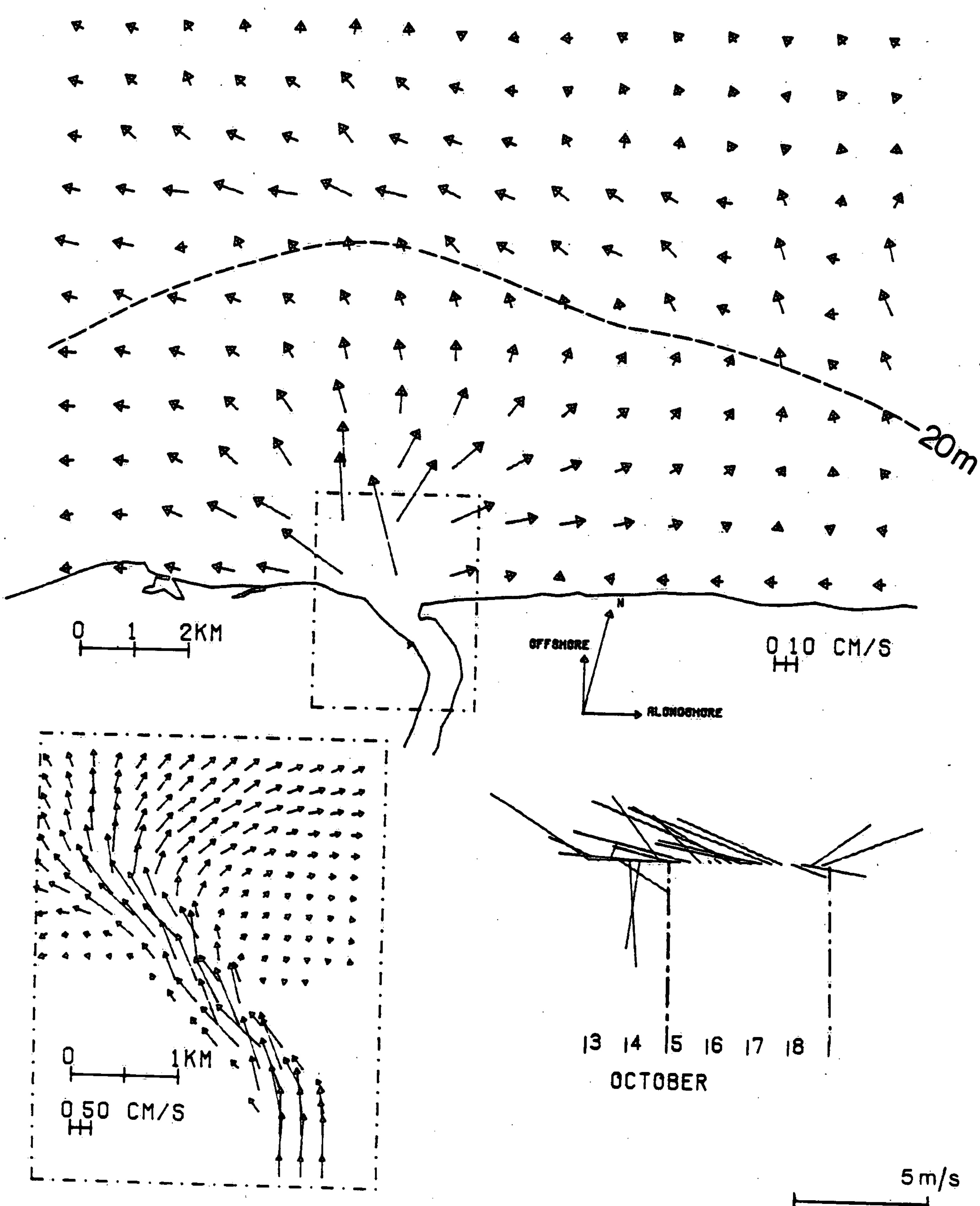

OCT 8, 1982 (14:00 GMT)

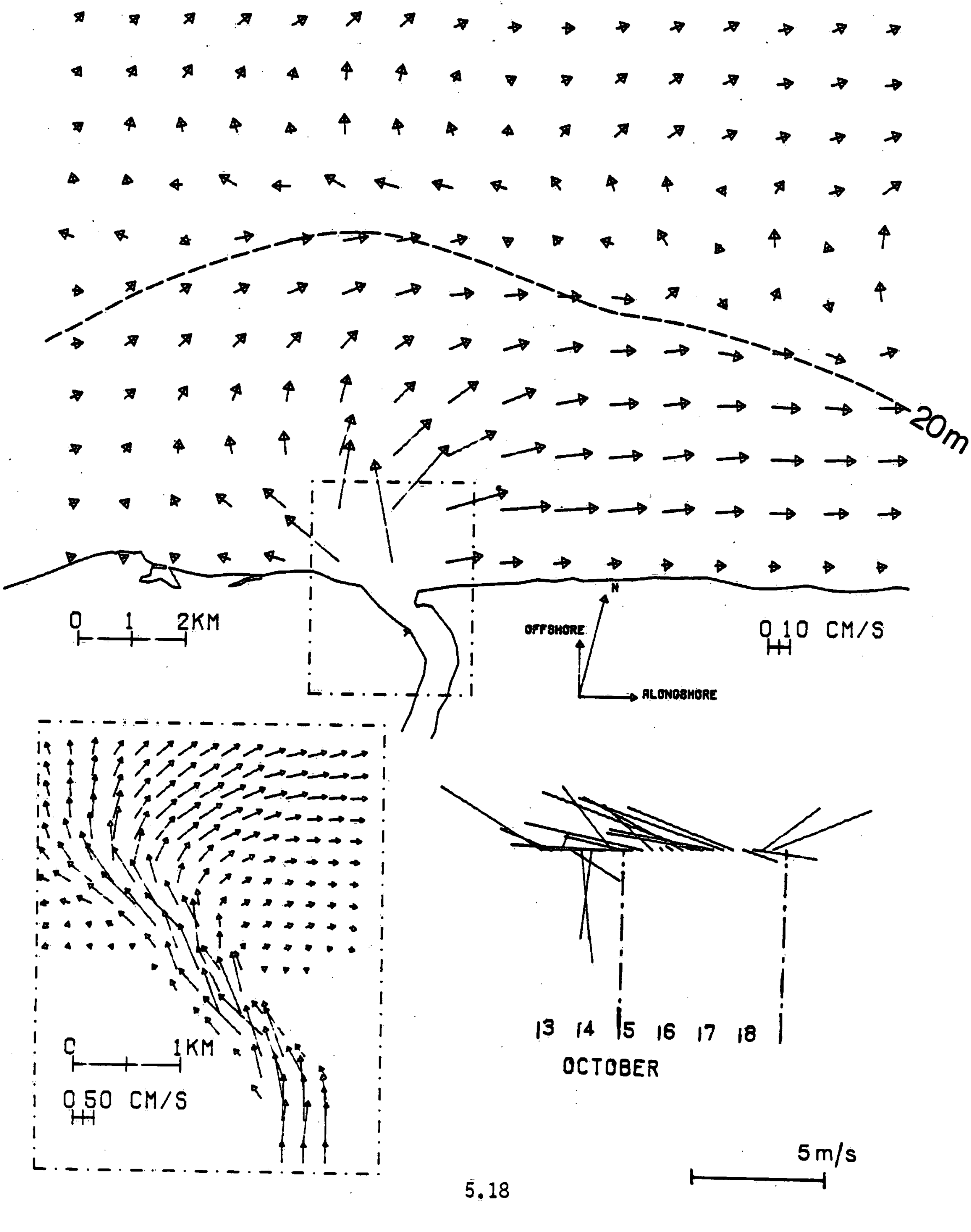

NOV 8, 1982 (14:00 GMT)

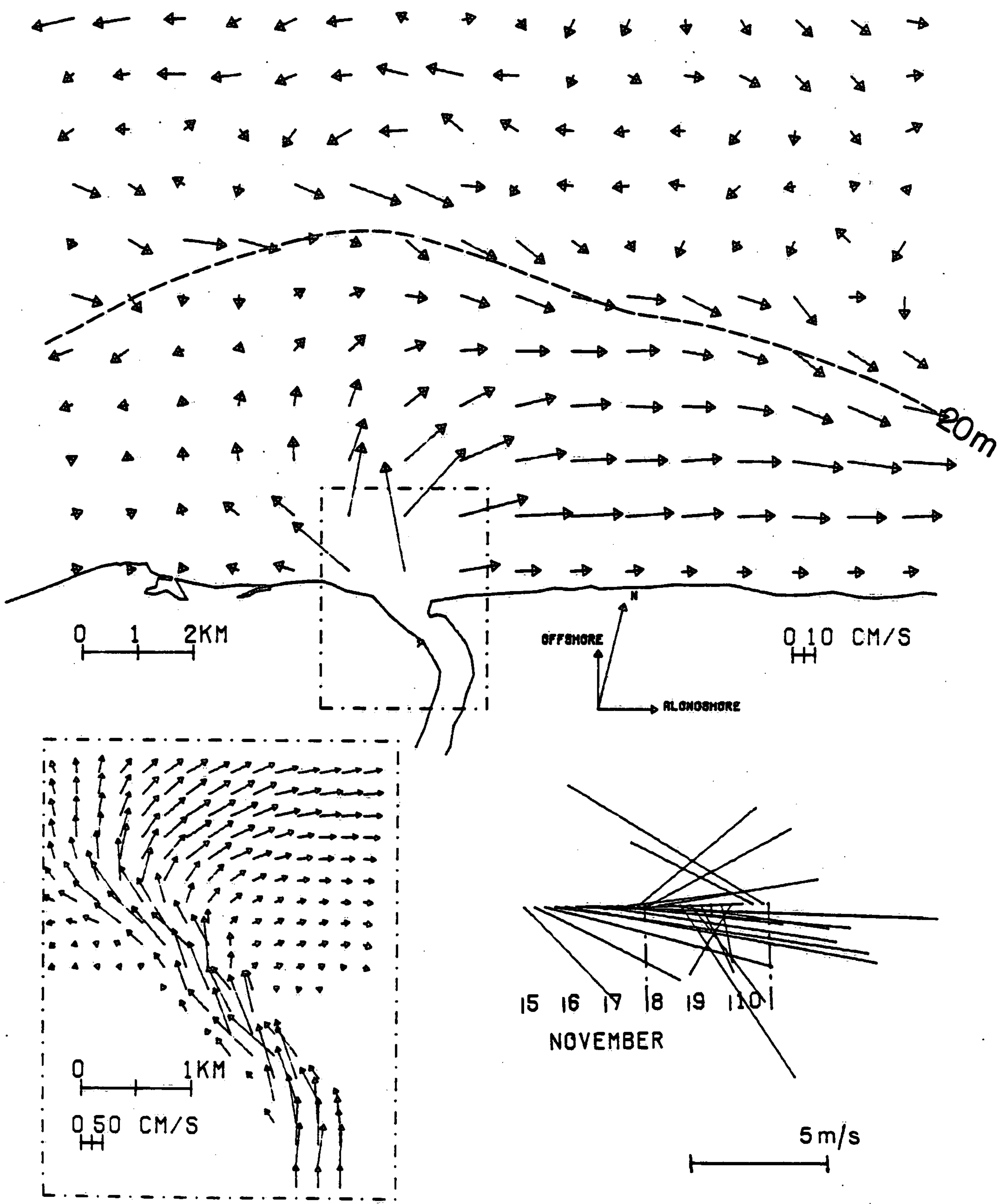

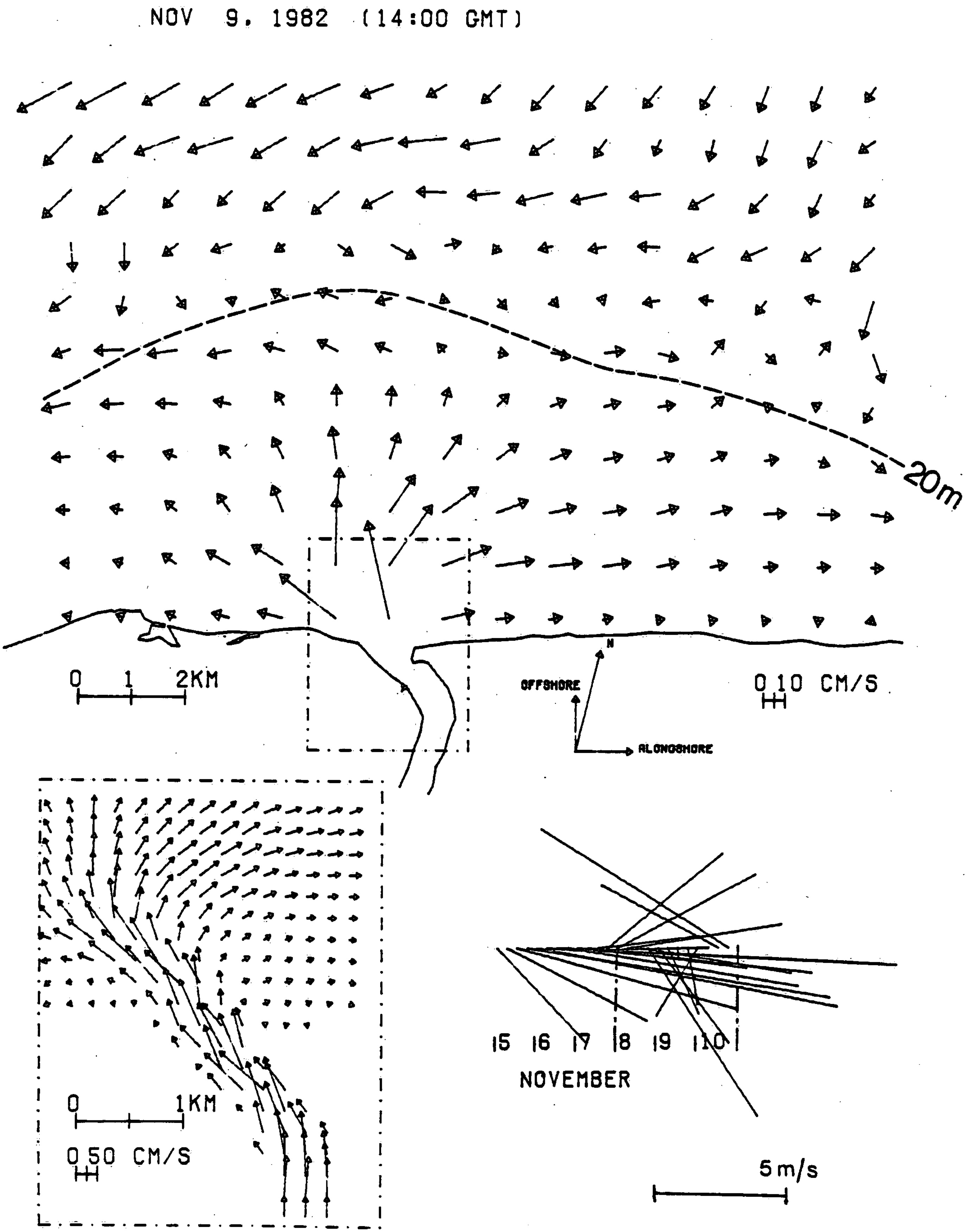
NOV 9, 1982 (14:00 GMT)
20m
0 1 2KM
N
OFFSHORE
ALONGSHORE
0 10 CM/S
0 1KM
0 50 CM/S
15 16 17 18 19 110
NOVEMBER
5 m/s

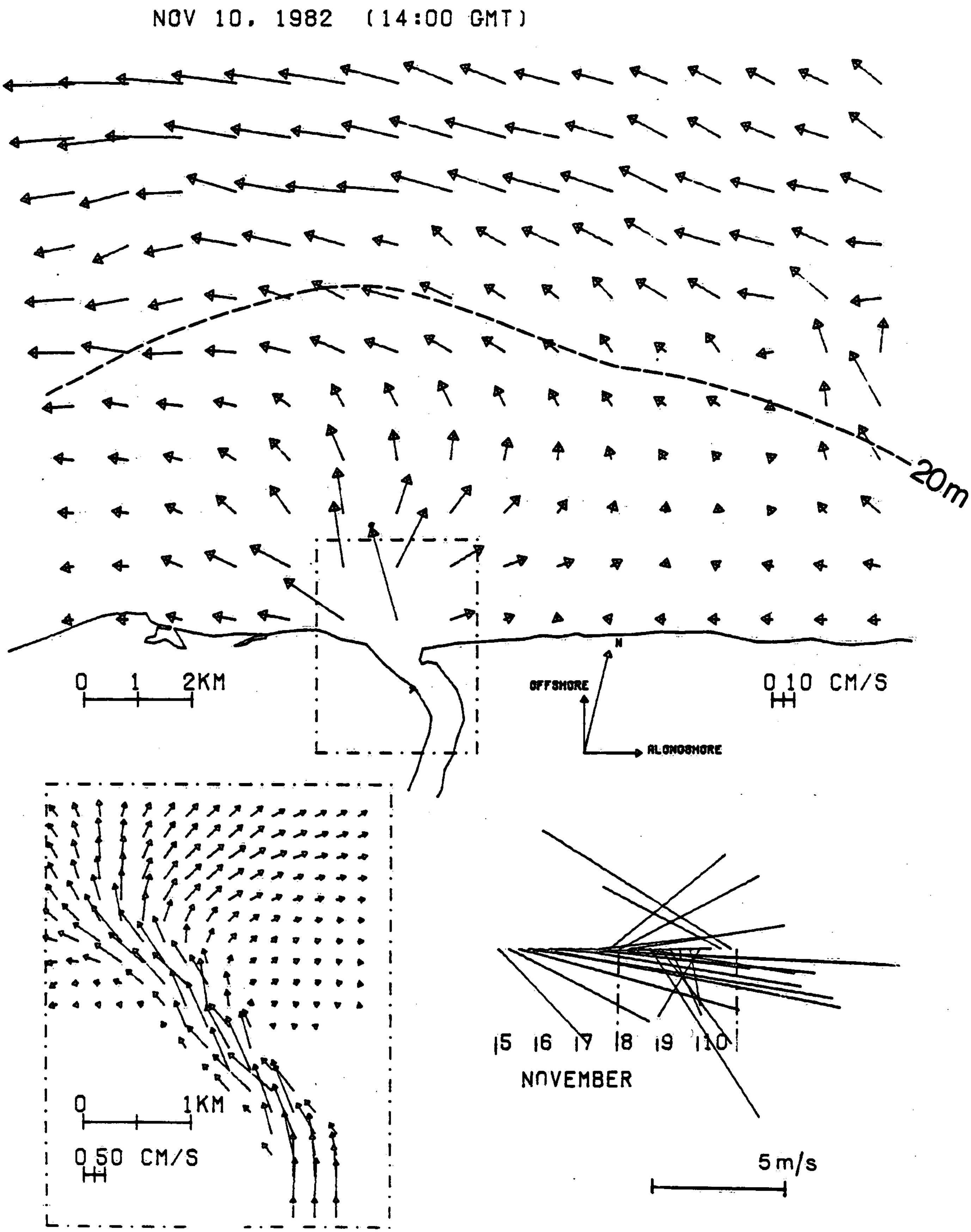
NOV 10, 1982 (14:00 GMT)
20m
0 1 2KM
OFFSHORE
N
ALONGSHORE
0 10 CM/S
0 1KM
0 50 CM/S
15 16 17 18 19 110
NOVEMBER
5 m/s

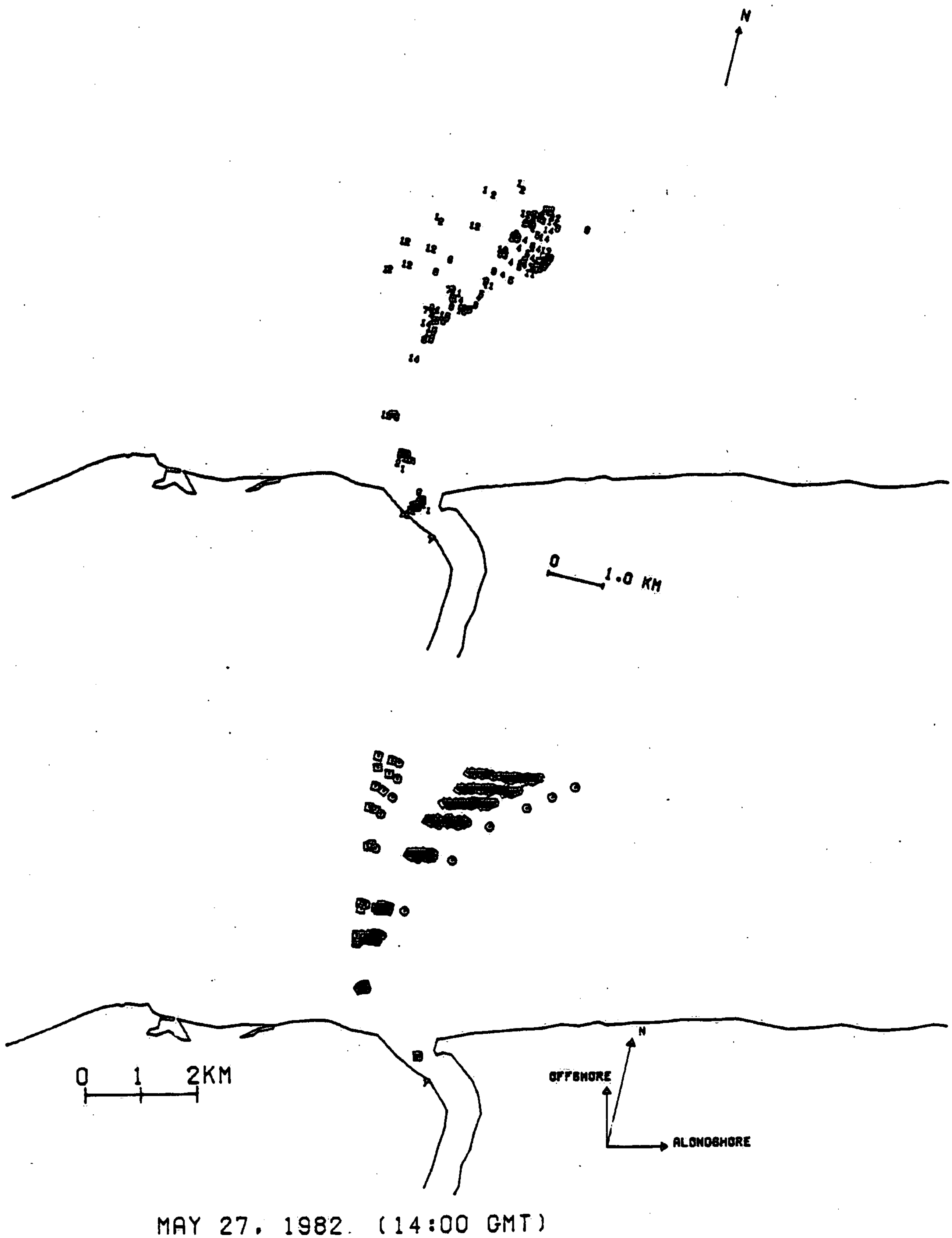

MAY 27, 1982 (14:00 GMT)

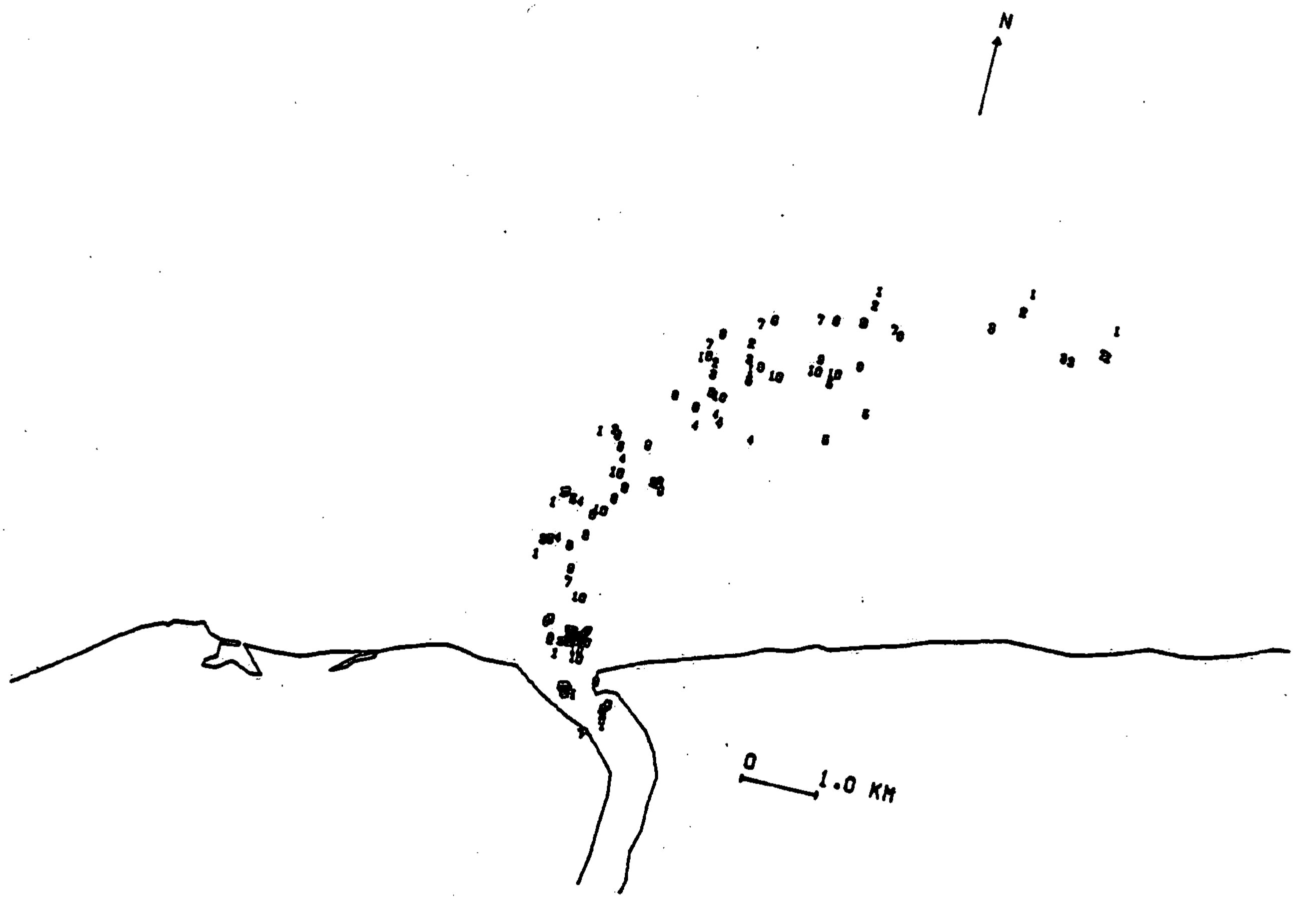

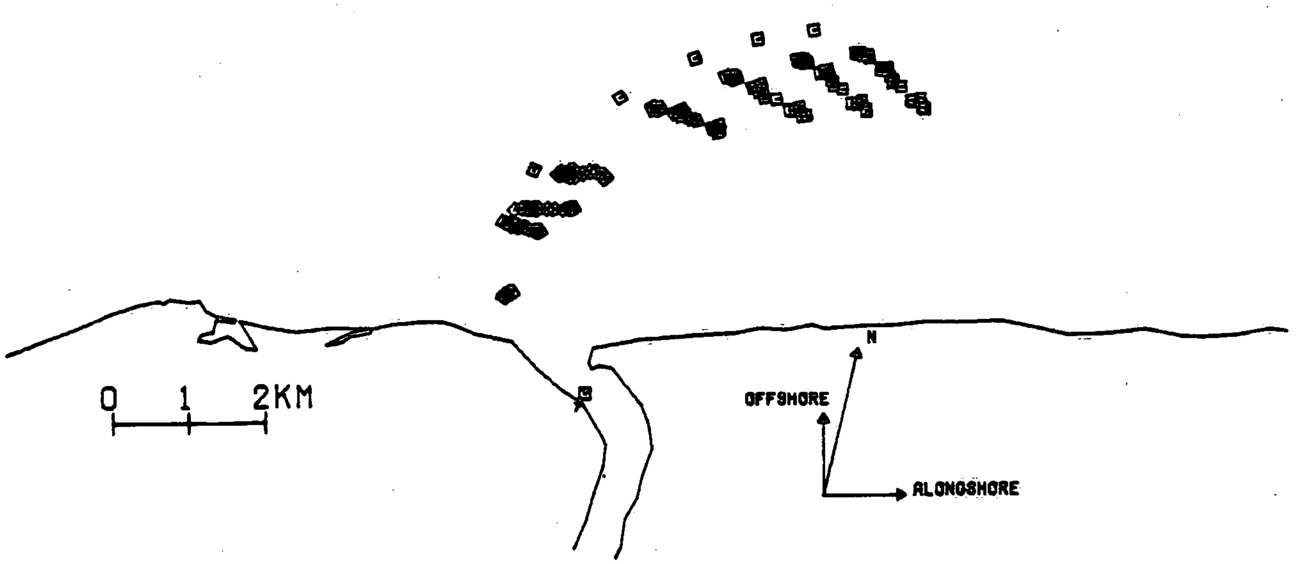

JUN 25, 1982 (14:00 GMT)

6.2

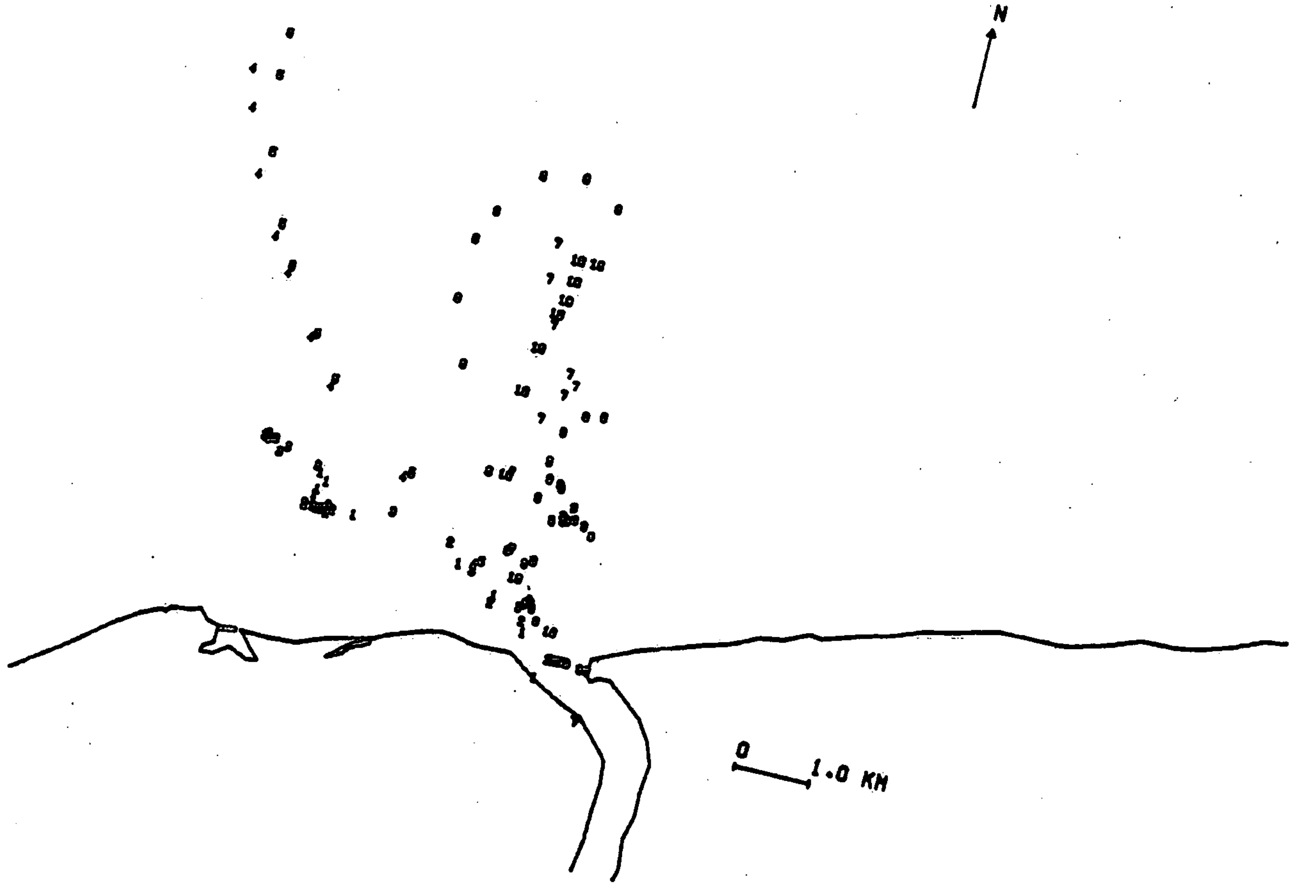

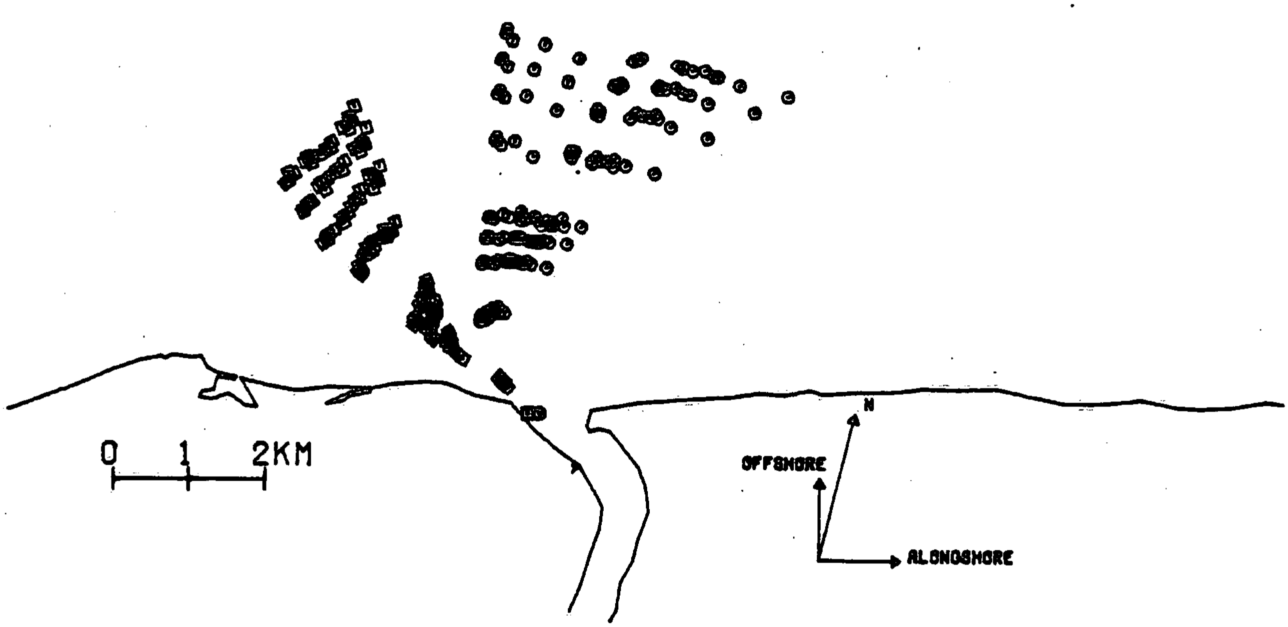

AUG 12, 1982 (14:00 GMT)

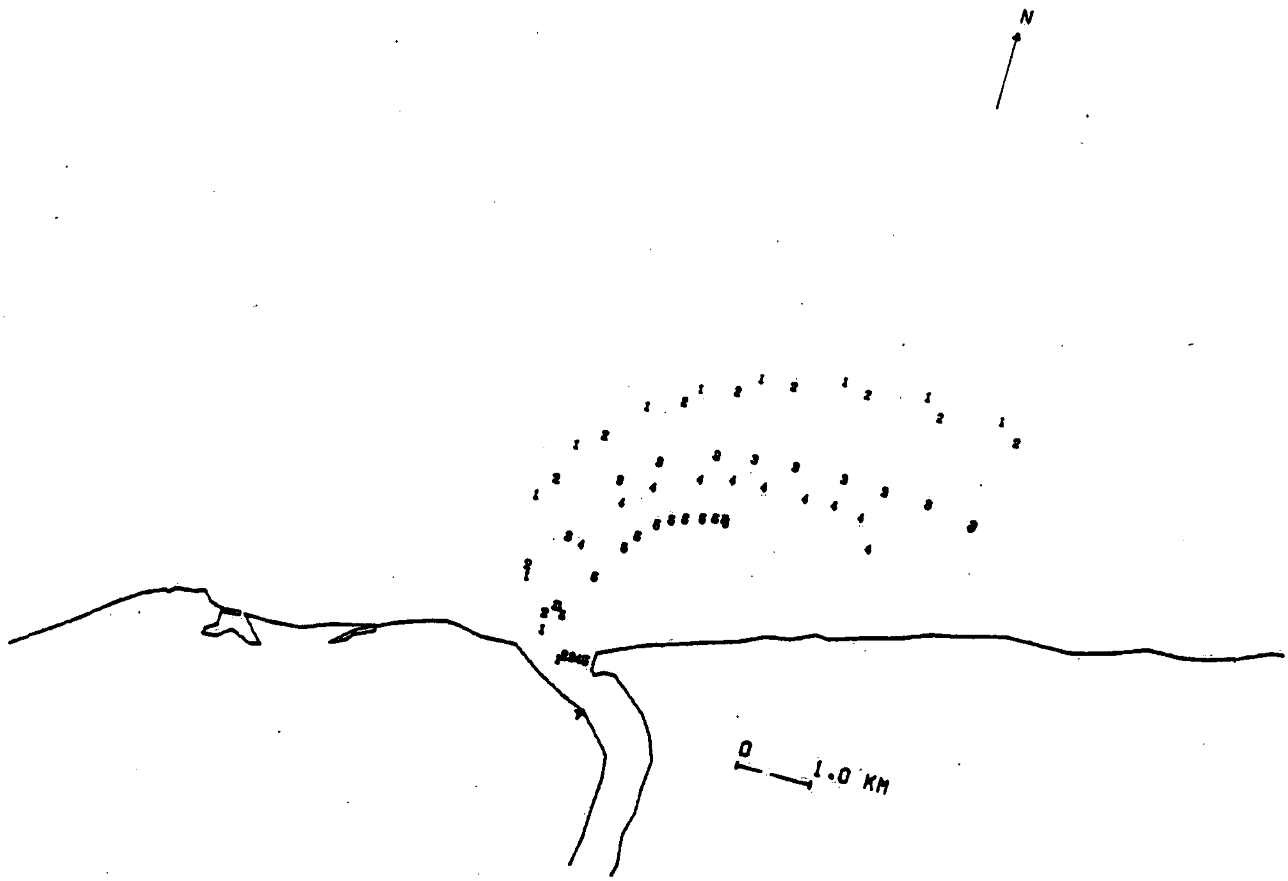

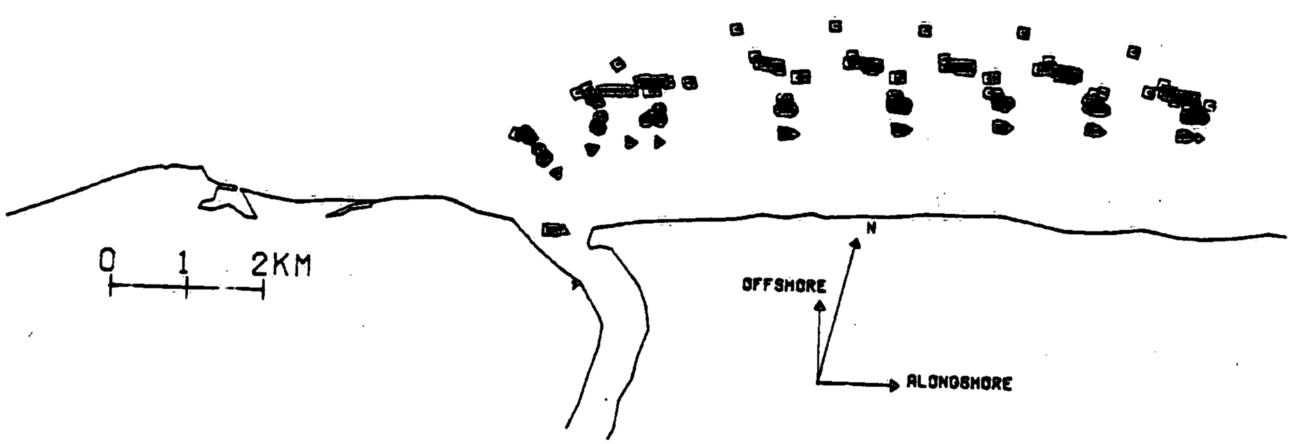

NOV 8, 1982 (14:00 GMT)

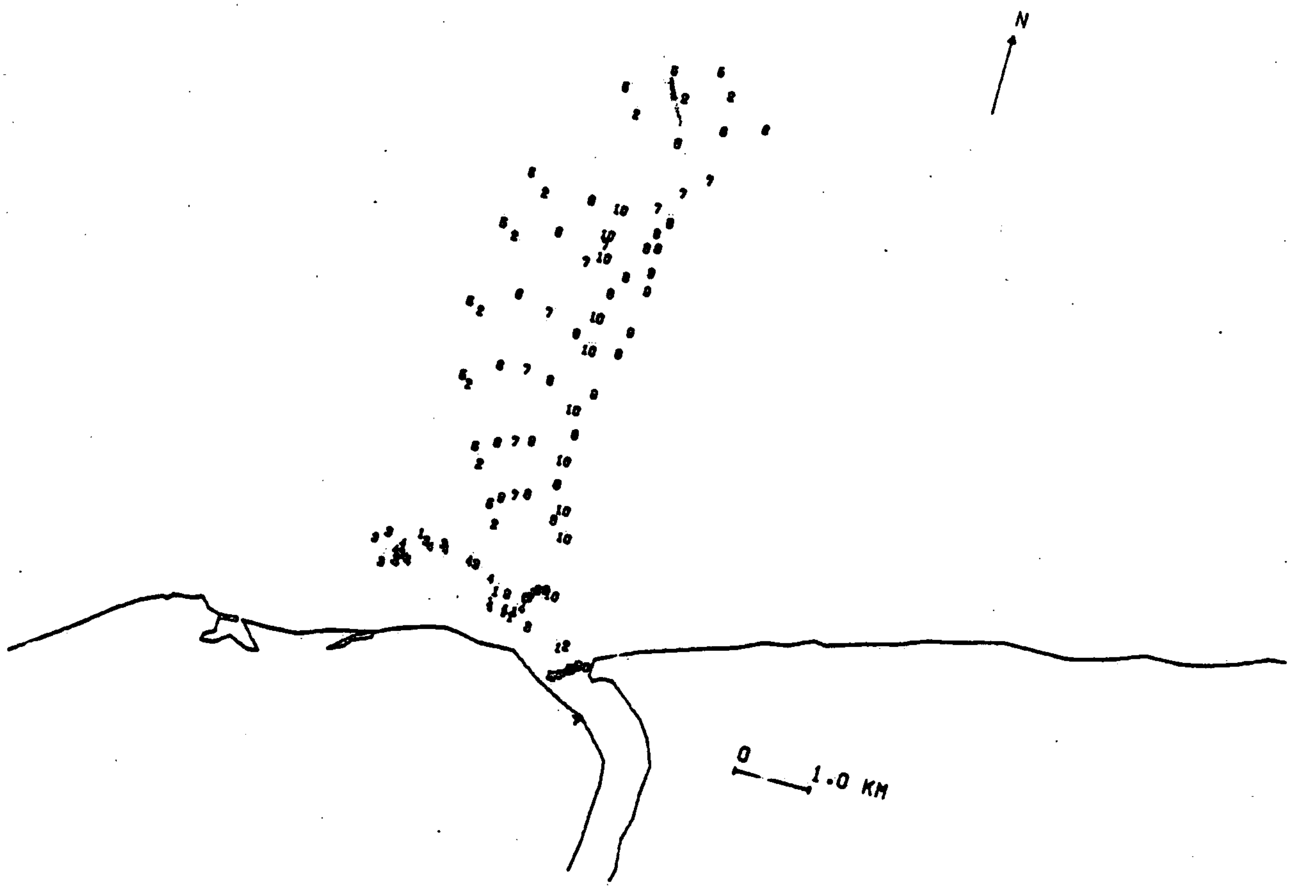

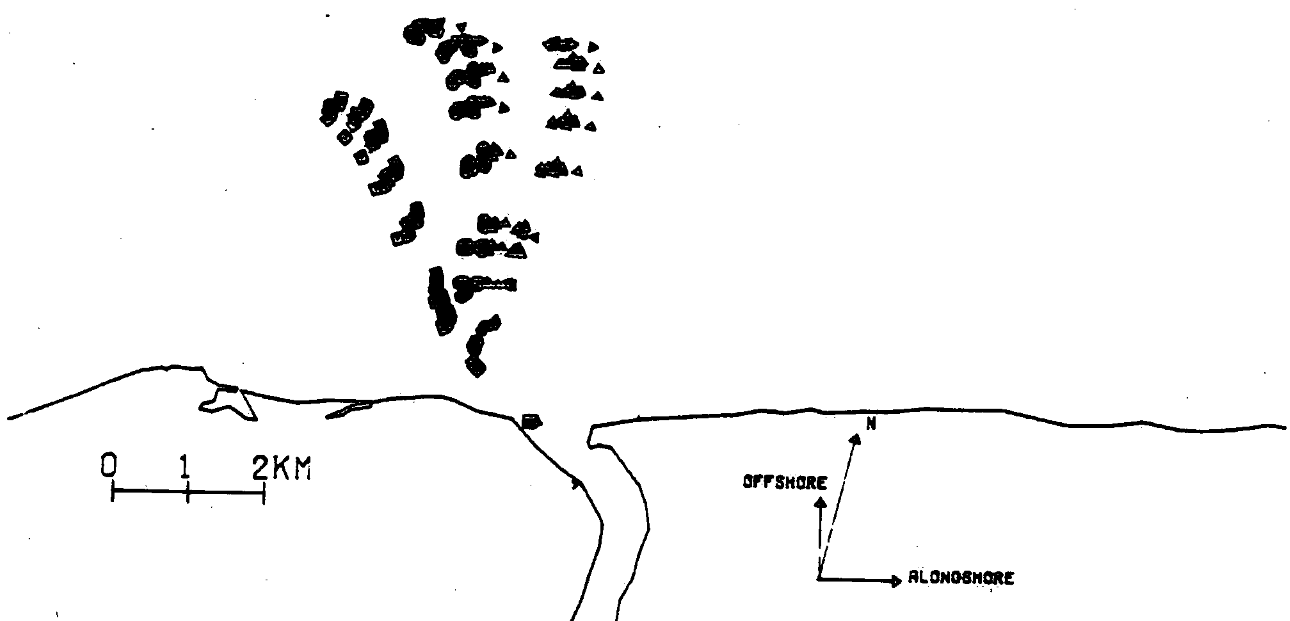

NOV 9, 1982 (14:00 GMT)

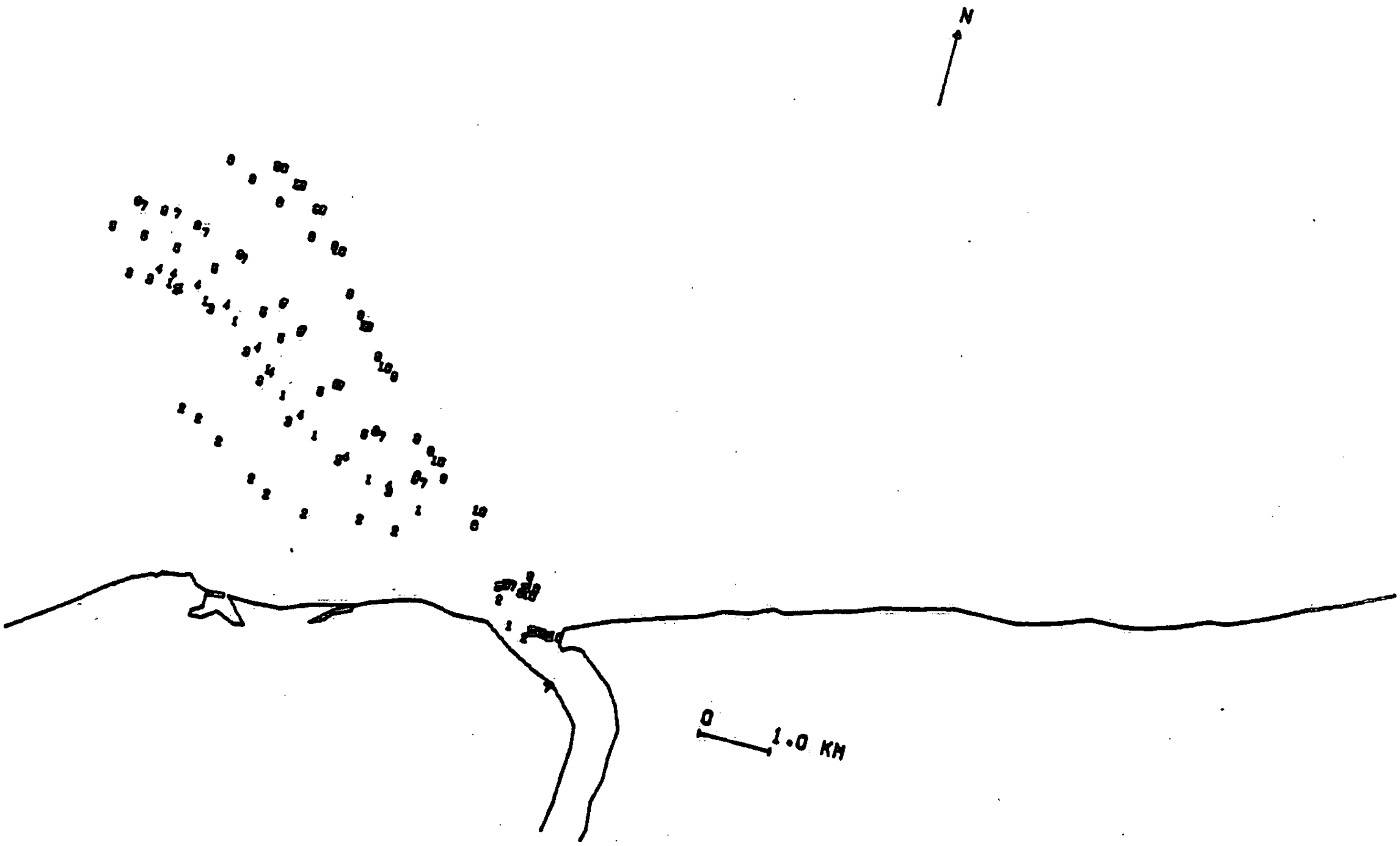

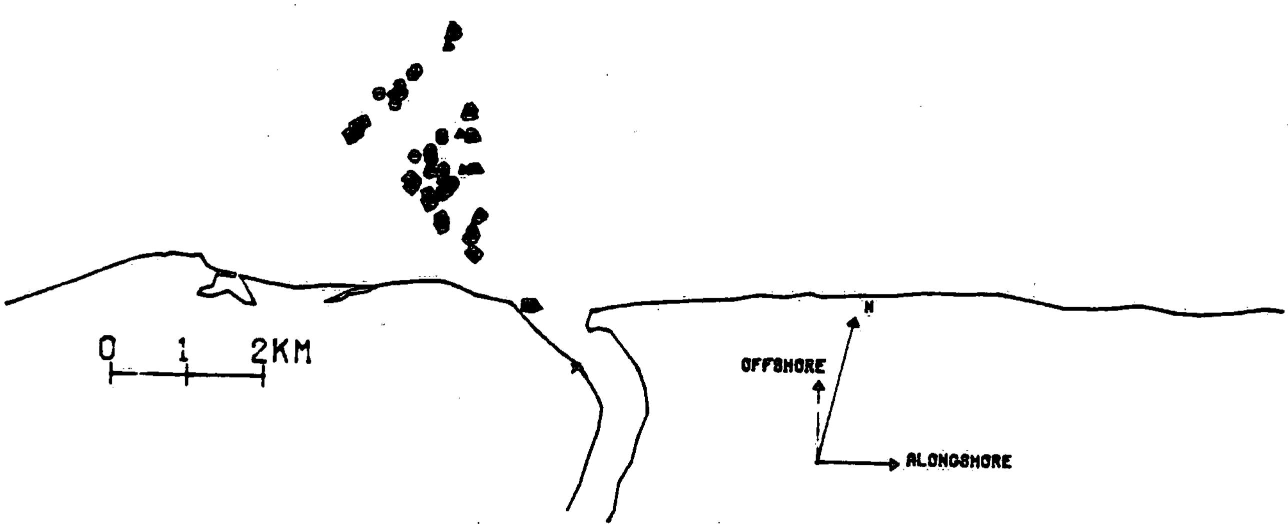

NOV 10, 1982 (14:00 GMT)

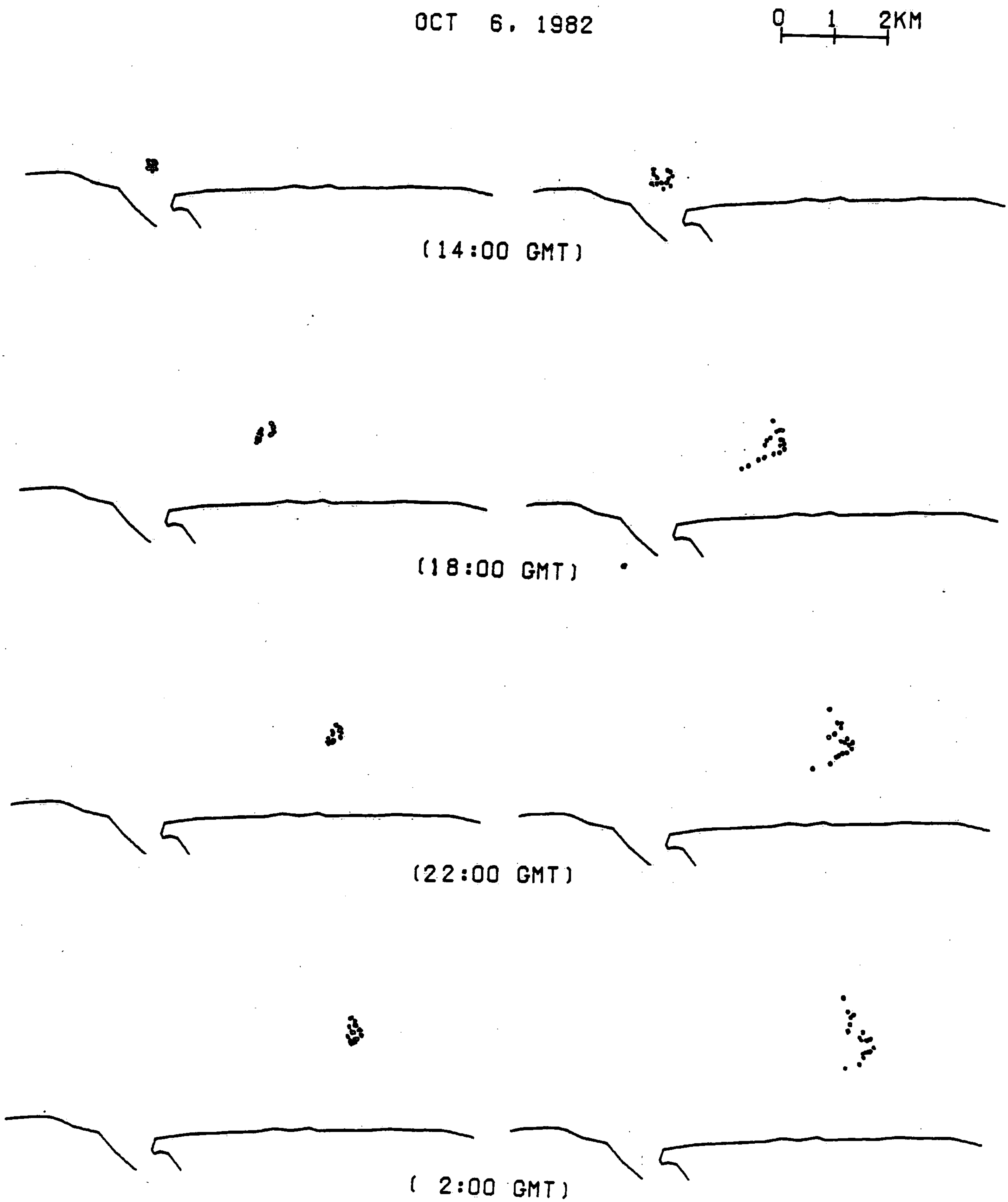
OCT 6, 1982
0 1 2KM
(14:00 GMT)
(18:00 GMT)
(22:00 GMT)
(2:00 GMT)

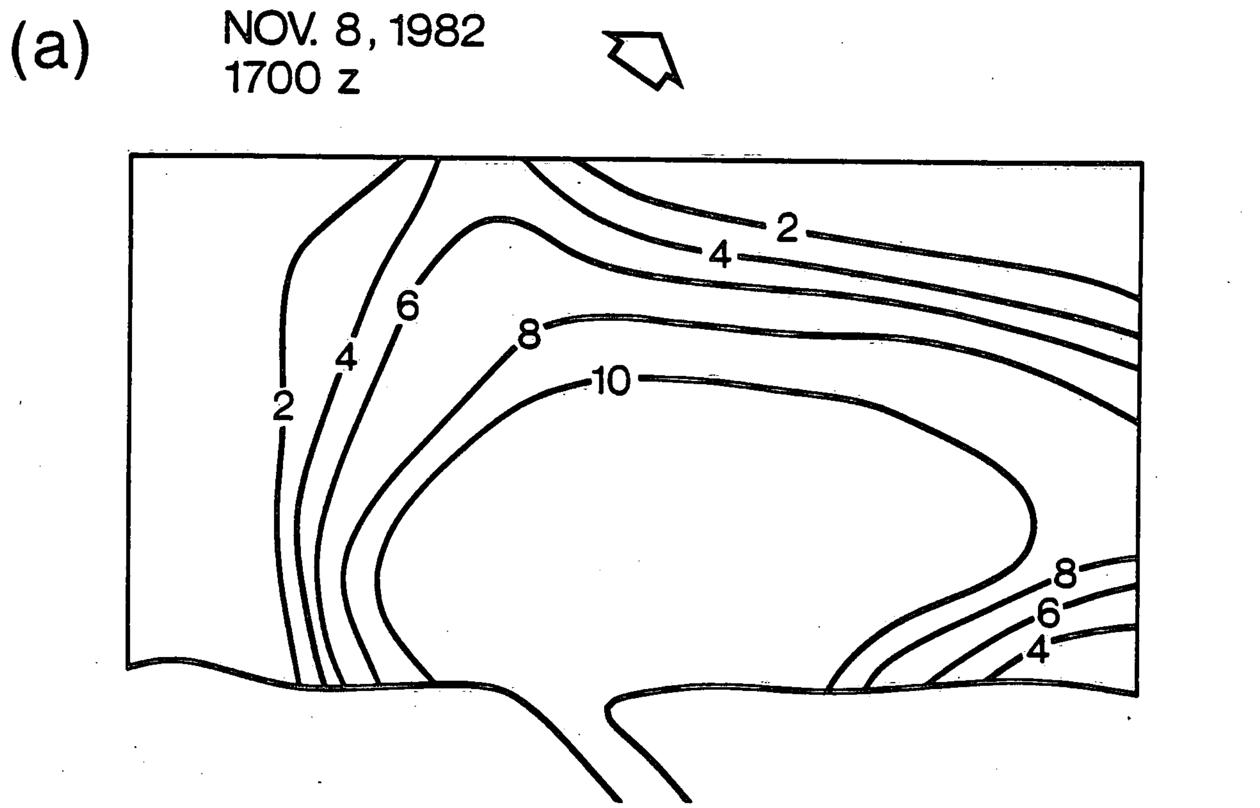

(a)
NOV. 8, 1982
1700 z
2
4
2
4
6
8
10
8
6
4
0
5km

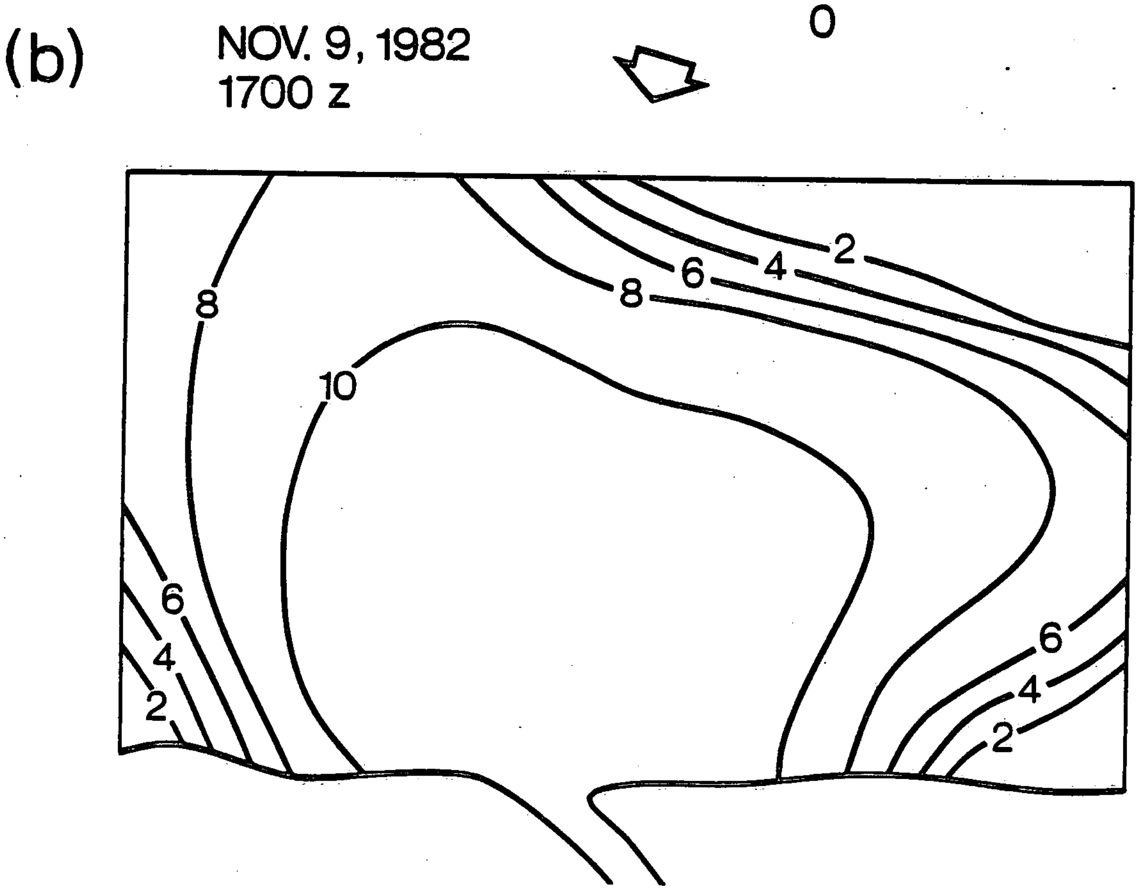

(b)
NOV. 9, 1982
1700 z
2
4
6
8
8
10
6
4
2
6
4
2

(c) NOV. 10, 1982
1700 z

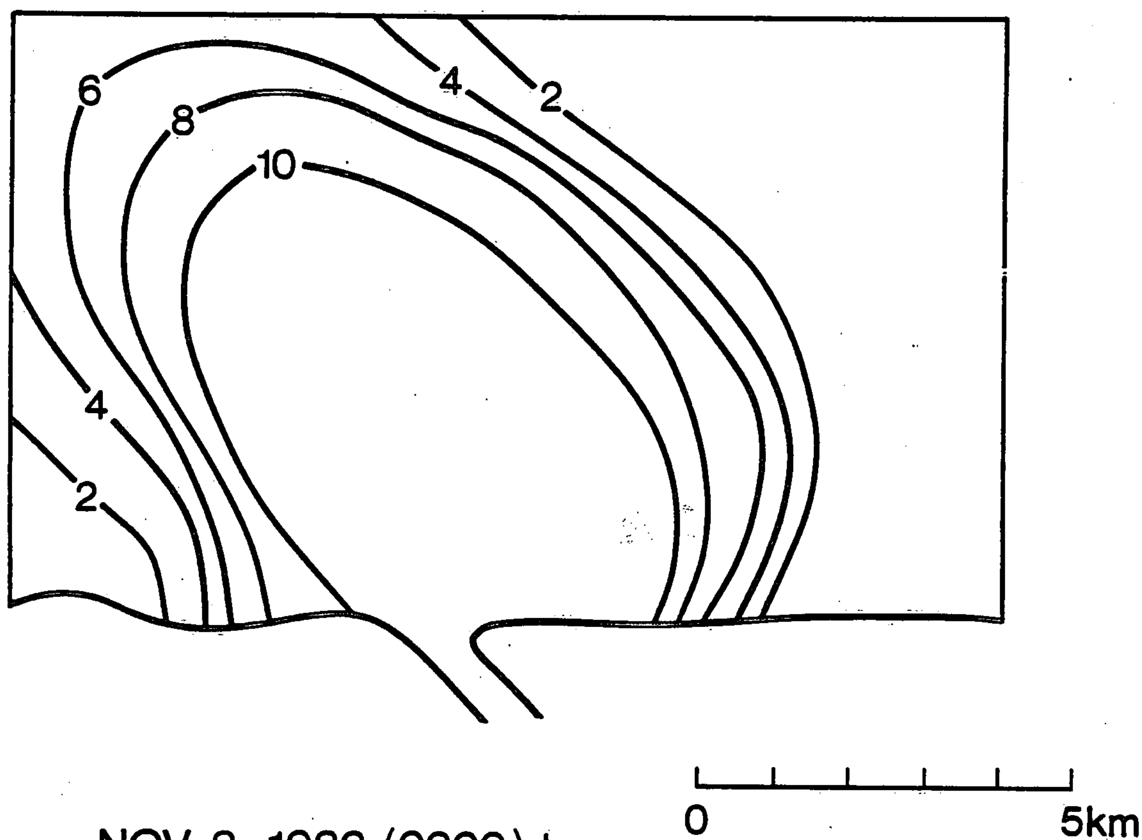

(d) NOV. 8, 1982 (0800) to
NOV. 10, 1982 (2300)

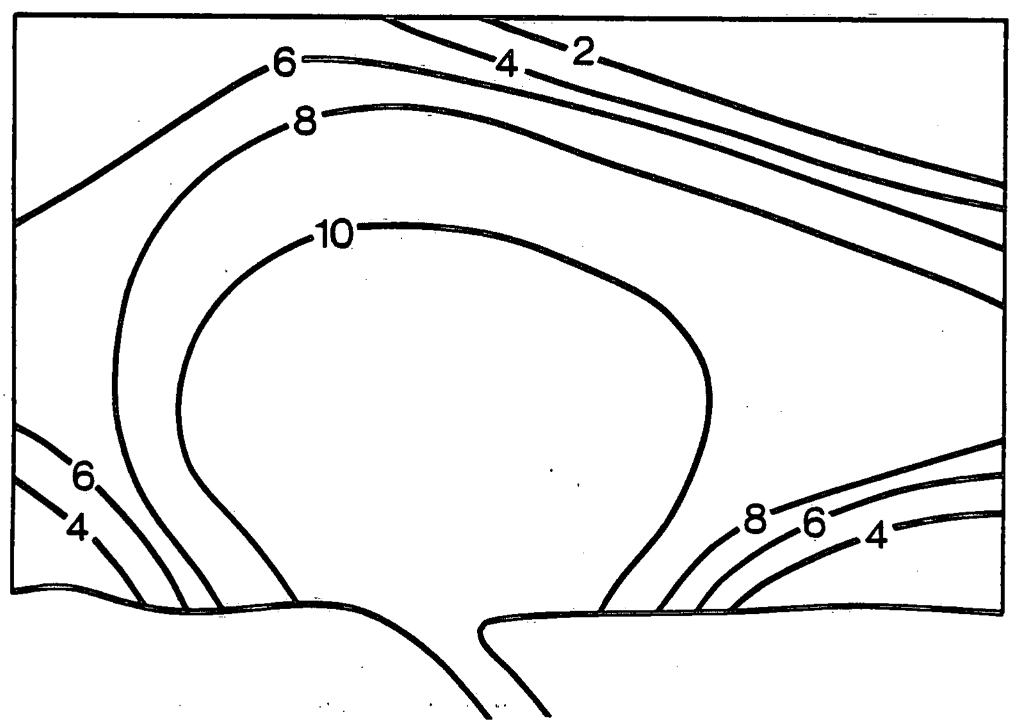

19581